January 2015

MICROBIAL CONTROLS ON THE ENVIRONMENTAL FATE OF CARBON NANOMATERIALS

Timothy Dale Berry
Purdue University

Graduate School Form 30
Updated 1/15/2015

PURDUE UNIVERSITY
GRADUATE SCHOOL
Thesis/Dissertation Acceptance

This is to certify that the thesis/dissertation prepared

By Timothy Dale Berry

Entitled
MICROBIAL CONTROLS ON THE ENVIRONMENTAL FATE OF CARBON NANOMATERIALS

For the degree of Doctor of Philosophy

Is approved by the final examining committee:

Timothy Filley
Chair

Chad Jafvert

Greg Michalski

Ron Turco

To the best of my knowledge and as understood by the student in the Thesis/Dissertation Agreement, Publication Delay, and Certification Disclaimer (Graduate School Form 32), this thesis/dissertation adheres to the provisions of Purdue University's "Policy of Integrity in Research" and the use of copyright material.

Approved by Major Professor(s): Timothy Filley

Approved by: Indrajeet Chaubey 12/1/2015

Head of the Departmental Graduate Program Date

MICROBIAL CONTROLS ON THE ENVIRONMENTAL FATE OF CARBON NANOMATERIALS

A Dissertation

Submitted to the Faculty

of

Purdue University

by

Timothy D. Berry

In Partial Fulfillment of the

Requirements for the Degree

of

Doctor of Philosophy

December 2015

Purdue University

West Lafayette, Indiana

To my loving family and friends.

ACKNOWLEDGEMENTS

This dissertation would not have been possible without the guidance of my advisory committee and primary advisor, Timothy Filley, and the contributions of my collaborators: Andrea Clavijo, Howard Fairbrother, David Goodwin, Chad Jafvert, Ron Turco, and Yingcan Zhao. I would also like to thank my colleagues in the Purdue Stable Isotope lab for their unwavering support - I couldn't ask for better people to work with. Most importantly, I would like to thank my family and friends for their continuous love.

TABLE OF CONTENTS

Page

Page

Page

LIST OF TABLES

LIST OF FIGURES

Figure Page

Figure Page

Figure Page

Figure Page

ABSTRACT

Berry, Timothy D Ph.D., Purdue University, December 2015. Microbial Controls on the Environmental Fate of Carbon Nanomaterials. Major Professor: Timothy Filley.

Since the synthesis of the first carbon nanomaterials (CNM) 30 years ago, researchers and manufacturers have recognized the potential of these materials to transform the world. The unique physical properties and incredible resilience of these materials gives them countless applications and has led to significant increases in their production over the last decade. However, despite their growing prevalence, the properties and processes controlling the degradation of CNM in the environment remain poorly understood. The primary purpose of this dissertation is to examine the role of environmental microorganisms in degrading CNM and to elucidate which CNM properties and environmental processes represent important controls on this degradation. To accomplish this, a series of incubation studies were conducted in which pure fungal cultures and soils were exposed to a CNM.

In pure culture studies the wood-decay fungi *Trametes versicolor* and *Phlebia tremellosa* were grown in the presence of single-walled carbon nanotubes (SWCNT) and CNT-polymer composites. By using CNT with varying purities and surface chemistries we were able to relate CNT properties to the production of degradative

enzymes by the fungi. While fungal enzyme activity and growth patterns were not affected by purified and unfunctionalized SWCNT, incubation with either impure SWCNT or purified SWCNT with 3% surface carboxylation altered fungal growth morphology and the activity of the extracellular laccase and peroxidase enzymes. The role of CNM surfaces in initiating microbial responses to these materials was further highlighted by the inability of cultured fungi to increase enzyme activity when grown with CNT-polymer composites in which the CNT surface was not accessible. To further explore the role of surface chemistry in controlling the degradation of CNM, laboratory soil incubations using ^{13}C-enriched C_{60} fullerenes were conducted. We observed that while pristine C_{60} was not degraded in the soil, C_{60} that had been previously abiotically transformed by prolonged photo-exposure were, with ~0.78 % of added C_{60} mineralized. In a follow up study using C_{60} fullerols, a hydroxylated analog of C_{60} fullerenes, were found to be rapidly mineralized in soils with a maximum mineralization of ~59.1 % of fullerol C mineralized. Analysis of microbial phospholipid fatty acids (PLFA) extracted from soils found that Gram negative PLFA contained the largest proportion of fullerol derived ^{13}C.

The works in this dissertation are the first to demonstrate that surface functionalization is necessary to induce an enzymatic response in saprotrophic fungi and first to confirm that abiotic degradative processes are able to significantly increase the rate of CNM decomposition in soils. The use of isotopically labelled CNM has allowed for sensitive quantification of microbial mineralization and uptake of CNM carbon. Together, these findings demonstrate the critical importance of surface chemistry in controlling the microbial degradation and environmental fate of CNM.

CHAPTER 1. INTRODUCTION

1.1 Research Background and Significance

1.1.1 A new allotrope of carbon

The synthesis of the first carbon nanomaterial (CNM) by Kroto, Smalley, and Curl at Rice University in 1985 continues to have far-reaching impacts in the fields of chemistry, physicals, materials science, engineering, and medicine. This first CNM, buckminsterfullerene, would become the first of a number of new allotropes of carbon in a material class known as fullerenes (Kroto *et al.* 1985). Like all nanomaterials, CNM are incredibly small structures with dimensions on the order of nanometers (10^{-9} m) but are comprised of an ordered physical structure that differentiates CNM from collections of other small carbon-based particles (e.g. amorphous carbon). Fullerenes, a type of CNM, have a graphenic (i.e. flat sheets of aromatic carbon) structure that has many similarities to what is found naturally in the mineral graphite. In addition to its planar form, fullerenes may be synthesized in a variety of three-dimensional forms ranging from simple cylinders and spheroids to more complex structures (Figure 1.1). Buckminsterfullerene or C_{60} is a fullerene made of a series of alternating 5- and 6-carbon rings that formed a spherical structure (the soccer ball like appearance of C_{60} gives rise to the alternate name of “buckyball”).

Similarly shaped fullerenes with different dimensions have also been synthesized and include C_{32}, C_{50}, and C_{70} among countless others. Carbon nanotubes (CNT) are cylindrical fullerenes that resemble a rolled-up graphene sheet (Iijima 1991). The resulting tube's diameter is determined primarily by the number of layers in the wall of the structure with single-walled carbon nanotubes (SWCNT) being more narrow than multi-walled carbon nanotubes (MWCNT). In either case, the length dimension of the tube often greatly exceeds its diameter and it is possible to synthesis CNTs with a 1:100,000,000 aspect ratio.

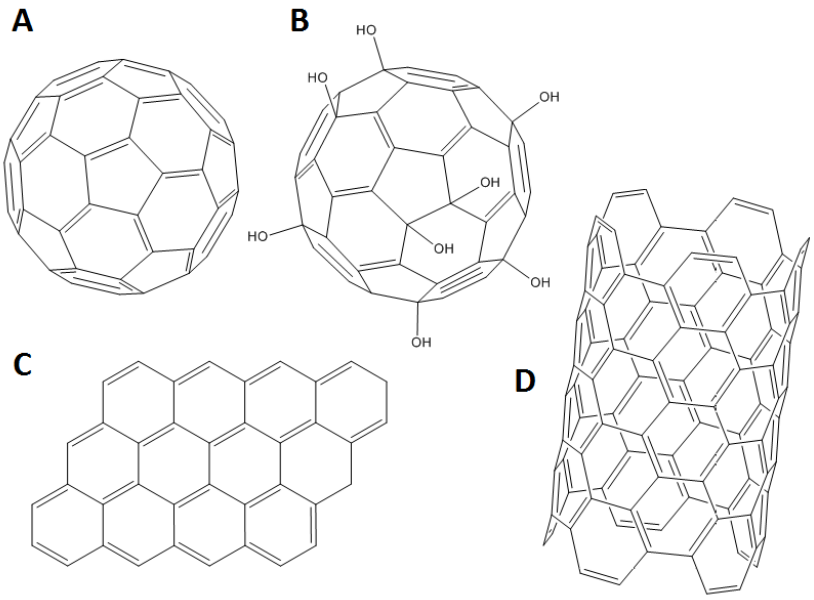

Figure 1.1 CNM exist in a variety of configurations that result in different physical and chemical properties; (A) C_{60} (Buckminsterfullerene), (B) $C_{60}(OH)_8$, a fullerol, (C) graphene sheet, (D) Single-walled carbon nanotube

Regardless of morphology, all fullerenes share a number of properties as a result of their structure that have elicited interest in a wide variety of fields. The highly aromatic structure of fullerenes results in an exceptionally high tensile strength (Ruoff

and Lorents 1995). MWCNT have been produced with an ultimate tensile strength of over 60 Gigapascals which greatly exceeds the tensile strength of conventional materials such as steel or wood (Yu *et al.* 2000). This strength makes the incorporation of fullerenes into materials that are workable at a macroscopic scale an active area of research (Coleman *et al.* 2006). The highly condensed nature of fullerenes also makes them chemically resilient, as only exposed edges and defect sites are viable reaction centers for covalent bonding (Hirsch 2002). Despite this resilience it is possible to modify the surface chemistry of fullerenes under certain conditions (e.g. high heat and exposure to strongly oxidizing acids (Liu *et al.* 1998)) to create a fullerene derivative with significantly different properties than the original material (Nakamura and Isobe 2003). For example, the addition of polyethylene glycol moieties to SWCNT dramatically increases the water solubility of the resultant nanomaterial (Zhao *et al.* 2005). Functionalization of fullerenes allows for a greater range of possible applications, e.g. as drug delivery vehicles (Bianco *et al.* 2005; Bakry *et al.* 2007).

As aromatic structures, the carbon atoms in fullerenes are sp^2 hybridized resulting in delocalized electrons that are free to convey charge depending on the morphology of the fullerene. CNTs, for example can be formed with varying degrees of curvature and with different alignments that impact electrical properties of the tube (Avouris 2002). This property allows CNT to be metallic, semimetallic, or semiconductive characteristics, depending on chiral angle. The fine-tuning of CNT conductivity allows fullerenes to be used to construct nanoscale electronic components

such as transistors (Franklin *et al.* 2012) and piezoelectric nanosensors (Hierold *et al.* 2007).

1.1.2 Environmental concerns about CNM

The myriad applications of CNM have led to considerable demand for fullerenes and other nanomaterial products, resulting in the formation of the nascent nanotechnology industry and commercialization of nanomaterials. Innovations in synthesis methods and development of production infrastructure have allowed for dramatic increases in the production capacity of CNM, resulting in a correspondingly sharp decline in the cost of nanomaterials. Considering MWCNT as an example, production by industry has increased over 100-fold in the last decade resulting in a 450-fold reduction in the price of MWCNT (De Volder *et al.* 2013; Zhang *et al.* 2013). The steadily falling cost of nanomaterials is expected to result in greater demand for CNM as mass-produced fullerenes become an economically feasible replacement for carbonaceous fillers such as carbon black in rubber and polymer applications (Zhang *et al.* 2013).

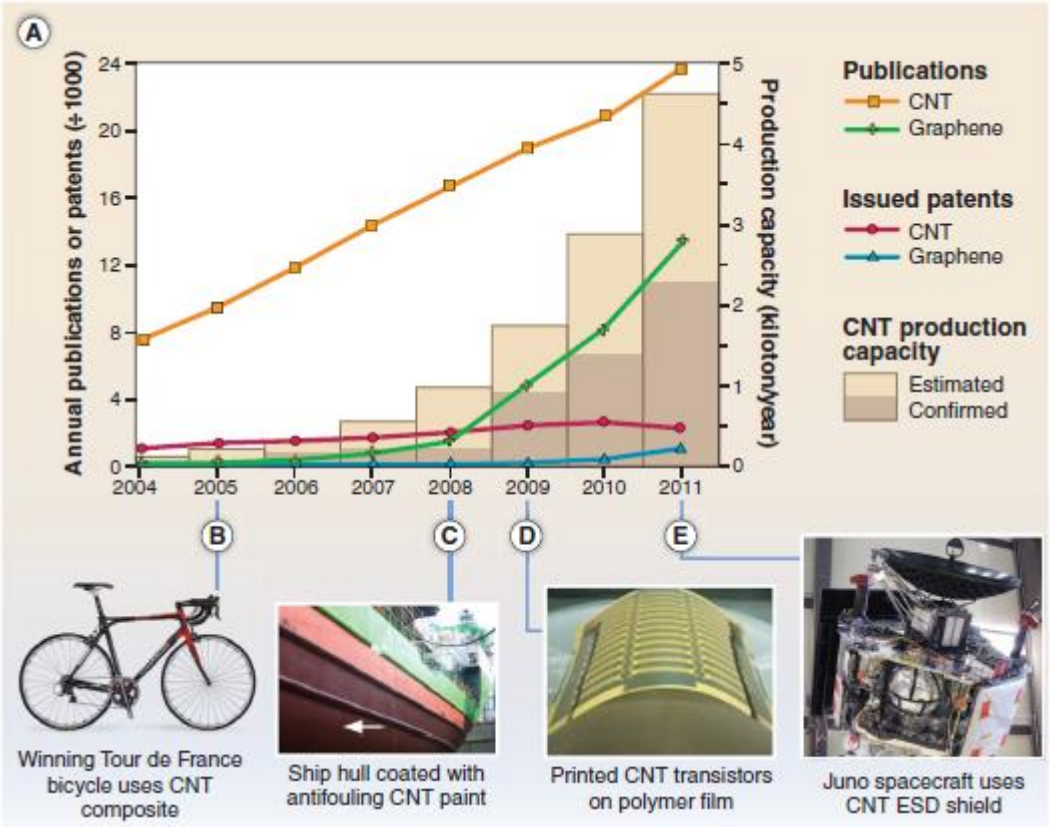

Figure 1.2 Trends in CNM research, commercialization, and synthesis (A) and a selection of CNT containing products. Reproduced with permission from De Volder *et. al* (2013).

Despite the advances in CNM synthesis and application, there is relatively little knowledge on how the eventual release of CNMs into the environment can be expected to impact the health and safety of ecosystems. Environmental exposure to nanomaterials such as fullerenes is expected to occur through accidental release from production facilities, as a result of the regular disposal of nanomaterial containing products at the end of their life-cycle, and through contamination of waste water following use of nanomaterial containing therapeutics and cosmetics (Gottschalk and Nowack 2011; Nowack *et al.* 2012; Yang *et al.* 2015). Accidental release of bulk CNM has the potential to distribute them over a wide area; the incredibly small mass and

relatively large surface area of nanomaterials powders allows them to be easily scattered by air currents outside of controlled conditions. The disposal of nanomaterial containing products in landfills presents the risk that fullerenes liberated by weathering of the product will infiltrate ground waters and become distributed throughout soils.

Environmental contamination of CNMs presents a potential threat to the health of organisms exposed to fullerenes. Laboratory studies have reported CNM toxicity in a wide variety of organisms ranging from soil microbes to humans (Navarro *et al.* 2008). Of particular concern are those studies that demonstrate detrimental effects of CNM on the microbes and invertebrates that regulate important ecosystem-sustaining processes like nutrient cycling in soils, as disruption of these services has the potential to damage entire ecosystems (Holden *et al.* 2013). The addition of low-purity SWCNT to low-carbon soils was found to alter soil microbial community while inducing metabolic changes in the soil (Tong *et al.* 2012). Even in the absence of the acute toxicity, CNM have the potential to influence ecologically important populations with chronic exposure. For example, MWCNT contamination of food at concentrations as low as 37mg kg^{-1} resulted in decreased reproduction rate in the earthworm *Eisenia veneta* while similar concentrations in soils resulted in DNA damage in the same species (Scott-Fordsmand *et al.* 2008; Hu *et al.* 2014). The inclusion of MWCNT in growth medium also been found to impact exposed plant species such as the tomato, *Lycopersicon esculentum,* which increased its expression of genes commonly associated with a stress response. Interestingly, tomatoes grown in the presence of MWCNT were observed to have MWCNT in root, leaf, and fruit tissues (Khodakovskaya *et al.* 2011). In a separate study

examining the exposure of Asian rice (*Orzya sativa)* to MWCNT, the nanomaterials could be traced into both leaf and seed tissues (Lin *et al.* 2009). These studies suggest that under some conditions CNM might enter food chains through contamination of primary producers.

Like many potential environmental toxins, the toxicity of CNM appears to be a complex function of a number of factors. Comparisons of fullerenes with differing morphological characteristics such as the size and shape report conflicting results. A number of studies have found that the smaller, spherical fullerenes such as C_{60} are less damaging that larger structures such as CNT (Jia *et al.* 2005; Scott-Fordsmand *et al.* 2008). However, a study assessing the antibacterial effects of C_{60} fullerenes found that decreased aggregate size resulted in increased cytotoxicity (Lyon *et al.* 2006) while a study on the toxicity of functionalized SWCNT found that highly compact aggregates correlated with decreased cytotoxicity (Pasquini *et al.* 2012). Conflicting results in toxicological studies on CNM are relatively common, and are possibly the result of failure to account for environmental factors in experimental design (Holden *et al.* 2013). Environmental factors such as the presence of organic matter and solution ionic concentration are important controls on CNM stability with importance consequences in determining toxicity. Lyon *et al*. for example, found that toxicity of fullerene suspensions towards *Escheria coli* and *Bacillus subtilis* was greater when the exposure occurred in a growth medium with low salt content that prevented aggregation of the fullerenes (Lyon *et al.* 2005). Stabilization of fullerenes by dissolved organic matter may also have a mitigating effect on the cytotoxicity of C_{60} clusters (Li *et al.* 2008). The ability

of organic matter to reduce the toxicity of CNM is further supported by the observation that SWCNT added to a low carbon soil had a measurable impact on soil microbial community while addition to a more organic matter rich soil failed to produce any significant changes (Tong *et al.* 2012). Although these studies highlight the necessity of considering environmental interactions with CNM when assessing their potential toxicity, a great deal more work is needed to fully understand the extent to which substrate characteristics are able to influence CNM toxicity.

1.1.3 The environmental fate of CNM

The resilience of highly condensed aromatic particles such as CNM suggests that following release into the environment, fullerenes in most forms are likely to be highly recalcitrant and thus have the potential to accumulate in sediments and soils (Batley *et al.* 2013). However, because fullerenes can be produced with a wide range of morphologies and surface chemistries, some fullerenes will be more susceptible to environmental transformation than others. As with toxicity, the environmental degradability of CNM is thought to involve a number of factors including nanomaterial morphology, surface chemistry, and purity; all of which may then interact with the geochemistry and microbiology at the location of release. The high aspect ratio of fullerenes such as CNT and formation of large nanomaterial aggregates under certain conditions are likely to prevent uptake of CNM by common degradative organisms, limiting biotic degradation to extracellular processes such as enzymatic oxidation. A number of studies have demonstrated the potential for such enzymes to modify CNMs. Cell-free studies involving the treatment of SWCNT with the oxidative enzyme

horseradish peroxidase have found that given long-term exposure, the enzyme is able to degrade the nanomaterials (Allen *et al.* 2008). Schreiner *et al*. (2009) demonstrated that white-rot fungi, which are capable of producing powerful lignin degrading enzymes, were able to enzymatically bleach hydroxylated C_{60} while being unable to modify the fully aromatic C_{60} (Schreiner *et al.* 2009). Other studies reported that degradation of MWCNT increased with surface functionalization (i.e. carboxylation) which further supports that surface chemistry is important in controlling microbial degradation of CNM (Zhao *et al.* 2011). In fact, Berry *et al.* (2014), the work conducted in CHAPTER TWO of this dissertation, demonstrated that only 2-3% surface carboxylation of purified SWCNT, was sufficient to induce oxidative enzyme activity in fungal cultures.

The transformation of fullerenes is not limited to biotic processes, the role of abiotic processes such as photo-oxidation in CNM degradation has been widely explored. Exposure of aqueous C_{60} suspensions to visible light results in the formation of reactive oxygen species (ROS) such as superoxide anion and singlet oxygen that facilitate the oxidation of C_{60} and the alteration of it surface properties (Hou and Jafvert 2009; Hou *et al.* 2010). Similar results are reported in suspensions of SWCNT, MWCNT, and planar graphene when exposed to light (Chae *et al.* 2011; Zhao and Jafvert 2015). ROS produced by photo-exposure of CNM increases as a result of SWCNT surface functionalization, suggesting that photo-degradation of CNM might result in a positive-feedback loop facilitating further ROS generation and surface oxidation (Chen and Jafvert 2011). The increased degradative potential of oxidative enzymes towards previously functionalized CNM suggests that degradation of CNM in the environment

might proceed synergistically via coupled abiotic and biotic processes. The study detailed in CHAPTER FOUR (Berry *et al.*, in review) provides the first evidence that interactions between degradative processes do have the potential to influence the environmental fate of CNM by increasing their mineralization in soils.

1.2 Dissertation Content and Structure

This dissertation addresses critical knowledge gaps related to the importance of coupled abiotic-biotic processes and CNM surface chemistry in controlling the environmental fate of CNM. The guiding hypotheses addressed in this dissertation are (1) CNM surface chemistry is a significant control on the ability of microorganisms to degrade CNM and (2) Abiotic transformative processes (e.g. photo-irradiation) are able to synergistically increase the environmental degradation of CNM via biological processes. We investigate these hypotheses using a multi-proxy (stable isotope, molecular microbiology) approach to track the fate of different pristine and functionalized CNM in soils and growth media. Each chapter examines the transformation of and response to CNM by microorganisms over the course of an incubation period and addresses these hypotheses in order to expand the current knowledge on the factors controlling the environmental fate of CNM.

CHAPTER TWO describes a fungal pure culture study that sought to determine the factors inherent to a specific nanomaterial that controlled the enzymatic response of saprotrophic organisms. A thorough understanding of the interactions between nanomaterial physiochemical characteristics and the ability of environmental organisms to degrade them have been largely neglected in lieu of studies focusing solely on

toxicity. This study placed pure cultures of the white-rot fungi *Trametes versicolor* and *Phlebia tremellosa* on growth media containing a variety of SWCNT, all produced by the same synthesis method, which allowed many of the confounding variables that often interfere with such studies to controlled. We found that the activity of oxidative enzymes produced by the fungi did not increase when exposed to purified, unfunctionalized SWCNT. However, exposure of fungi to either unpurified or purified but carboxylated SWCNTs did result in increased enzymatic activity, though the exact nature of these enzymatic responses varied between fungi and different media types. This chapter has been published in the journal *Environmental Pollution* (Berry *et al.* 2014) and has been reformatted for inclusion in this dissertation with permission from Elsevier.

CHAPTER THREE is an expansion on the study undertaken in CHAPTER TWO that seeks to understand the affect that CNM inclusion in products such as polymer composites has on the degradation of these materials. This approach is relevant as many previous studies seeking to understand the degradation of CNM are limited in scope to include aqueous suspensions or dry deposition of fullerene powders. Again the white-rot fungi *T. versicolor* was used a model organism to assess the enzymatic response of saprotrophic organisms to CNT containing polymer composites. In contrast the previous chapter we found that surface functionalized CNT did not increase oxidative enzyme activity in white-rot fungi when embedded in polymer composites. This finding further highlights the crucial role of surfaces in controlling microbial interactions with CNM.

CHAPTER FOUR explores the extent to which abiotic photochemical processes influence the biotic degradation of CNM. Although evidence from several studies suggests a mechanism for interactions between abiotic and biotic processes, no study has demonstrated that an environmental relevant abiotic process can meaningfully impact biotic CNM transformation. To address this lack of experimental evidence a laboratory soil microcosm experiment was conducted in which C_{60} fullerenes that were enriched in the stable isotope ^{13}C were progressively photo-oxidized before addition to an agricultural soil. The use of isotopically labelled nanomaterials greatly increased our ability to track the fate of that carbon as it was degraded in the soils, allowing for the. This study, Berry *et al.* (in review) generated the first numbers for the microbially-driven decay of photo-irradiated C_{60}. Although prolonged exposure of $^{13}C_{60}$ to visible light (60 days of constant exposure) resulted in measurable chemical and structural modification of the C_{60}, the mineralization rate of the photo-oxidized product when added to soil was still quite low with an average mineralization of 180.9 ng/day.

CHAPTER FIVE details an experimental follow-up to CHAPTER FOUR in which custom synthesized ^{13}C-enriched C_{60} fullerols are used to represent a highly oxidized end-member product of abiotic oxidation of CNM. The addition of the fullerols to the same soils used in CHAPTER FOUR resulted in significant nanomaterial mineralization, with an observed mineralization rate of 2.7 and 21.3 µg/day in low- and high-carbon soils respectively. Additionally, the ^{13}C from the fullerols was tracked into microbial phospholipid fatty acids from the high-carbon soil, revealing that microbial preference for that carbon was dominated by Gram negative bacteria. This study, in conjunction

with the study discussed in CHAPTER FOUR provides additional novel results demonstrating that surface functionalization can significantly increase CNM mineralization in environmental substrates.

CHAPTER SIX summarizes the findings of the previous chapters and discusses additional research questions that warrant further investigation to improve our understanding of the environmental fate of CNM.

CHAPTER 2. OXIDATIVE ENZYMATIC RESPONSE OF WHITE-ROT FUNGI TO SINGLE-WALLED CARBON NANOTUBES

2.1 Abstract

Although carbon nanomaterials such as single-walled carbon nanotubes (SWCNT) are becoming increasingly prevalent in manufacturing, there is little knowledge on the environmental fate of these materials. Environmental degradation of SWCNT is hindered by their highly condensed aromatic structure as well as their size and aspect ratio, which prevents intracellular degradation and limits microbial decomposition to extracellular processes such as those catalyzed by oxidative enzymes. This study investigates the peroxidase and laccase enzymatic response of the saprotrophic white-rot fungi *Trametes versicolor* and *Phlebia tremellosa* when exposed to SWCNTs of different purity and surface chemistry under different growth conditions. Both unpurified, metal catalyst-rich SWCNT and purified, carboxylated SWCNTs promoted significant changes in the oxidative enzymes activity of the fungi while pristine SWCNT did not. These results suggest that functionalization of purified SWCNT is essential to up-regulate enzymes that may be capable of decomposing CNT in the environment.

2.2 Introduction

Single-walled carbon nanotubes (SWCNTs), formed from single-atom thick sheets of carbon wound into nanometer scale tubes (Iijima 1991), display a number of remarkable properties ranging from superior tensile strength, thermal and electrical conductivity, and relative ease of chemical modification (Collins *et al.* 1997; Georgakilas *et al.* 2002). These properties make CNTs promising components in next-generation thermopolymers, electronics, and drug delivery systems (Bianco *et al.* 2005; Trojanowicz 2006). As a result of their wide range of uses and the rapidly advancing production methods, carbon nanotubes are increasingly prevalent in manufactured products. Despite the increase in CNT production, very little is known about the eventual fate of CNTs once introduced into the environment through accidental release, dispersal in landfills, and as a part of biosolid waste for land application (Wiesner *et al.* 2009; Turco *et al.* 2011; Holden *et al.* 2013).

As with the vast majority of industrial products, the environmental fate of CNTs is partially dependent on degradation by microorganisms found in soils, sediments, and landfills (Klaine *et al.* 2008). Commercially produced CNTs have lengths on par, or much larger than, many biological cells with aspect ratios of up to 1,000,000 to 1 making intracellular degradation unlikely. Instead, the most likely mechanism by which environmental CNTs are microbially transformed and degraded are via extracellular redox processes, such as those catalyzed by oxidative enzymes (Allen *et al.* 2008; Zhao *et al.* 2011). Of particular interest are enzymes of the peroxidase and polyphenol oxidase groups (Collins *et al.* 1996; Novotny *et al.* 1999). These lignin-modifying

enzymes catalyze the oxidation of aromatic structures by generating highly reactive radicals, which interact with aromatic structures in a variety of ways (Blanchette 1991; Leonowicz *et al.* 1999; Rabinovich *et al.* 2004). Laccase, for example, oxidizes phenolic compounds into their corresponding phenoxy radicals; following radical formation, ring fission can be caused by spontaneous rearrangement and reaction with other nearby compounds (Thurston 1994; Leonowicz *et al.* 2001). Peroxidase enzymes utilize heme cofactors in the presence of peroxides to facilitate a wide range of redox reactions (Dunford and Stillman 1976). Environmentally important peroxidase enzymes include manganese peroxidase, which generates reactive Mn(III)-chelates (Forrester *et al.* 1988; Wariishi *et al.* 1988; Wariishi *et al.* 1992), in addition to more versatile peroxidases that are able to reduce and oxidize a variety of substrates (Camarero *et al.* 1999). Peroxidase and polyphenol oxidase enzymes, such as laccase, may also interact synergistically. For example, reactive species generated by oxidation of phenolic compounds by laccase are able to serve as substrates for versatile peroxidases; this synergy allows lignin-modifying enzymes to function as powerful degraders of highly condensed compounds (Leonowicz *et al.* 2001), including functionalized SWCNT (Allen *et al.* 2008).

As a result of their repertoire of degradative enzymes, saprotrophic fungi, such as the wood-rotting Basidiomycetes *Trametes versicolor* and *Phlebia tremellosa,* are considered excellent candidates for the degradation of a wide range of industrially-produced xenobiotics (Rabinovich *et al.* 2004; Riva 2006). However, there is limited research demonstrating enzymatic or direct microbial decomposition of manufactured carbon-based nanomaterials. Allen *et al.* demonstrated that pristine CNT where

unreactive toward purified solutions of horse radish peroxidase, while mildly carboxylated, analogs exhibited chain shortening and oxidation under the same conditions. Previous research by our group has demonstrated that lab-cultured white rot fungi are able to successfully degrade partially hydroxylated C_{60} fullerenes, i.e., C_{60} fullerols (Schreiner *et al.* 2009). The distinction between pristine and functionalized, hydroxylated or carboxylated, may be crucial when estimating the potential for microbial decay of CNT's as the highly condensed nature of unfunctionalized CNTs, may dramatically impede microbial decomposition and increase the potential for long-term environmental accrual as has been seen for pristine fullerenes.

Research on the impacts of carbon nanomaterials on microorganisms has been largely focused on the impact of nanomaterials on bacterial monocultures where both CNT and fullerenes have demonstrated antimicrobial properties (Lyon *et al.* 2006; Kang *et al.* 2007; Arias and Yang 2009; Kang *et al.* 2009). In a study using a variety of different fullerene suspensions, the nanomaterials were found to function as potent antibacterial agents against the gram-positive bacteria *Bacillus subtilis* (Lyon *et al.* 2006), while unfunctionalized multiple-walled carbon nanotubes (MWCNT) were found to significantly decrease sporulation of the fungus *Paecilomyces fumosoroseus* in pure culture but had no effect on hyphal growth (Gorczyca *et al.* 2009). Kang et al. (2007, 2009) found that SWCNT were effective in inactivating pure cultures of *Escheria coli, Pseudomonas aeruginosa, Bacillus subtilis,* and *Staphylococcus epidermis* in defined media, though the authors found that antimicrobial activity against pure cultures was a

poor indicator of microbial deactivation in more complex environmental samples (Kang *et al.* 2007; Kang *et al.* 2009).

It has been suggested that in more complex environmental systems, natural organic matter aids in the sorption of nanoparticles, diminishing their apparent toxicity (Li *et al.* 2008; Navarro *et al.* 2008). Studies of fullerene toxicity in soil have found little impact on soil respiration or on bacterial and fungal communities (Tong *et al.* 2007). Additionally, a recent study found that unpurified CNTs that contain residual amorphous carbon and catalysts from synthesis are able to influence microbial community composition in soils with low organic matter content, diminishing certain fungal and bacteria groups, while having less impact in soils with higher organic matter content (Tong *et al.* 2012). Such findings are also consistent with reports of the microbial toxicity of carboxylated SWCNT in soils with low organic content (Rodrigues *et al.* 2013).

The surface chemistry of CNT may not just control their chemical "lability" with respect to microbial enzyme decay, but may also play an important role controlling cytotoxic interactions of CNTs with soil microbial communities (Karakoti *et al.* 2006; Rodriguez-Yanez *et al.* 2013). For example, the cytotoxicity of both SWCNTS and MWCNTs has been reported to significantly increase once their surface has been oxidized (Bottini *et al.* 2006; Fenoglio *et al.* 2008). Other studies, however, have demonstrated that increased density of surface functionalization of SWCNTs may actually decrease cytotoxicity (Sayes *et al.* 2006). These seemingly contradictory responses are most likely a function of the propensity of functionalized CNTs under certain conditions to either bind to cells, or to homo and heteroaggregate and thus self-

mitigate certain toxicological effects (Handy *et al.* 2008; Arias and Yang 2009; Pasquini *et al.* 2012).

Impurities in CNTs derived from the manufacturing process, e.g. amorphous carbon and metal catalysts, must also be considered as potential influences on soil microbial activity. Although a broad range of synthesis methods exist for commercially available CNTs, many rely on formation of the nanomaterials around metallic nanoparticles catalysts (Melechko *et al.* 2005). As a result, the majority of CNTs contain metal impurities (Ge *et al.* 2011). For example, one popular method of large-scale SWCNT synthesis, electric arc discharge, uses nickel and yttrium catalysts(Journet *et al.* 1997). Liu et al. (2007) reports that catalytic nickel from a variety of SWCNT synthesized by this method is readily bioavailable, more so than the nickel salt $NiCl_2$ used as a reference (Liu *et al.* 2007). As is the case with the carbon nanomaterials themselves, bioavailability of the metal nanoparticles is highly dependent on environmental factors such as presence of soil organic matter and local redox conditions (Degryse *et al.* 2009; Auffan *et al.* 2010). One recent study in agricultural systems found that dissolution of natural organic matter by surfactants greatly increased mobility of heavy metals (Hernandez-Soriano and Jimenez-Lopez 2012). Mitigation of metal toxicity by organic matter has previously been thought to render the catalyst's toxicity negligible in short-term soil incubations, although the authors acknowledge that some evidence suggests CNTs act to compound the toxic effects of metals by increasing the mobility of catalytic metals (Liu *et al.* 2007; Tong *et al.* 2012).

To improve our understanding of the interaction between growth environment, in this case the nutrient richness of growth media, and fungal response to SWCNT of different purity and surface chemistry we compare the measured changes in oxidative enzymatic activity of the saprotrophic white-rot basidiomycetes *Trametes versicolor* and *Phlebia tremellosa* in inoculation experiments on both a simple, defined minimal media and a complex malt media high in organic and phenolic compounds. To minimize variables we use one commercial source of SWCNT, all prepared using the same electric arc process and an yttrium nickel catalyst, but treated to different levels of purity and surface functionalization.

We expect that purified SWCNT will induce a minimal enzymatic response in either media treatment given its lack of chemical functionality, low metal content and large aspect ratio. However, SWCNT with either high metal content or surface functionalization will induce oxidative enzymes activity, either as a detoxification response or an induction of aromatic/lignin-like decay processes. Growth media nutrient content, which may be considered as a proxy for soil nutrient status available to microbes in a natural system, should modulate the ability of fungi to produce oxidative enzymes and thus we expect fungi on minimal media to have significantly reduced responses to metals or functionalized SWCNT.

2.3 Materials and Methods

2.3.1 Carbon Nanomaterials

Carbon nanotubes used in this study were purchased from Carbon Solutions Inc. (Riverside, CA, USA). Carbon Solutions uses an electric arc discharge method with an

yttrium/nickel catalyst to produce the nanotubes (Niyogi *et al.* 2002). Transmission electron microscopy (TEM), using a FEI/Philips CM-100 Transmission Electron Microscope (FEI Company, Hillsboro, Oregon, USA) was employed to investigate the physical form, relative proportion of amorphous materials, and bundling of the SWCNT and compared with the manufacturers specifications to ensure conformity of the products. A summary of the chemical and physical characteristics of the SWCNT is provided in Table 2.1. The unpurified product, AP-SWCNT, contains single-walled carbon nanotubes, amorphous carbon, and metal catalyst. To produce P2-SWCNT, an unfunctionalized but high-purity SWCNT, and the carboxyl functionalized and purified analog, P3-SWCNT, the AP-SWCNT stock is oxidized by reflux in concentrated nitric acid (Hu *et al.* 2003) and purified by cross-flow filtration. P2-SWCNT and P3-SWCNT can then be separated by differences in charge (Rinzler *et al.* 1998). P3-SWCNT have a surface functionalization of 1.0-3.0 % carboxylic acid which is the only significant difference between it and the purified but unfunctionalized P2-SWCNT. Catalytic metal content and carbonaceous purity are determined by the manufacturer by thermogravimetric analysis and near-IR spectroscopy respectively (Itkis *et al.* 2003).

Table 2.1 Contents of Carbon Solutions nanocarbon added to media treatments. Nanocarbon was analyzed for purity by vendor as discussed in Itkis *et al*, Functionalization is given as the percentage of carbon atoms in nanocarbon with attached functional groups.

Nanomaterial	Carbon content	Catalyst content	SWCNT content	Functionalization	Bundle diameter (nm)
AP-SWCNT	60-70%	30%	30%	None	10-25
P2-SWCNT	>90%	4-8%	>90%	None	4-20
P3-SWCNT	>90%	5-8%	>90%	1-3% COOH	5-15

2.3.2 Media and Plating

A two-layer media plating strategy with a denser base-layer was used to prevent carbon nanomaterials from settling to the bottom of the plate, away from the fungi which predominantly occupy the surface of the media. Specifically, each plate contained a 7.5 mm deep base layer of 3 % agar (w/w) with a second 2.5 mm layer of malt extract or minimal media agar poured on the surface of this layer. The malt extract media contained barley malt extract (2 % w/w) (VWR LLC., Randor, PE, USA) and minimal media contains glucose (2 % w/w) and 1 mL yeast nitrogen base without amino acids made to manufacturers recommendations (Sigma-Aldrich, St. Louis, MO, USA) in addition to 2 % agar (w/w). It is important to note that malt extract agar is a relatively complex chemical media as compared to the minimal agar media as it contains an array of plant-derived aromatic compounds and micronutrients (Bell *et al.* 1991; Zhao *et al.* 2008). Treatments containing SWCNT were prepared by adding 50 mg of the desired nanomaterials (AP-SWCNT, P2-SWCNT, or P3-SWCNT) to 80 mL of media prior to autoclaving. Cultures of *Trametes versicolor* (strain MAD697-R) and *Phelbia tremellosa*

(strain PRL 2845) were maintained on malt extract agar and transferred to experimental plates after two weeks of growth. In order to establish the fungi on each plate, a plug of inoculum was placed on a 15 mm by 2.5 mm disc on malt extract agar at the center of each dish. Plates were incubated in darkness at room temperature (~22 °C) for 60 days before sampling. See Figure 2.1 for schematic and examples of plating scheme used in this study.

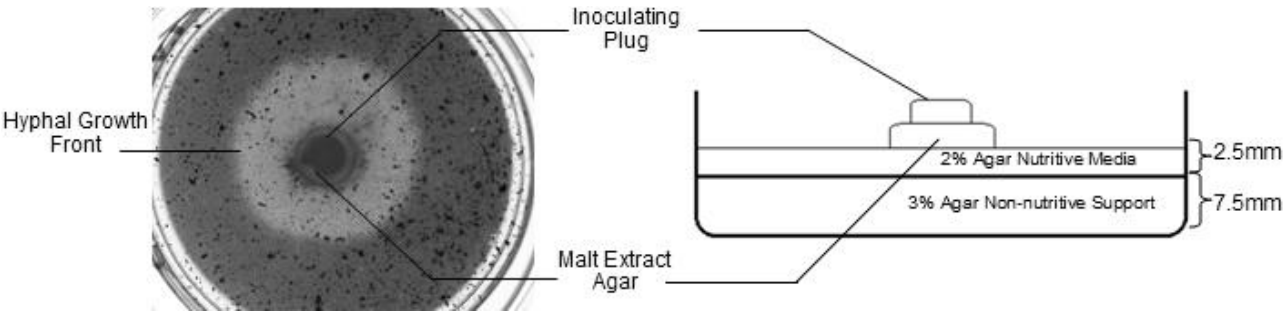

Figure 2.1 Photo of fungal growth assay (left) and schematic diagram of media layers (right) used in this study.

2.3.3 Enzyme Assays

Oxidative enzymes were extracted from growth media and assayed using a modification of the methods presented in (Heinonsalo *et al.* 2012). Briefly, four 8mm circular plugs were taken from each plate in positions corresponding to 25 % (referred to as zone 1) and 75 % (zone 2) of the distance between the center and edge of the plates; since fungal hyphae radiate outwards from the point of inoculation this sampling strategy allowed for a comparison of enzyme activity between more mature (central) and juvenile (peripheral) hyphae. Agar plugs for each treatment were halved and randomized before being loaded into 0.45 µm cellulose acetate membrane filtered

microcentrifuge tubes (Costar Spin-X, Corning Inc., Corning, NY, USA). Tubes were centrifuged at room temperature and 15,700 g for 30 minutes.

The activity of laccase and peroxidase enzymes in the resulting supernatant was determined in a coupled colorimetric assay utilizing 2,2'-azino-bis(3-ethylbenzothiazoline-6-sulphonate) (ABTS) as a substrate. Each milliliter of reaction solution contained 50 mM sodium malonate (at pH = 4.5), 0.5 mM $MnSO_4$, 1.0 mM ABTS, and 0.1 mM H_2O_2 - to be added following an initial measurement (Sigma-Aldrich). The entire volume of liquid extracted from each tube (~200 µL) was added to the reaction solution and laccase activity was measured by absorbance at 420 nm after 20 seconds. H_2O_2 was then added to serve as a peroxidase substrate, and absorbance was measured again after an additional 20 seconds. Enzyme activity was quantified against a standard curve prepared by reacting purified laccase of known activity from *T. versicolor* with reaction solution.

2.3.4 ICP-MS Analysis

The nickel and yttrium content of SWCNT-supplemented media and associated fungi was analyzed by inductively coupled plasma mass spectroscopy using a Perkin Elmer DRC-e ICP-MS (Perkin Elmer, Waltham, MA, USA). Fungal tissue was collected by using sterile forceps to peel the surface hyphae from the plates, taking care not to remove any non-fungal material on the media surface; to insure that media components didn't contaminate fungal samples, only treatment conditions resulting in dense surface mycelium were sampled. Removal of *T. versicolor* hyphae from plates was facilitated by freezing over night at -20 °C and thawing to separate media layers. As SWCNT are

dispersed evenly throughout, two 8 mm plugs of media were taken from each plate and homogenized and considered one replicate. Metals present in media and fungal hyphae were extracted by dissolving the media or tissue in 10 % nitric acid at 100 °C for 60 minutes. Following extraction and filtering to remove insoluble materials, solutions were diluted ten-fold to produce an extract in 1 % nitric acid matrix for introduction into mass spectrometer by nebulizer. A low concentration of nitric acid was used in the extraction in order to insure that SWCNT in the media plugs were not readily oxidized to release encapsulated catalyst, limiting the metals measured to that which have diffused from the surface of the nanomaterials. Nickel and yttrium were quantified against external yttrium and nickel standards. An internal standard of 3.75 ppm gallium was used to correct for instrument drift. The aluminum, chromium, manganese, iron, copper, and zinc content of the initial supporting media, prior to SWCNT loading, was also determined by ICP-MS using the same extraction procedures.

2.3.5 Statistical Analyses

Effects of SWCNT and media treatment on fungal enzyme activity were compared using two-way ANOVA with interaction using a standard least squares type model. Treatment effects were analyzed separately for each sampling zone. Significance of inclusion of catalytic metals in media and differences between enzyme activity of SWCNT containing plates and controls was determined using student's t-test. All statistical analysis was performed with JMP 8 (v8.0.2.0 SAS Institute, Cary, NC, USA). Statistical significance was determined for $\alpha = 0.05$ for all tests unless otherwise noted.

2.4 Results and Discussion

2.4.1 Catalyst metal uptake into fungal tissue and dispersal in growth media

T. versicolor mycelia harvested from the AP-SWCNT/malt media treatment had a significantly higher concentration of both catalytic metals in comparison to mycelium grown on malt media control. Similarly, *T. versicolor* mycelium also had significantly increased metal concentrations when grown on P3-SWCNT supplemented media in comparison to control despite the manufacture's chemical purification of the nanomaterials (see Table 2.2). Unfortunately, the methods used in this study are unable to determine whether *T. versicolor* accumulated catalytic metals when plated on minimal media due to insufficient mycelia for harvest.

Table 2.2 Concentration of SWCNT catalytic metals in *T. versicolor* hyphae grown on malt extract media (mean ± SD). Reported in mg metal/L digest after reflux of media plug or 10mg mycelia in 1.5mL of nitric acid (see methods section).

Nanomaterial	**Media [Ni]**	**Mycelia [Ni]**	**Media [Y]**	**Mycelia[Y]**
Control	<0.005	<0.005	<0.005	<0.005
AP-SWCNT	1.490±0.218	0.146±0.044	0.588±0.154	0.118±0.064
P3-SWCNT	0.079±0.029	0.007±0.001	0.018±0.009	0.006±0.001

As expected, the inclusion of unpurified AP-SWCNT in growth media greatly increased concentrations of nickel and yttrium in each media type compared to controls. The purified P2 and P3-SWCNTs, however, contribute significantly lower but still measurable quantities of the catalyst metals to the media (Figure 2.2). There was no significant difference in nickel concentrations between different media types when supplemented with the same nanomaterials, indicating that media type does not impact

mobilization of this metal into media and that the extraction method used can be consistently applied with both minimal and enriched media. The differences in yttrium concentrations between malt extract media containing AP-SWCNT when plated with *T. versicolor* or *P. tremellosa* suggests that under nutrient rich conditions *P. tremellosa* may have a role in sequestration of yttrium but no significant effect on nickel concentration of the media.

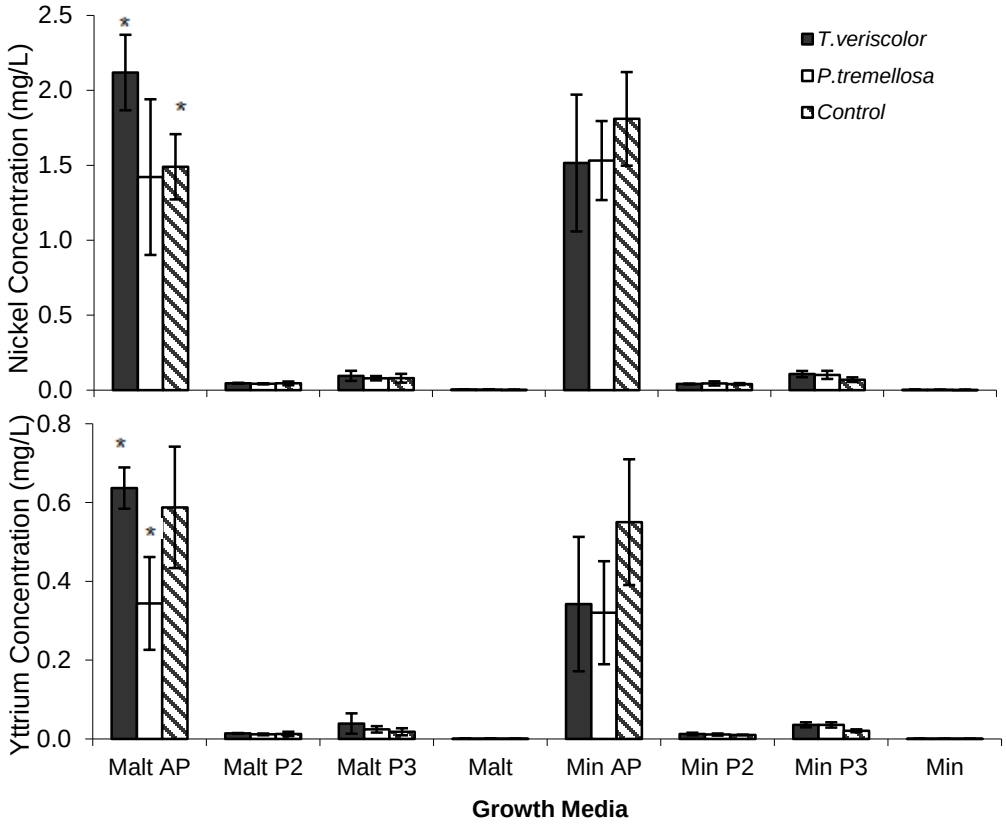

Figure 2.2 Concentrations of residual CNT catalyst metals in minimal and malt extract agar media containing AP, P2, or P3 SWCNTs for media plates inoculated with *T. versicolor and P. tremellosa*. Asterisks indicate significant difference between fungal treatments when grown on the same combination of SWCNT/media at $\alpha = 0.05$;no significant difference was found between any SWCNT/fungi combination grown on different media.

The effect of heavy metals on fungi have been widely studied, particularly in the context of fungal-based bioremediation processes, as environmental metal contamination frequently coincides with xenobiotic and organic wastes (Baldrian 2003). One such study of contaminated soil demonstrated that the white-rot fungi *Phanerochaete chrysosporium* and Pleurotus *pulmonarius* were able to colonize contaminated soil and degrade a variety of aromatic pollutants despite contamination with various heavy metals, including nickel (D'Annibale *et al.* 2005). In environments with significant concentrations of heavy metals, fungi often serve as major sinks of the metals (Gast *et al.* 1988; D'Annibale *et al.* 2005; Svoboda *et al.* 2006). The primary method of fungal accumulation of metal is sorption to fungal cell walls (Gabriel *et al.* 2001). With respect to the present study, sorption to fungal cell walls is the most likely mechanism of fungal uptake of catalytic metals, as the large physical size of SWCNT-bundles would prohibit the direct uptake of nanomaterials. Studies on the absorptive capacity of nickel by *T. versicolor* have found that the fungus is capable of significant nickel uptake and growth in a liquid media with nickel concentrations of up to 400 mg/L which is far below the concentrations of nickel found in the media of the present study (Yetis *et al.* 1998; Dilek *et al.* 2002).

Although the inclusion of these SWCNTs did not necessarily introduce toxic concentrations of catalytic metals into growth media, their concentrations may still be physiologically relevant. For example, morphological changes to basidiomycetes upon exposure to heavy metals has included increased density of mycelium as a result of more frequent branching and looping of hyphae (Darlington and Rauser 1988; Lilly *et al.*

1992). Additionally, a large number of fungi are found to produce both extracellular and cell-bound pigments in response to metal exposure (Gadd 1993; Baldrian 2003); these protective pigments include various melanins which are able to bind to and insolubilize metals (Fogarty and Tobin 1996). In previous studies, *T. versicolor* and the related *Trametes pubescens* were observed to produce a dark brown melanin pigment in response to heavy metal exposure, these same studies reported greater changes in morphology (hypothesized to indicate increased toxicity) in less complex media than in corresponding cultures grown in enriched media (Baldrian and Gabriel 1997; Galhaup and Haltrich 2001). In the present study, *T. versicolor* grown on minimal media containing AP-SWCNT were found to produce dark melanin-like pigments, which were easily observed by visual inspection (see Figure 2.3). These pigments were not produced by cultures grown with purified SWCNT suggesting a metal-induced response in this experiment, consistent with previous studies using this fungus. It is also worth noting that only the minimal media with AP-SWCNT treatment did not have confluent growth at the end of the study, all other treatments showed symmetric growth rings about the initial fungal plug. Melanin production and asymmetric growth highlight the high metabolic cost of mitigating environmental metal exposure (Gadd 1993; Baldrian 2003).

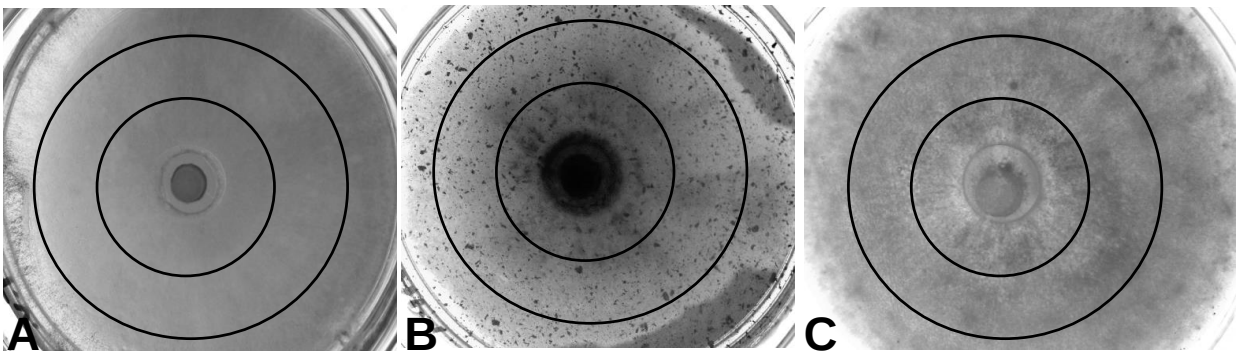

Figure 2.3 *T. Versicolor* colonies after one month growth on minimal media (A), minimal media with AP-SWCNT (B), and malt extract media with AP-SWCNT (C). Mycelia density is increased when grown on malt extract agar in comparison to minimal media; growth in the presence of AP-SWCNT is confluent on malt extract media (surface mycelia conceal SWCNT in media). *T. versicolor* cultured on minimal media with AP-SWCNT produced a dark pigment not found in cultures grown on other media types. Concentric circles indicate distance representing 25% (zone 1) and 75% (zone 2) of the distance between center of plate and plate wall.

2.4.2 Enzyme Activity

Differences in enzyme activity between cultures grown with and without SWCNT are presented in Figure 2.4. Inclusion of unpurified or carboxylated SWCNTs has a significant impact on the activity of oxidative enzymes produced by both tested fungi whereas purified, unfunctionalized SWCNTs have little impact on enzyme activity in either the malt or minimal media used in this experiment. Additionally, the inclusion of unpurified AP-SWCNT to malt extract agar resulted in significant increases in both the laccase and peroxidase activity of *T. versicolor* cultures while only laccase activity is elevated when AP-SWCNT is included in minimal media. Cultures of both species exposed to AP-SWCNT in minimal media also had significantly increased laccase production, while only *P. tremellosa* demonstrated increased peroxidase activity under

these conditions. These results are thought to reflect the differing nutrient requirements and substrate interactions important in controlling enzyme production by the two fungi. Similarly complex interactions between nutrient availability and the presence of aromatic compounds in media have been reported previously in white-rot fungi and were found to vary between fungal strains (Rogalski *et al.* 1991).

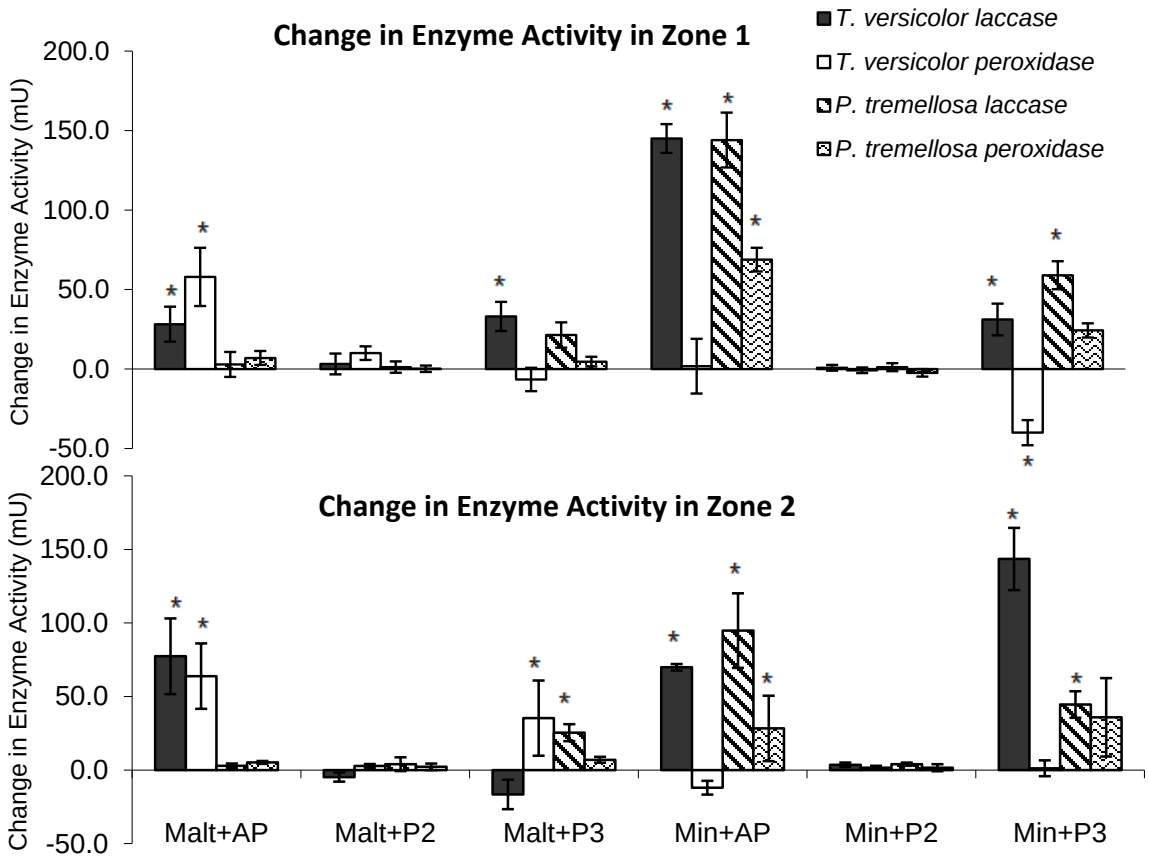

Figure 2.4 Differences in laccase and peroxidase activity in growth zones 1 (top) and 2 (bottom) in response to SWCNT inclusion in minimal and malt extract media containing AP, P2 or P3 SWCNTs inoculated with *T. versicolor* or *P. tremellosa*. Activity is reported in mU/mL liquid extract from media. Asterisks indicate a significant difference between SWCNT treatment and control as determined by student's T-test with $\alpha = 0.05$.

Melanin production by *T. versicolor* was also observed in the older hyphae of zone 1 when grown under nutrient limited conditions with AP-SWCNT (see Figure 2.3). The significant increase in laccase activity in this growth zone is consistent with the role played by oxidative enzymes in the formation of extracellular melanin in white-rot fungi (Bell and Wheeler 1986). Extracellular melanin can be produced by the oxidative degradation of phenolic compounds, either located in the environment or secreted by the fungus itself for that purpose. Similar responses have been demonstrated in other white-rot fungi in response to high metal concentrations; Galhaup et al. found that both laccase activity and melanin formation increased with copper concentration (Galhaup and Haltrich 2001).

Exposure to the purified and unfunctionalized P2-SWCNTs to either growth media did not significantly affect the enzymatic activity of either fungus, while the effect of inclusion of P3-SWCNT on enzyme activity was dependent on a combination of hyphal location and media composition. Specifically, in the presence of P3-SWCNT, *T. versicolor* peroxidase activity was suppressed in minimal media when sampled in zone 1, near the original fungal plug, but was not significantly altered when sampled distally in zone 2. In contrast, growth in the presence of P3-SWCNT on malt agar led to a significant increase in peroxidase activity of hyphae in zone 2. *T. versicolor* laccase activity was elevated with P3-SWCNT exposure in zone 1 on both media types and dramatically increased under minimal conditions when sampled in zone 2. As P2 and P3-SWCNT contain similar quantities of residual catalyst, the presence of metal is not likely to be the source of the elevated enzyme activity – the primary distinction between two SWCNTs is the inclusion

of carboxyl into the structure of P3-SWCNT as a result of carboxylic acid functionalization. This indicates that the carboxyl functional groups on P3-SWCNT directly induced oxidative enzyme activity and thus that functionalization may be a necessary condition for fungal-driven decomposition of CNT.

In contrast to *T. versicolor* peroxidase activity when grown on minimal media containing P3-SWCNT, *P. tremellosa* peroxidase activity was dramatically increased under these same conditions. Although *P. tremellosa* produces a compliment of manganese-independent peroxidases (Hatakka *et al.* 1992) which might be expected to limit the reliance of peroxidase activity on media Mn(II) availability, no difference was found in Mn(II) between media types. White-rot fungi are known to exhibit complex enzyme patterns and responses that are mediated by a variety of factors including media composition and age of the hyphae, both of which must be taken into account when evaluating enzymatic responses to SWCNT exposure (Hatakka 1994).

The results of the enzyme assays in this study indicate that the enzymatic response of white-rot fungi to SWCNT is complex and mediated not solely by fungal species, media composition, or substrate functionalization, but also by interaction between these factors (Table 2.3). Previous studies have demonstrated that the age of mycelium is important in determining enzyme activity; some species focus on enzymatic production during expansion while others have greater enzymatic activity once expansive growth has been completed and the fungi enters a secondary metabolic stage (Hatakka 1994). Decreased age of mycelia (by proxy of sampling from zone 2 rather than zone 1; Figure 2.3) was found to only interact with the variable of SWCNT addition

on *T. versicolor* laccase activity and of media type on *P. tremellosa* peroxidase activity (compare zones 1 and 2 on table 2.3). These findings suggest that the drivers of enzymatic response to SWCNT exposure may differ in less-mature mycelia between fungi, with *T. versicolor* enzyme production being controlled by media composition while *P. tremellosa* enzyme activity is more impacted by SWCNT characteristics.

Table 2.3 P values from two-way ANOVA on fungal enzyme activity to determine significance of media type and SWCNT addition. Bolded values indicate a significant effect (α=0.05).

	T. versicolor **laccase**	***T. versicolor*** **peroxidase**	***P. tremellosa*** **laccase**	***P. tremellosa*** **peroxidase**
Zone 1				
Media Type	**0.0048**	**<0.0001**	**<0.0001**	**<0.0001**
SWCNT	**<0.0001**	**<0.0001**	**<0.0001**	**<0.0001**
Media Type *SWCNT	**<0.0001**	0.0857	**<0.0001**	**<0.0001**
Zone 2				
Media Type	**<0.0001**	**0.0003**	**<0.0001**	0.0666
SWCNT	0.6262	**<0.0001**	**0.0014**	**0.0297**
Media Type *SWCNT	**<0.0001**	**0.0004**	**<0.0001**	0.3742

2.5 Implications of study in fungal/nanomaterial interactions

The patterns of enzyme activity outlined in this study offer valuable insights on the interactions between SWCNT surface chemistry, nutrient growth conditions, and type of saprotrophic fungi. As purified, carboxylated SWCNT resulted in increased activity of oxidative enzymes while purified but unfunctionalized analogs exhibited no change in activity it can be concluded that surface chemistry of the nanomaterial has a direct influence on fungal response to SWCNT. Contrary to our original hypothesis that nutrient rich media would allow for a more significant change in enzyme activity in response to functionalized SWCNT, we found oxidative enzyme activity to be diminished

when compared to nutrient poor growth conditions. This suppressed response may be a result of phenolic compounds in the malt extract media, which could bind to or help aggregate surface functionalized tubes, thus reducing effective exposure to the hyphae. Although some changes in enzyme activity in the AP-SWCNT treatments might be explained as an induction of enzyme production by metals and other impurities in the AP product, not all enzymatic responses can be considered a result of non-SWCNT factors. Specifically, the induction of oxidative enzyme activity by P3-SWCNT but not by the unfunctionalized and purified P2-SWCNT, nanomaterials which differ only in surface functionalization, indicates that the 1-3% carboxyl content of P3-SWCNT is the driver of the observed changes in enzyme activity.

Given the low concentration of residual metal catalysts measured in the growth media, we conclude that it is unlikely that the Ni/Y catalysts present in these SWCNTs were a significant source of cytotoxic interactions, though they may play an important role in the enzymatic response of some fungi towards SWCNTs. The observed elevation of oxidative enzyme activity when fungi were exposed to unpurified SWCNT and functionalized SWCNT stands in contrast to the lack of significant enzymatic response to purified, unfunctionalized SWCNT. This finding suggests that pristine SWCNT released in the environment would not promote a degradative response by saprotrophic fungi in soils. Although this study provides no direct evidence of SWCNT transformation by fungal oxidative enzymes, we have demonstrated for the first time that activity of oxidative enzymes in the laccase and peroxidase family are significantly impacted by exposure to certain formulations of SWCNT in pure cultures and in doing so

provide important context for future mechanistic studies of interactions between white-rot fungi and SWCNT.

2.6 Acknowledgements

The authors acknowledge support from the Environmental Protection Agency under award RD-83485801-0 and would like to thank Mr. Stephen Sassman and Mr. John McMillan for performing the ICP-MS analysis in this study and Ms. Laurie Mueller for her assistance in TEM analysis.

CHAPTER 3. FUNGAL INTERACTIONS WITH CARBON NANOTUBE COMPOSITES

3.1 Abstract

The exceptional physical and chemical resilience of carbon nanotubes (CNTs), combined with their light-weight and high aspect ratios make them promising fillers for next generation composite materials. Despite growing production capacity and demand for composites of CNT, very little is known about how these composites degrade or are otherwise transformed in the environment. In the previous study (CHAPTER TWO) we demonstrated a significant enzymatic response by the white-rot fungi *T. versicolor* to surface functionalized single-walled carbon nanomaterials. In the present study we discuss the results of a 60 day incubation of *T. versicolor* with thin wafers of CNT-chitosan and CNT-polycaprolactone (PCL) composites. We report no significant changes in the activity of either laccase or peroxidase produced by the fungi when incubated with CNT-PCL composites. CNT-chitosan composites, however, resulted in an apparent decrease in fungal laccase activity. Incubation of both CNT-chitosan and CNT-PCL wafers on growth media resulted in significant changes in both FTIR and XPS spectra as compared to the initial composites. However, these changes from the initial proved to be identical between fungal and non-fungal control treatments and were ascribed to alterations due to interaction with the growth media or exposure to air.

Although the results of the composite experiments were equivocal, when contrasted with the results of CHAPTER TWO, it further highlights the importance of accessibility to CNT surfaces as a driver of the microbial response to these materials.

3.2 Introduction

With easily modifiable surface-chemistry, exceptional tensile strength, and a high surface area to volume ratio, carbon nanotubes (CNT) have a wide variety of applications including microelectronics, drug delivery platforms, and light-weight, wear-resistant materials (Georgakilas *et al.* 2002). Despite the incredible potential of CNTs, their tendency to form large aggregates as a result of Van Der Waals interactions between tubes frequently results in an unstable suspension (Thess *et al.* 1996) that limits their use in applications which require an even distribution of CNTs (Capek 2009). The formation of large aggregates by CNT has important implications in the use of CNT-containing products for biological uses as a number of previous studies report that increased aggregated size corresponds to increased cytotoxicity to a variety of cell types (Handy *et al.* 2008; Pasquini *et al.* 2012). In order for CNT to be used successfully in these applications the tendency to homoaggregate must be overcome and the CNTs dispersed. Covalently functionalizing CNT to make them less hydrophobic is popular in a number of applications, however to achieve useful dispersal larger CNTs may require significant functionalization. Covalent surface functionalization of CNT is not always suitable however, as extensive functionalization disrupts the distributed π-bonding networks responsible for the conductive properties of some CNTs (Ausman *et al.* 2000). Other approaches to prevent aggregation include dispersal in specialized solvents

(Ausman *et al.* 2000) and/or polymeric substances (Star and Stoddart 2002) that disrupt Van Der Waals interactions and encourage aggregate stability. These approaches may be used in combination; in applications requiring well-dispersed nanomaterials for structural or conductive purposes, deposition of slightly functionalized CNTs suspended in stabilizing polymers to form nanocomposites is an attractive solution (Wang and Keddie 2009). As a result of nanomaterial inclusion, polymer nanocomposites often have superior mechanical, electrical, and thermal properties than polymer composites with more traditional filler materials (Wang and Keddie 2009). These properties make CNT nanocomposites promising materials for use in next-generation packaging (Lopacka 2013), data storage, electronic displays, biosensors, and other microelectronic applications (Avouris 2002; Zhang *et al.* 2016).

Although an increasingly active area of research, there are relatively few studies exploring the environmental impact and fate of nanomaterials, especially when included in composites. Studies investigating the interactions of carbon nanomaterials with microorganisms have found that toxicity and degradation of nanomaterials depend on complex factors such as nanomaterial morphology and functionalization, for example the oxidative enzyme horseradish peroxidase is able to more quickly degrade carboxylic acid functionalized CNT than similar pristine CNT (Allen *et al.* 2008; Zhao *et al.* 2011).

While developing an understanding of microbial interactions with free CNTs (as highlighted in CHAPTERS ONE and TWO) is important in assessing their environment impacts, the inclusion of nanomaterials as fillers in polymer composites is likely to complicate their transformation in the environment and is projected to be a major use

of these materials in industry. As CNT surface chemistry appears to be an important factor in initiating an enzymatic response to these materials (Berry *et al.* 2014) inclusion in nanocomposites is expected to limit biological interactions by occluding the surface of the CNTs. A decrease in exposed surface area can also be expected to result in a significantly different response from degradative microorganisms that are challenged with CNT nanocomposites than would be in exposed to nanomaterials alone.

In this chapter the results from a study investigating the enzymatic response of the model white-rot fungus *Trametes versicolor* towards CNT containing nanocomposites are presented. Wood-decay fungi such as *T. versicolor* possess a number of powerful oxidative enzymes to facilitate the degradation of natural highly condensed substances such as lignin (Leonowicz *et al.* 1999). The fungi can also degrade a variety of highly condensed xenobiotics including dyes, coal residues, and polyaromatic hydrocarbons (Ollikka *et al.* 1993; Gramss *et al.* 1999; Hofrichter *et al.* 1999). Previous studies from this research group have highlighted the important role of nanomaterial surface chemistry in the enzymatic response of saprotrophic fungi. In laboratory incubations, pure cultures of white-rot fungi were found to enzymatically bleach surface oxidized C_{60} fullerols but not their unfunctionalized fullerene analogs (Schreiner *et al.* 2009). The importance of surface chemistry is further demonstrated by a study that links increased oxidative enzyme activity to the presence of CNT in fungal growth media only when nanomaterial surfaces have functionalized with carboxylic acid (Berry *et al.* 2014). Because CNT included in CNT-Composites little exposed surface area, we hypothesize that there will be limited enzymatic activity towards the

nanomaterial filler in these composites. After long term exposure however, fungal enzymes might be expected to 'weather' the polymer component of the nanocomposites enough to expose carbon nanomaterials, as has been previously demonstrated *in vitro* with PCL coated nanotubes (Zeng *et al.* 2006).

3.3 Materials and Methods

3.3.1 Nanotube composite synthesis

To prepare CNT/chitosan nanocomposites, a 20 mg/mL aqueous stock solution of chitosan (MW 20,000; Sigma-Aldrich, St. Louis, MO, USA) in 2% v/v acetic acid (Thermo Fisher Scientific, Waltham, MA, USA) was stirred and heated at 50 °C for approximately four hours. Surface oxygenated single-walled carbon nanotubes (SWCNT; Carbon Solutions Inc., Riverside, CA, USA) or similarly functionalized multi-walled carbon nanotubes (MWCNT, Nanocyl, Auvelais, BE) were weighed separately and added to the chitosan stock solution to produce 0.1 % and 1 % w/w mixtures (refer to Table 3.1 for CNT characteristics). Each mixture was then sonicated for 4 hours with frequent stirring to produce stabile suspension of CNT and chitosan macromolecules. Following sonication, the suspension was centrifuged at 4000 rpm to remove any aggregates. The wafers were cast by transferring 5 mL of each suspension into aluminum dishes (44 mm diameter, 12.5 mm height) for drying overnight. Finally the wafers were soaked in a 1 M NaOH bath for 1 hour to remove excess acetic acid and washed thoroughly with deionized water.

To produce PCL nanocomposites ethylcellulose was used as a natural, biocompatible surfactant at a ratio of 2:1 ethylcellulose to MWCNT (described above).

Ethylcellulose (0.2 % and 2 %) and MWCNT (0.1 % and 1 %) were added to 40 mL tetrahydrofuran and sonicated for four hours with frequent stirring to produce a stable CNT and ethylcellulose suspension. Following sonication, polycaprolactone (Sigma-Aldrich, 0.1 % and 1 % w/w) was added to the appropriate suspension to produce suspensions with a final ethylcellulose to MWCNT to PCL ratio of 2:1:1. This suspension was sonicated for 2 hours and cast in aluminum dishes as above. Dishes were soaked in DI water to facilitate removal of PCL nanocomposites wafers.

Table 3.1 Characteristics of CNT included in polymer composites. NC7000 were oxygenated by HNO_3 reflux for 5 hours at 110 °C before purification by filtration and inclusion in composites.

CNT Type	CNT Walls	Synthesis Method	Surface Oxygen (%)	Average Length (µm)	Average Diameter (nm)
P3-CNT	Single	Electric Arc	3	1	1.4
NC7000	Multiple	Chemical Vapor Deposition	4	1.5	9.5

3.3.2 Fungal inoculation experiments

Plates containing malt extract agar (2 % w/w; VWR LLC., Randor, PE, USA) were inoculated in the center with *T. versicolor* (strain MAD697-R). Two pieces of nanomaterial composite wafer were placed 2 cm away from the inoculating plug on either side (Figure 3.1). Because the nanomaterial composite wafers used in this study did not remain intact through autoclaving, they were sterilized by bathing in ethanol for 30 minutes before being air-dried under sterile conditions. An additional complication arose with the lignin-MWCNT composites as they immediately dissolved when placed on

the growth media and over the course of the incubation diffused throughout the plate. Both inoculated and no fungi control plates were incubated in darkness at 23 °C for 60 days.

3.3.3 Oxidative enzyme assays

Oxidative enzymes were extracted from growth media and assayed using a modification of the methods presented in (Heinonsalo *et al.* 2012). Briefly, two 8 mm circular plugs were taken from each plate at sampling positions near or away from the location of the nanomaterial composites (see Figure 3.1). Agar plugs for each treatment and sampling location were then loaded into 0.45 µm cellulose acetate membrane filtered microcentrifuge tubes (Costar Spin-X, Corning Inc., Corning, NY, USA) and centrifuged at room temperature and 15,700 g for 30 minutes.

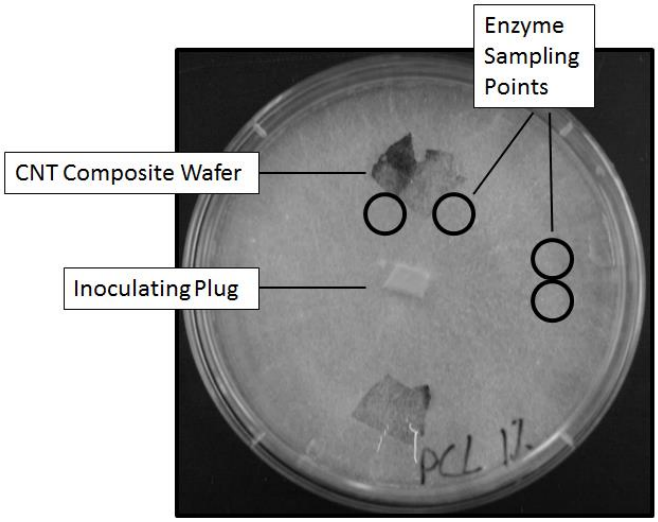

Figure 3.1 Schematic of fungal incubation plates with locations of enzyme sampling indicated

The activity of laccase and peroxidase enzymes in the resulting supernatant was determined in a coupled colorimetric assay utilizing 2,2'-azino-bis(3-

ethylbenzothiazoline-6-sulphonate) (ABTS) as a substrate. Each milliliter of reaction solution contained 50 mM sodium malonate (at pH = 4.5), 0.5 mM $MnSO_4$, 1.0 mM ABTS, and 0.1 mM H_2O_2 - to be added following an initial measurement (Sigma-Aldrich). The entire volume of liquid extracted from each tube (~200 µL) was added to the reaction solution and laccase activity was measured by absorbance at 420 nm after 20 seconds. H_2O_2 was then added to serve as a peroxidase substrate, and absorbance was measured again after an additional 20 seconds. Enzyme activity was quantified against a standard curve prepared by reacting purified laccase of known activity from *T. versicolor* with the reaction solution.

3.3.4 Nanomaterial composite surface characterization

ATR-FTIR was used to qualitatively determine the change in functional group distribution before and after fungal degradation of wafers using a Thermo Scientific Nicolet iS5 ATR-IR (500 scans) with a diamond crystal and a dTGS room-temperature detector (< 0.8 cm^{-1} resolution). Analysis was carried out on 2-4 spots of the wafers. X-ray photoelectron spectroscopy (XPS) was used to assess the peak shape changes in the C(1s) and N(1s) regions after wafers had been exposed to *T. versicolor*. The C(1s) region was too difficult to deconvolute due to the many oxidized carbon environments in the chitosan molecular structure, but the N(1s) region could be more easily used to assess transformations due to a less complex nitrogen environment. Analysis was carried out on 2-4 spots of the wafers using a PHI 5600 XPS system (P_{base} < $5x10^{-9}$ Torr) with Mg Kα X-rays (1253.6 eV, 15 kV, 300 W). An electron energy analyzer operating at a constant pass energy of 58.7 eV collected a spot size of approximately 800 x 2000 μm^2 at a rate of

0.125 eV/step (50 ms/step). Data was processed using CasaXPS (Casa Software Ltd., UK). All spectra were energy-adjusted to 284.5 eV using the C(1s) region and given a Shirley background. Peak-fitting of the N(1s) region was carried out using the same full-width at half max (FWHM) for both nitrogen components to determine the percentage of oxidized nitrogen present relative to the total nitrogen peak area.

3.3.5 Statistical analysis

Differences in enzymatic activity between plates containing nanomaterial composites and controls were assessed by one-way ANOVA with a Tukey HSD post-hoc test. After initial analysis determined that enzyme activity was not significantly different between sampling locations, activities were pooled together for a given nanocomposite treatment. Statistical analysis was performed with JMP 8 (v8.0.2.0 SAS Institute, Cary, NC, USA) with significance set for $\alpha = 0.05$ and marginal significance set at $\alpha = 0.10$ respectively.

3.4 Results and Discussion

3.4.1 Fungal growth and oxidative enzyme activity

Over the course of the 60 day incubation, *T. versicolor* exhibited confluent growth in all treatments, with the exception of the surfaces covered by chitosan containing nanocomposite wafers (see Figure 3.2). The inability of the fungi to grow over these wafers was not dependent on CNT loading as the CNT-free chitosan wafers were also found to be free of fungal hyphae after 60 days. This observation is consistent with a number of studies that have demonstrated the broad-spectrum anti-microbial activity of chitosan and its derivatives (Rabea *et al.* 2003; Kong *et al.* 2010), particularly

against fungi such as *T. versicolor* that do not contain chitosan as a cell-wall component *(Allan and Hadwiger 1979).*

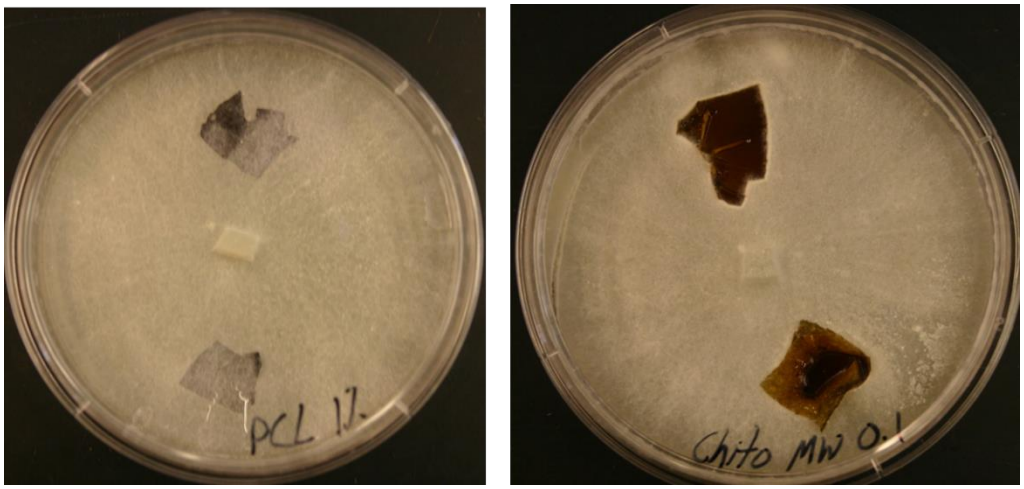

Figure 3.2 Fungal growth on plates containing PCL/MWCNT composites (left) and chitosan/MWCNT composites (right) after 60 days of incubation. Note the growth of white fungal hyphae across the surface of the PCL, but not chitosan composite surface. Also noteworthy is the presence of transparent sections on the chitosan composite wafer.

The activity of extracellular oxidative enzymes in the laccase and peroxidase families was measured following the incubation period (Figure 3.3). Fungal growth media was sampled near and away from composite wafers in order to capture any spatial heterogeneity in enzyme production (refer to Figure 3.1). Enzyme activity was not found to vary between sampling locations for any treatment, indicating that any enzymatic response to the wafers is broadly distributed throughout the hyphal network. Activity could not be assayed in plates containing lignin/MWCNT composite wafers due to the dissolution of the wafers on contact with growth media. The diffusion of the lignin throughout the media resulted in a high background absorbance at 420 nm which prevented consistent measurement of oxidized ABTS for these treatments.

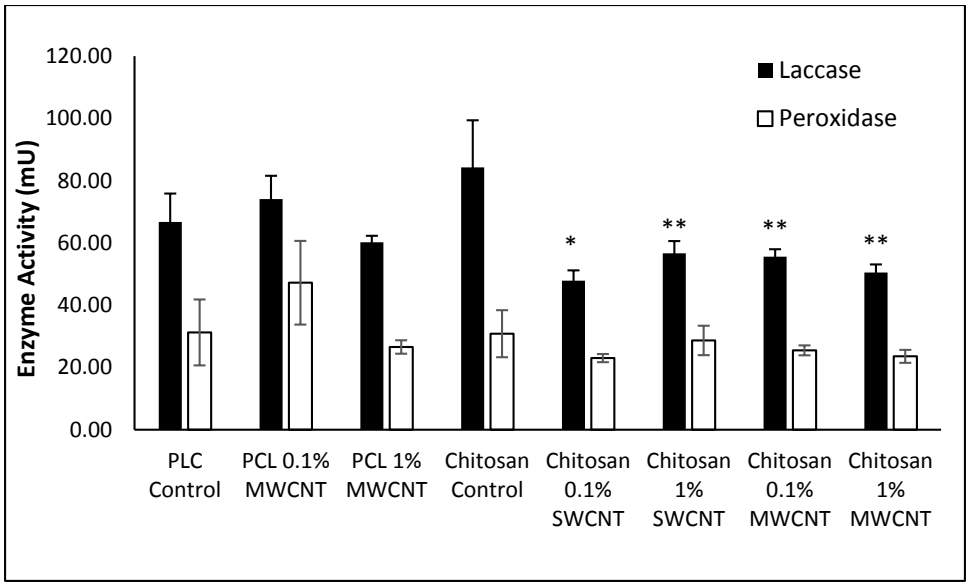

Figure 3.3 Activity of extracellular oxidative enzymes produced by fungi after 60 days of incubation on media containing CNT composite wafers. Asterisks indicate significant differences (*, α = 0.05; **; α = 0.10) between plates containing a CNT composite and the corresponding CNT-free controls. Error bars represent standard error.

The oxidative enzyme activity of *T. versicolor* in plates containing PCL/CNT wafers did not significantly differ from PCL only controls. This finding contrasts with that from our previous study using free CNT and the same fungi, which demonstrated a significant enzymatic response as a result of fungal exposure to surface oxygenated CNT (Berry *et al.* 2014). These results are consistent with a nanocomposites in which CNT are completed embedded with copolymer, preventing surface interactions with the fungi. Indeed, SEM analysis of a PCL/MWCNT wafer surface demonstrates that the CNT are not exposed on the surface (Figure 3.4). Although PCL is often considered to be biodegradable (Shimao 2001; Zeng *et al.* 2006) and is readily broken down by a variety of common microorganisms, basidiomycetes such as *T. versicolor* have not been observed to do so (Kim and Rhee 2003).

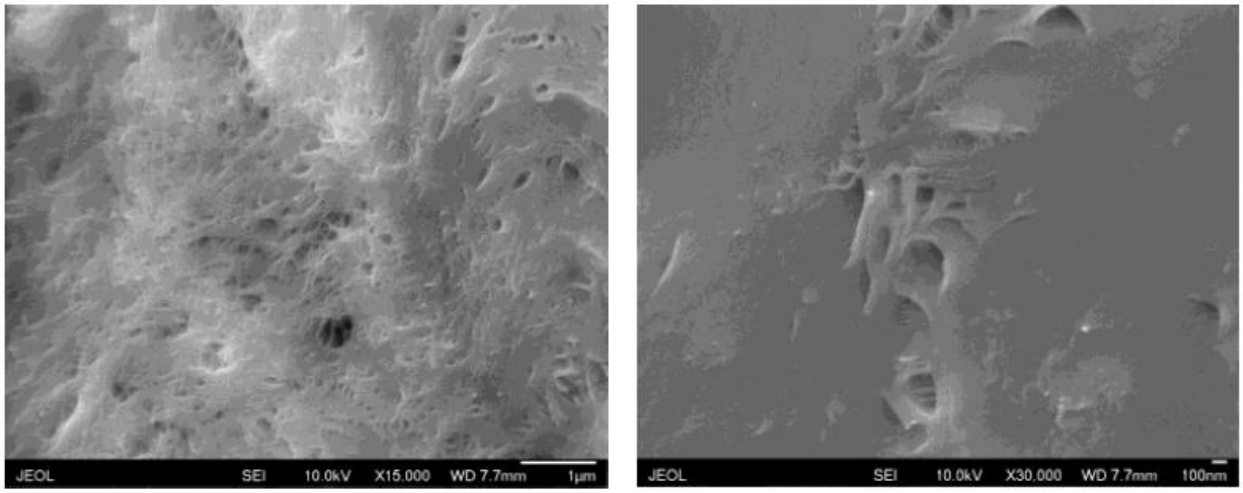

Figure 3.4 Scanning electron micrographs of PCL nanocomposites with a 1% MWCNT loading at 15,000 and 30,000X magnification. Note that although the surface is heterogeneous there is no indication of MWCNT bundles or aggregates on the wafer surface.

In contrast to the PCL/MWCNT composites, fungal exposure to both Chitosan/SWCNT and Chitosan/MWCNT composites resulted in significant changes in laccase activity ($p \leq 0.05$ in chitosan wafers containing 0.1 % SWCNT, $p \leq 0.1$ in chitosan wafers containing 1 % SWCNT, 0.1 % MWCNT, and 1 % MWCNT). Interestingly, the inclusion CNT in chitosan composites decreased, rather than increased the apparent activity of fungal laccases. Increased laccase activity by *T. versicolor* in response to chitosan exposure is not unexpected, and has been previously documented (Adekunle *et al.* 2015) though it is important to note that *T. versicolor* has not been found to be able to actually depolymerize chitosan directly. A decrease in extracellular enzymatic activity in a system typically reflects a change in nutrient acquisition strategies or sorption/inactivation of the enzymes by some environmental component. However, as with PCL/CNT composites, SEM characterization of the chitosan/CNT surface found no

evidence of exposed CNT surfaces making direct sorption or inhibition of enzymes by CNT unlikely (Figure 3.4). The apparent decrease in laccase activity observed in this study then cannot be directly attributed to fungal interactions with CNTs and may instead reflect the interactions between the extracellular enzymes and the surface structure of the chitosan polymer surface which has been altered by the presence of CNT deeper within the composite wafer.

3.4.2 CNT composite surface characterization

CNT composite wafers were characterized with XPS and ATR-FTIR before and after exposure to *T. versicolor* to assess any transformations that had occurred as a result of exposure to the fungus. In wafers containing only PCL, there was no change in functional group distribution in the infrared spectrum aside from a small hydroxyl band growing in around 3300 cm^{-1} (not shown). Although this could indicate the occurrence of PCL chain scission or further oxidation, the presence of a strong hydroxyl band in the spectra of the underlying growth media makes the origin of this feature ambiguous. The same hydroxyl band was present in PCL wafers containing 0.1 % MWCNT but this band was not observed in wafers with a 1 % MWCNT loading, though the significant of this finding is unclear given the possibility of contamination by the growth media signal.

Surface analysis of chitosan wafers showed significant functional group changes with ATR-FTIR (Figure 3.5). In particular, the doublet feature of the amine group (NH_2 stretch, 3400 and 3300 cm^{-1}), which overlaps with the broad hydroxyl band in this region, is lost following incubation. Following incubation, the hydroxyl band itself is also observed to decrease in intensity. Additionally, the carbonyl feature at 1650 cm^{-1}

increases in intensity and shifts slightly towards lower wavenumbers. The C-H bending modes between 1300-1500 cm^{-1} also show a decrease in wavenumber after incubation, which is more typical of a CH_3 stretch. The C-H stretching around 2950 cm^{-1} also shows a change after incubation. These same changes, however, were present in the no-fungi nanocomposite treatments, indicating that these spectral features cannot be ascribed to fungal chemistry.

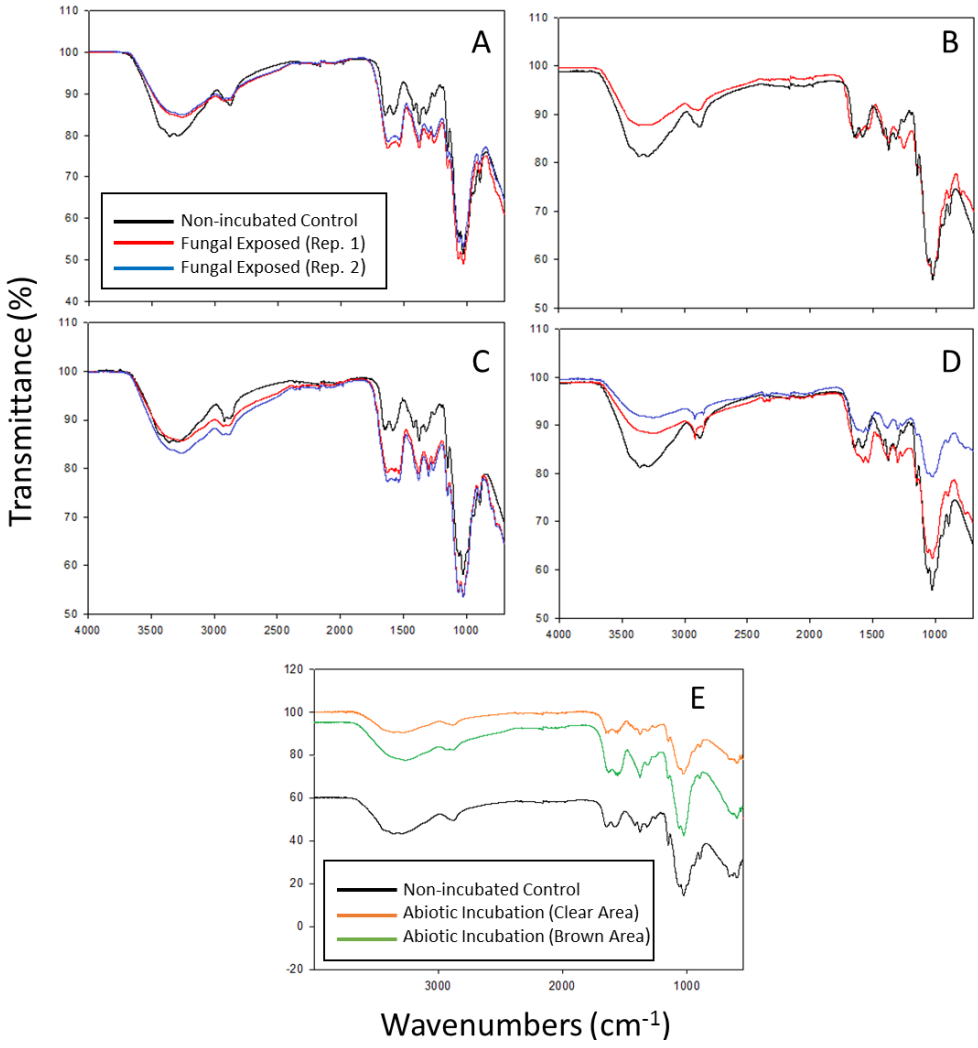

Figure 3.5 ATR-FTIR spectra of Chitosan CNT composites before (black trace) and after (blue and red traces) incubation with fungi. (A) 0.1% MWCNT, (B) 1% MWCNT (C) 0.1% SWCNT, (D) 1% SWCNT, (E) Abiotic chitosan composite controls

XPS analysis of the chitosan before and after incubation showed changes in the C(1s) and N(1s) regions but these changes were present regardless of the presence of fungi. The C(1s) region was not chosen to track any changes in the chitosan structure as a result of fungal degradation, as the region contained a large number of oxidized carbon environments due to the nature of the chitosan molecular structure. The N(1s) region, however, provided clearer and consistent peak shapes that facilitated the interpretation of chitosan structural changes following incubation (Figure 3.6). The pristine chitosan samples exhibit a nitrogen peak centered on 398 eV. In contrast, the incubated samples had an additional peak present at 400 eV. In XPS, features at higher binding energies typically indicate a more highly oxidized atomic environment. This second feature is consistent with an amide nitrogen atom in a more oxidized state than the original amine nitrogen, though other processes such as protonation of chitosan amines can cause similar effects. The peak at 400 eV contributed 28 ± 2 % to total N(1s) area in chitosan only wafers following incubation compared to only 4 % in the non-incubated control wafers. There were no significant differences in the N(1s) region for chitosan wafers containing either SWCNT or MWCNT and the control either before or after incubation. Interestingly, XPS analysis of the dark brown and transparent yellow sections of chitosan wafers revealed significant differences in relative contribution of the at 400 eV peak N(1s) region. In the transparent regions of the wafer this peak contributed ~18 % of the N while in the dark brown regions it comprised ~38 %. Overall these analyses indicate that there were no observable chemical changes to either

control or CNT composite wafers due to the presence of fungi in any of the incubation treatments.

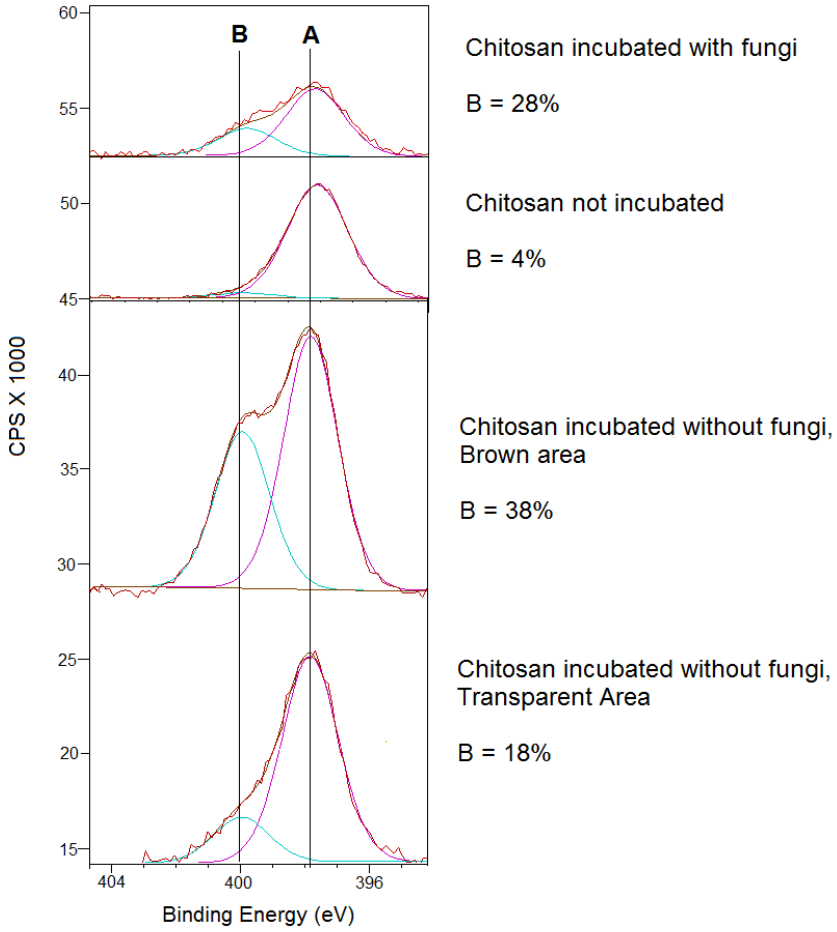

Figure 3.6 XPS spectra of chitosan wafer N (1s) region. Lines A and B indicate approximate peak centers of amine nitrogen and the nitrogen feature that developed during incubation, respectively. Neither the presence of fungi or CNT inclusion (not shown) significantly impacted the spectra in the N (1s) region.

3.5 Conclusions

In contrast to previous studies investigating the transformation of CNT and CNT composites by microorganisms we found little evidence of differential enzymatic activity or composite degradation as a result of the presence of CNT in the composites. The

notable exception to this was a decrease in laccase activity in plates containing CNT-chitosan composites. This decrease in fungal laccase activity upon exposure to CNT-chitosan composites is noteworthy, because our surface chemical characterization of the composites found no significant differences in composite surface chemistry, thus no causal link between fungal enzyme activity and surface chemistry can be made. The use of the white-rot fungi *T. versicolor* in this study was based in part on the observed increase in the fungi's oxidative enzyme activity following exposure to functionalized but free SWCNT previously observed in CHAPTER 2 (Berry *et al.* 2014) The lack of response of *T. versicolor* to is likely the result of the fungus being unable to sufficiently decompose either the chitosan or PCL copolymers to expose the CNT surfaces.

3.6 Acknowledgements

This work was made possible by funding from the Environmental Protection Agency under award RD-83485801-0. The author thanks collaborators D. G. Goodwin and D. H. Fairbrother whose significant material and analytical contributions were vital to the study.

CHAPTER 4. SOIL MICROBIAL RESPONSE TO PHOTO-DEGRADED C_{60} FULLERENES

4.1 Abstract

Recent studies indicate that while unfunctionalized carbon nanomaterials (CNMs) exhibit very low decomposition rates in soils, even minor surface functionalization (e.g., as a result of photochemical weathering) may accelerate microbial decay. We present results from a 90-day laboratory soil incubation of ^{13}C-labeled photo-oxidized C_{60} that investigated the potential link between photochemical and microbial degradation. Irradiating aqueous C_{60} with solar-wavelength light resulted in a complex mixture of intermediate products with decreased aromaticity. Although irradiated C_{60} had little effect on respiration rates in soil microcosms after one week of incubation, excess ^{13}C in the respired CO_2 demonstrates that irradiating C_{60} for 60 days enhanced its degradation in soil, with ~0.78 % of the C_{60} mineralized. Community analysis by DGGE found that soil microbial community structure was altered and depended on the photo-treatment duration. These findings demonstrate how abiotic and biotic transformation processes can couple to influence degradation of CNMs in the natural environment.

4.2 Introduction

Since the discovery of the first fullerenes in 1985, manufactured carbon nanomaterials (CNMs) have resulted in significant material advances in the fields of bioengineering and microelectronics (Kroto *et al.* 1985). These nanoscale materials, with a rigid framework composed entirely of condensed aromatic carbon rings, can be found in many geometric configurations ranging from planar graphene sheets to spherical buckminsterfullerene (C_{60} fullerene) and can be chemically modified to generate a wide variety of carbon nanomaterials (Nakamura and Isobe 2003). The small size and high surface area of these nanomaterials makes them attractive components in a variety of applications ranging from drug delivery to inclusion in next-generation photovoltaic panels (Mwaura *et al.* 2005; Bakry *et al.* 2007; Thompson and Frechet 2008). In recent years, CNMs have become increasingly prevalent in manufacturing due to their robust physical properties, variety of available chemical modifications, and the versatility that these modifications confer on electrical and biological interactions (Guldi and Asmus 1997). Despite these advances in the synthesis and application of carbon nanomaterials, little is still known about the fate of CNMs that might enter the environment following accidental release, disposal in landfills, or accumulation in biosolids (Westerhoff *et al.* 2013). The same highly condensed structure that makes nanomaterials ideal as structural components makes them relatively resistant to biodegradation. As a result of this environmental recalcitrance, nanomaterials have the potential to accumulate in soils and sediments following environmental releases (Batley *et al.* 2013).

Recent work has illustrated a wide range of interactions and reactions of CNMs in the environment which occur as a result of physiochemical properties (e.g., particle size, surface functionalization, metal content, etc.). For example, the surface functionalization of CNMs has been found to play a particularly significant role in the stability of CNM homo-aggregates in suspension and thus their solubility, as the aggregation of CNM into clusters predictably results in flocculation (Smith *et al.* 2009; Batley *et al.* 2013). The formation of aggregates renders long-term suspensions of nanomaterials in aqueous environments unlikely unless they are stabilized by interaction with other environmental compounds such as dissolved organic matter. In the absence of such stabilizers, however, CNMs can be expected to partition into sediments (Handy *et al.* 2008). Recent studies on the movement of CNMs through soil columns have found that C_{60} exhibits greater transport than single walled nanotubes (Jaisi and Elimelech 2009). Transport of nanotubes through soil was also found to increase with soil pore-size (Kasel *et al.* 2013). These studies highlight the importance of properties such as nanomaterial cluster size and aspect-ratio in controlling environmental interactions.

Physiochemical properties of CNMs are dependent on the degree and type of functionalization, with functionalization often intended at synthesis, but also occurring upon exposure to different natural environmental conditions; for example, in aqueous environments C_{60} is able to undergo a wide variety of chemical transformations that can alter its molecular properties and eventual fate (Taylor and Walton 1993; Klaine *et al.* 2008). Photo-transformation of C_{60} in aqueous environments is one such example.

Exposure of nC_{60} clusters to both short-wavelength (Hou and Jafvert 2009) and long-wavelength (Hou *et al.* 2010) visible light has been reported to result in decreased cluster size and increased water solubility as the surface of the C_{60} is progressively modified to include oxygen containing functional groups (Hou *et al.* 2010). This functionalization of C_{60} is thought to be the result of carbon oxidation by reactive oxygen species (ROS) such as singlet oxygen ($^1O_2$), which is also produced upon light exposure to C_{60}. Hou et al. (2009) reported that transformation of nC_{60} clusters into more water soluble C_{60}-derivatives increased in rate, alongside ROS production as the duration of exposure to solar spectrum light was increased (Hou and Jafvert 2009). These findings are similar to those reported in a recent study in which aqueous suspensions of graphene oxide were found to produce superoxide anion ($O_2^{\cdot-}$) upon exposure to solar light, resulting in alteration of surface defects (Zhao and Jafvert 2015), demonstrating that abiotic transformation of CNMs is not limited to C_{60} alone.

Transformation reactions of CNMs fundamentally alter their stability in soil and aquatic systems, which in turn controls the interactions between CNMs and microorganisms. Lyon *et al.* (2005) found that, although C_{60} had an antibacterial effect on cultures of *Eschericia coli* and *Bacillus subtilis* when grown on low-salt media, this effect was diminished when using media with a higher salt content, likely due to greater aggregation of C_{60} under this condition (Lyon *et al.* 2005). In agreement with these findings, an additional study on the relationship between CNM particle size and cytotoxicity found that particle size and antibacterial activity were inversely related (Lyon *et al.* 2006). Studies on microbial-nanomaterial interactions in more complex

substrates, such as soils and sediments, have provided additional insights on the interactions between microbial populations, CNM physiochemical properties, and the environment in which the interactions takes place. For example, Li *et al.* (2008) found that sorption of C_{60} to organic matter in soil pore water diminished the antimicrobial activity of nC_{60} clusters (Li *et al.* 2008). This finding helps to explain the observed toxicity of C_{60} fullerenes on defined media but the apparent inability of nC_{60} clusters to significantly impact the structure or the function of microbial communities in soils (Tong *et al.* 2007) or sediments (Nyberg *et al.* 2008).

Few studies have examined how nanomaterial surface chemistry might control the activity of extracellular degradative enzymes (that may have the potential to degrade CNMs) produced by soil microorganisms. Although studies on unfunctionalized C_{60} in soils have found little evidence of mineralization or induction of enzymatic activity (Tong *et al.* 2007), there are a number of cell-free enzyme studies that demonstrate the increased activity of oxidative enzymes such as horseradish peroxidase against other functionalized CNMs (Allen *et al.* 2008; Zhao *et al.* 2011). Schreiner *et al.* (2009) reported enzymatic bleaching and oxidative degradation of manufactured C_{60} fullerols by cultures of the white-rot fungi *Trametes versicolor* and *Phlebia tremellosa* (Schreiner *et al.* 2009). In Berry *et al.* (2014) we reported the induction of oxidative enzymes by these fungi in the presence of carboxyl-functionalized single-walled carbon nanotubes (SWCNT) but not by unfunctionalized SWCNT (Berry *et al.* 2014). These studies suggest that biotic transformation and/or degradation of CNMs requires at least some degree of surface functionalization to facilitate enzymatic interactions. In an environmental

context for C_{60}, this functionalization might be achieved by abiotic transformation by photo-exposure, suggesting the importance of coupled abiotic/biotic mechanisms for the degradation/mineralization of this particular CNM.

In this study we investigated the hypothesis that exposure of C_{60} to solar wavelength light will transform it into intermediate products that are more conducive to degradation by soil microorganisms. We utilized a stable isotope mass balance approach to trace the fate of light irradiated ^{13}C enriched C_{60} in laboratory soil microcosms. The use of isotopically labelled C_{60} enabled us to determine the extent to which the abiotic transformation increased subsequent microbial oxidation in soil by measuring ^{13}C abundance in the respired CO_2. Additionally, the impact of the light irradiated C_{60} photoproducts on soil microbial communities was assessed through denaturing gradient gel electrophoresis (DGGE) analysis. As an important component of soil health (Garbeva *et al.* 2004), the ability of the C_{60} photoproducts to affect soil microbial diversity has important implications in assessing the overall environmental implications posed by this material.

4.3 Materials and Methods

4.3.1 Fullerene Preparations

To prepare 5 atom% ^{13}C C_{60} clusters, highly ^{13}C enriched C_{60} (> 99 % pure C_{60}, as per manufacturer; MER Corp., Tucson, AZ, USA) and unlabeled sublimed C_{60} (99.9 %, per manufacturer; MER Corp., USA) were combined, finely mixed, and added to ultra-pure water to achieve a final concentration of 3.3 g/L C_{60}. The resulting slurry was bath sonicated overnight before mixing in the dark on an elliptical motion shaker for 6

months at 60 revolutions/minute to insure even distribution of $^{13}C_{60}$ within the slurry. Following this mixing period the fullerene slurry was divided into 600 µL aliquots (each containing 2 mg C_{60}) and placed in sterilized 12 mL borosilicate glass vials (LabCo, High Wycombe, Buckinghamshire, UK). Sealed vials were then placed in a rotary carousel and irradiated in a Rayonet RPR-100 photochemical reactor (Southern New England Ultraviolet Company, USA) containing 16 black-light phosphor lamps (24 Watt, wavelength range: 300-410 nm) for 10, 30, or 60 days. Light intensity inside the reactor was determined to be 1.6×10^{-4} einstein$\cdot L^{-1}s^{-1}$ using the chemical actinometer potassium ferrioxalate. Non-irradiated C_{60} (i.e., 'pristine' controls) were prepared by wrapping vials in aluminum foil and incubating them in the dark.

A parallel irradiation experiment was performed using unlabeled and sublimed MER C_{60} in order to produce photo-decomposition products for intermediate product characterization, rather than for generation of microcosm feedstock material. The C_{60} concentration in the aqueous suspension used in this experiment was 12.8 mg/L. Light irradiation occurred under identical lamp and mixing conditions as described above and irradiated and control (non-irradiated) vials were removed and extracted for analysis on days 5 and 10 (UV-Vis) or 15 (HPLC) .

4.3.2 Fullerene Characterization

C_{60} starting materials and 5 and 15-day samples were characterized using HPLC after toluene-salt extraction. Specifically, 3 mL of aqueous nC_{60} clusters, 3 mL toluene, and 1.2 mL 0.1 M $Mg(ClO_4)_2$ were combined in a 15 mL glass centrifuge tube and gently

shaken overnight to extract C_{60} and less polar photoproducts into the toluene phase. Destabilization of C_{60} clusters by $Mg(ClO_4)_2$ facilitated transfer of C_{60} from the aqueous to the toluene phase. The C_{60} concentration in the toluene was determined by HPLC analysis of 100 µL samples on a Varian 9012/Varian 9050 (solvent delivery system, detector; Agilent Technologies, Santa Clara, CA, USA) fitted with a Cosmosil Buckprep (Nacalai Tesque, Kyoto, Japan) column with the detection wavelength set at 336 nm. The mobile phase was 100% toluene at a flow rate of 1 mL/min for a total run time of 12 minutes. C_{60} and photo-products were also spectrally characterized with a Cary 50 UV/Vis Spectrophotometer (Agilent Technologies, Santa Clara, CA, USA) using quartz cuvettes with 1 cm path lengths.

4.3.3 Soil Microcosm Incubations

The soil microcosm design was modified from Creamer et al. (2011). Briefly, microcosms were assembled by gently mixing 3 grams of air dried soil, sieved to remove large plant fragments and stones (0.5 cm), 1.5 g of ashed quartz sand (53-250 µm) to prevent caking and promote aeration, and the fullerene treatment, into 12 mL glass vials with screw-caps fitted with re-pierceable septa (LabCo, UK) and allowed to incubate for one week prior to the first measurement of headspace CO_2 (Creamer *et al.* 2011). A silty loam soil with 2.3% organic matter (see Table 4.1 for complete characterization) was chosen for this study. Because low carbon soils generally respire less rapidly than those with more organic carbon, using a low carbon soil provided lower background CO_2, making it easier to discern small changes in isotopic composition resulting from mineralization of the labeled material. The specific soil used in the

experiments originated from a field with a long history of agricultural production (soy/corn rotation) and was used in a previous study that investigated the effect of nanomaterials on soil microbiota (Tong *et al.* 2012).

Table 4.1 Physical properties of the soil used in microcosm incubations.

	Clermont Series Soil
Taxonomic Class	Fine-silty, mixed, superactive, mesic Typic Glossaqualf
Sand (%)	27
Silt (%)	57
Clay (%)	16
Texture	Silt Loam
Organic Matter (%)	2.3
pH	4.8
MAT* (ºC)	11
MAP* (cm)	10.54
Soil Moisture (%)**	23.72
*As described in official USDA series description. **Water holding capacity at 1/3 Bar	

The fullerene treatments consisted of addition of either dark control C_{60} material or 10-, 30-, or 60- day photo-treated C_{60} clusters (2 mg dry weight) suspended in sterile ultra-pure water; the resulting suspension was used to bring soils to field moisture conditions (i.e., water holding capacity at 1/3 bar). Controls with only water (i.e., no nanomaterial) were also prepared. Three replicates were prepared for each fullerene

treatment. Microcosms were incubated in the dark at 26 °C for 90 days with gas tight caps to prevent moisture loss. When not accumulating headspace for sampling, the microcosms were periodically uncapped under aseptic conditions to maintain headspace oxygen.

Abundance and isotopic composition of CO_2 in the microcosm headspace were measured using a Sercon (Crewe, Cheshire, UK) TGA2 trace gas analyzer interfaced to a Sercon 20/20 isotopic ratio mass spectrometer, quantified against laboratory standards of known abundance and composition. Isotopic compositions of headspace samples are reported in standard delta (δ) notation relative to Vienna Pee Dee Belemnite (VPDB). To prepare the microcosms for CO_2 accumulation experiments, they were flushed with 10 times their volume of humidified CO_2-free air and capped. The humidified air was generated by passing atmospheric air over NaOH pellets and bubbling the air through sterile ultra-pure water. Headspace was sampled after two days of accumulation, allowing for determination of respiration rates over this time interval. Because headspace was flushed after each sampling event, cumulative carbon respiration was calculated by integrating the measured respiration rates between time points.

4.3.4 Oxidative Enzyme Assays

Following the disassembly of microcosms after 90 days, the soil was assayed to determine the activity of phenol oxidase and peroxidase enzymes using a colorimetric test with L-3,4-dihydroxyphenylalanine (L-DOPA) as the substrate (Sinsabaugh and Linkins 1988). Soil homogenates were prepared by stirring for 30 minutes 1.5 g of field moist soil in 75 mL of 50 mM sodium acetate buffered to a pH of 5.0. Phenol oxidase

activity was assayed by combining 750 µL of soil homogenate with 750 µL of an aqueous 20 mM L-DOPA solution directly in the assay cuvettes. Peroxidase assays were similarly prepared with the addition of 10 µL of 3 % hydrogen peroxide (H_2O_2) to the cuvettes in addition to the soil homogenate and substrate solutions. Cuvettes were incubated in the dark at 26 °C for 15 hours (as determined by preliminary incubations), before absorbance was measured at 460 nm. Absorbance was corrected against soil homogenate- and substrate- only blanks.

4.3.5 Soil DNA Extraction and Analysis

DNA was extracted from ~250 mg of soil using the PowerSoil DNA isolation kit (MOBIO, Carlsbad, CA, USA) following the manufacturer instructions. Initial attempts to quantify extracted DNA by spectrometry yielded poor results as DNA abundance in some samples was below the range in which accurate quantification by the instrument could be made. As a result, DNA was quantified by fluorometry using the Qubit 2.0 fluorometer and the Qubit dsDNA BR assay kit (Life Technologies, Grand Island, NY, USA) according to the manufacturer instructions.

Bacterial community structure was analyzed using the 16S rRNA gene through PCR-DGGE. The PerfeCTa qPCR supermix (Quanta Biosciences, MD, USA) was used to amplify the V3 region of the 16S rRNA gene with 40 picomoles of the primers 534R and 388F-GC (Muyzer *et al.* 1993), and 50 ng of DNA in a 100 µL reaction. The temperature profile for the PCR consisted on an initial denaturation at 95 °C for 5 minutes, followed by 35 cycles of denaturation at 95 °C for 30 seconds, annealing at 56 °C for 30 seconds and extension at 72 °C for 1 minute. The final extension was carried out for 15 minutes

at 72 °C. After amplification, the resultant 236 base-pair product was identified by gel electrophoresis.

DGGE was used to separate the amplification products from the 16S rRNA genes. It was carried out in a 35-70 % denaturing gradient (7 M Urea and 40 % formamide comprised 100 % denaturant) in 8 % acrylamide gels. Gels were loaded with 55 µL PCR product and run for 15 hours at 65 V and 60 °C in the DCode system (Biorad, Hercules, CA, USA) before staining with a 1:100,000 dilution of SYBR Green I (Lonza, Charleston, TN, USA). Gels were digitized and analyzed using the GelCompare II software (Applied Maths, Inc., Austin, TX, USA) using a 4 % intensity cutoff for band detection. A total of 20 bands were scored based on migration distance in the gel and used in clustering analysis. A binary matrix was created according to the presence and absence of bands, similarities between samples were determined by Dice coefficient (Dice 1945) and UPGMA was used for clustering.

The bacterial abundance was determined by qPCR of the 16S rRNA using the same primers used for PCR-DGGE without the GC clamp. The Sso Advanced Universal Inhibitor-tolerant SYBR green supermix (Biorad, Hercules, CA, USA) at 1X was used in the amplification reaction with 8 picomoles of each primer and ~10 ng DNA, in a final volume of 20 µL. The temperature profile consisted of an initial denaturation at 98 °C for 3 minutes, followed by 40 cycles of denaturation at 98 °C for 30 seconds and annealing and extension at 60 °C for 1 minute. Melting curve consisted of an initial denaturation at 95 °C for 15 seconds followed by renaturation at 60 °C for 15 seconds, and 35 subsequent 1 °C temperature steps. Standard DNA for absolute quantification

was constructed using pCR2.1 TOPO TA vector (Life Technologies, Grand Island, NY, USA) containing a full-length copy of the 16S rRNA gene from *Bacillus subtilis*.

4.3.6 Statistical Analyses

The significance that prior solar light irradiation of C_{60} had on microcosm respiration rates and isotopic composition of headspace CO_2 was assessed by one-way ANOVA with a Tukey HSD post-hoc test. Treatment effects were analyzed separately at each time point. This method was also used to determine significant differences in laccase and peroxidase activity between C_{60} treatments. Statistical analysis was performed with JMP 8 (v8.0.2.0 SAS Institute, Cary, NC, USA) with significance set for $\alpha = 0.05$ in all tests.

4.4 Results and Discussion

4.4.1 Nanomaterial Characterization

Despite prolonged exposure to artificial sunlight, we found few significant changes in the cluster characteristics of the C_{60} fullerenes added to soil microcosms. Due to the high polydispersivity index of the fullerene suspensions, determination of particle size by dynamic light scattering was not possible. Characterization by TEM found that C_{60} particles of greatly differing sizes were present in all treatments with maximum and minimum particle sizes of >2 µm and approximately 20 nm, respectively. ζ-Potential of the fullerene clusters was found to be consistent between treatments (Table 4.2). The very small ζ-potentials of each treatment are also consistent with aggregation into micrometer size aggregates.

Past studies on the photochemistry of C_{60} have reported polydispersivity indices and ζ-potentials with values that contrast those found in this study. For example Su (2013) reported that even at 120 days of irradiation under natural sunlight, the PDI did not exceed 0.35, and ζ-potential remained below -20 mV (Su 2013). This difference in physical characteristics is best explained by comparing the initial C_{60} concentrations in the suspensions: Su et al. irradiated C_{60} with a maximum starting concentration of 48.5 mg/L, while the slurry used in this study contained 3.3 g/L C_{60} in order to generate sufficient C_{60} photoproducts for the subsequent microcosm studies. As a result, the optical density of the resulting suspensions and the size to which the C_{60} particles aggregated can be expected to differ.

Table 4.2 Physical characteristics of C_{60} fullerene aggregates. Zeta potential and polydispersivity index are presented as mean ± standard deviation (n=3 and n=7 respectively)

C_{60} Photo-irradiation Duration (Days)	**Minimum Observed Diameter (nm)**	**Maximum Observed Diameter (μm)**	**Zeta Potential (mV)**	**Polydispersivity Index**
0	10	4	-1.33 ± 0.078	0.885 ± 0.133
10	10	5	-0.917 ± 0.160	0.714 ± 0.130
30	25	5.5	-1.15 ± 0.106	0.804 ± 0.198
60	20	3	-0.872 ± 0.051	0.893 ± 0.175

HPLC analysis (with detection at 336 nm) of C_{60} dissolved in toluene yields a prominent peak at a retention time of approximately 8.5 minutes (Figure 4.1) (Bachilo *et al.* 2001). It should be noted that although C_{60} clusters were used in experiments, extraction into toluene results in dissolution of the clusters in the toluene phase so that molecular C_{60} is separated and monitored by HPLC. Upon solar light irradiation, the C_{60} concentration decreased, with over 70 % of the original C_{60} lost after 15 days of

irradiation. This result is consistent with previous studies that also found a decrease in the parent compound peak upon solar irradiation (Hou and Jafvert 2009; Hwang and Li 2010). These studies have shown that as oxidation proceeds, the resulting intermediate products (i.e., fullerols) become more polar and less susceptible to extraction by toluene. However, some less-functionalized intermediates are apparent after 15-days of irradiation, as evidenced by the additional peaks with retention times between 2 and 3.5 minutes, indicating that C_{60} was indeed undergoing reaction. The dark control samples were indistinguishable from non-irradiated C_{60} dissolved directly in toluene (not shown) indicating that the observed loss of parent C_{60} (and formation of product peaks) resulted from the exposure to light.

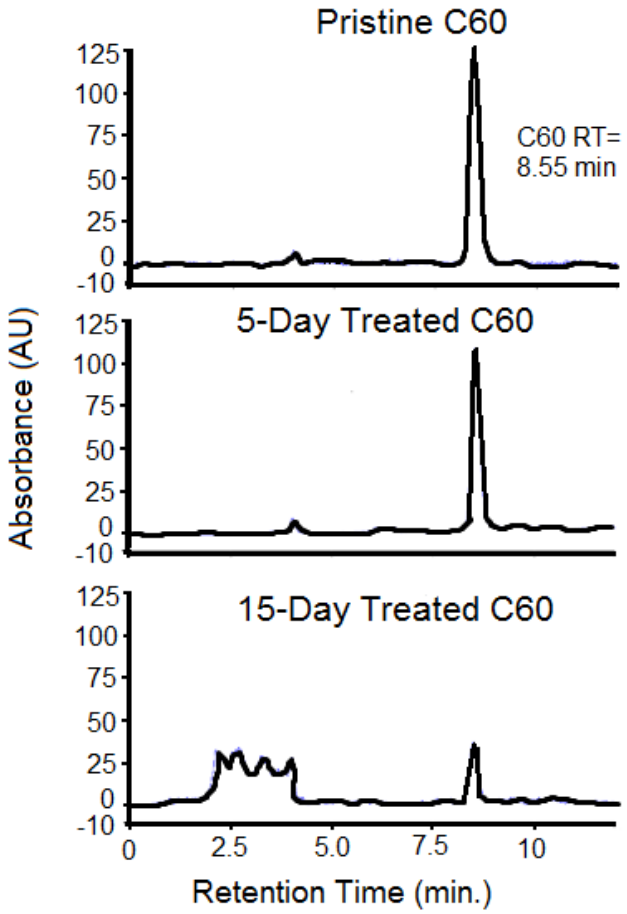

Figure 4.1 HPLC Analysis of C_{60} and Irradiated C_{60} Monitoring Absorbance at 336 nm.

The UV/Vis spectra of aqueous C_{60} clusters following irradiation also demonstrated progressive changes (Figure 4.2). Two prominent absorption bands centered at 270 and 350 nm are found on all three spectra (0, 5, and 10 day irradiations), in addition to the broad band between 410 and 555 nm that indicates the C_{60} was present in cluster form. The absorbance at all wavelengths (200 - 800 nm) decreased with irradiation time, including at 350 nm, a wavelength used to assess the concentration of C_{60} in clusters (Fortner *et al.* 2005). Dark control samples were found to be spectrally identical to C_{60} directly dissolved in toluene (not shown in figure). These

results indicate a general reduction in aromaticity consistent with parent compound loss measured by HPLC analysis, and are very similar to our previous work on the fate C_{60} molecules upon prolonged solar light irradiation. Specifically, significant $^1O_2$ is generated by aqueous C_{60} clusters when exposed to dissolved O_2, which in turn reacts with photochemically excited triplet state C_{60} ($^3C_{60}$) to produce oxidized C_{60} structures that are much more water-soluble (Hou and Jafvert 2009; Hou and Jafvert 2009; Hou *et al.* 2010). These seminal studies on solar light irradiated C_{60} were conducted using the same batch of C_{60} from MER Corporation as used in this study, so the characterization information provided previously are applicable to the current study. The FTIR spectra of irradiated and dark control C_{60}, reported by Hou et al. demonstrate that solar-spectrum light irradiation significantly increases absorbance at 1370 and 1080 cm^{-1} indicating in plane C-O-H bending and C-O stretching respectively (Hou *et al.* 2010), features that are consistent with the oxidative cleavage of C_{60} double bonds (Figure 4.3).

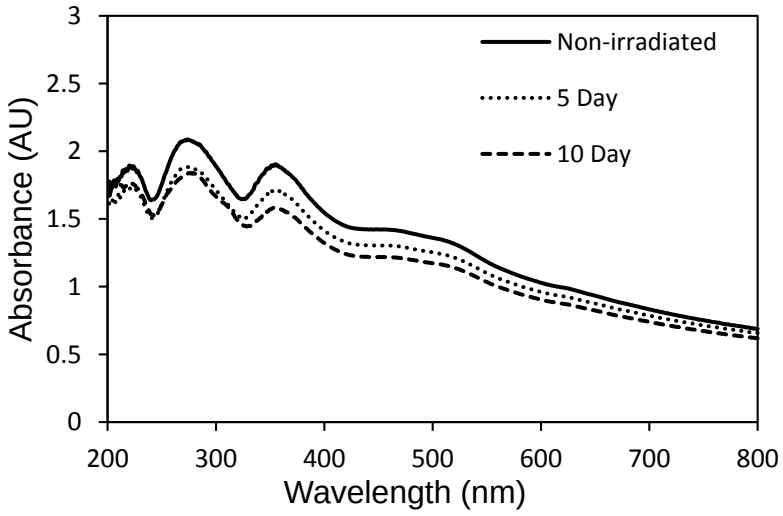

Figure 4.2 UV/Vis Spectra of C_{60} and Irradiated C_{60}.

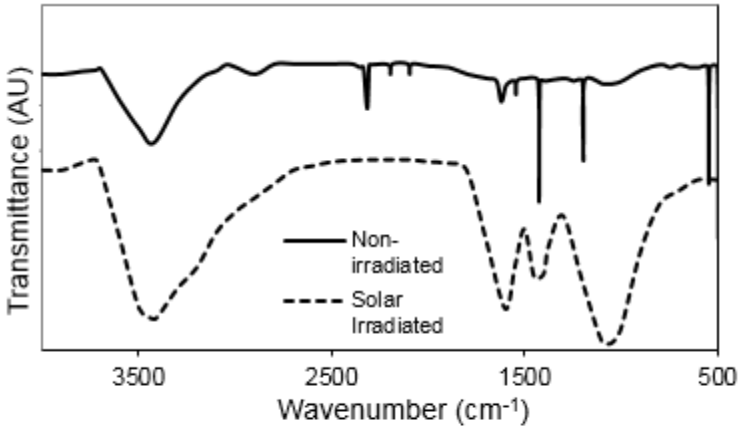

IR Band Assignment	Band Position (cm^{-1})
C=C stretch	1600
C-O-H in plane bend	1370
C-O stretch	1080

Figure 4.3 ATR-FTIR Spectra of solar irradiated and dark control sublimed MER C_{60} fullerenes. Irradiated fullerenes were exposed to solar radiation for 947 hours (~40 days). The dramatic increase in width and intensity of bands located at wavenumbers 1370 and 1080 are characteristic of carbon-oxygen interaction and indicate extensive oxidation and decreased aromaticity following irradiation. Spectra adapted from Hou *et al.* (2010) and IR assignments taken from Kokubo *et al.* (2008).

4.4.2 Soil Microcosm Respiration

A high degree of variability was observed in the isotopic composition (Figure 4.4) and respiration rates for all treatments when measured on days 3 and 7 (Figure 4.5), likely due to small differences in physical disruption upon mixing the soil with the quartz sand during pre-incubation. On day 7, headspace CO_2 in microcosms containing 30-day irradiated C_{60} showed significant enrichment (+ 4.2 ‰) of headspace CO_2 (-13.6 ± 0.9 ‰) in comparison to microcosms containing C_{60} that had not been previously irradiated (-17.8 ± 0.5 ‰). As the incubation progressed, headspace CO_2 in the microcosms containing 60-day irradiated C_{60} became significantly more enriched than all other

treatments, except for the 30-day irradiated C_{60}, indicating that 30 and 60 day irradiations resulted in C_{60} intermediates that were similarly amenable (i.e., labile) to further biological mineralization. Although there was a measurable decrease in headspace ^{13}C-enrichment on day 65, it was not found to be statistically significant and is likely the result of the natural variation in soil respiration or because of a minor disturbance of the soil microcosms during the preceding accumulation period. The addition of 30-day irradiated C_{60} to microcosms also resulted in discernable headspace enrichment when compared to microcosms containing 10-day irradiated C_{60} or C_{60} that had not been exposed to light, although this enrichment was not found to be significant at $\alpha = 0.05$ after day 7. The rapid decrease in headspace $^{13}CO_2$ in the microcosms containing 30-day irradiated C_{60} after this time-point may indicate that the early spike in enrichment was the result of mineralization of a high concentration of highly labile $^{13}C_{60}$ intermediates potentially present in these microcosms. Unfortunately, the sampling of microcosms was not performed early enough to quantify these early "spikes" in $^{13}C_{60}$ mineralization. Although differences were not always significant, the isotopic composition of headspace CO_2 in microcosms containing 30- and 60- day irradiated C_{60} was always ^{13}C-enriched compared to control microcosms, indicating that the continual mineralization of C_{60} photo-intermediates occurred throughout the experiment at measurable levels. At no time point during the incubation was the isotopic composition of headspace in the no-C_{60} control microcosms significantly different from those containing dark control C_{60} or 10-day irradiated C_{60}, suggesting that there may be a critical level of photo-oxidation that needs to occur before the C_{60} cage structure is

amenable to further microbial degradation in the soil. Further, this critical level may be associated with microbial availability (i.e., water solubility).

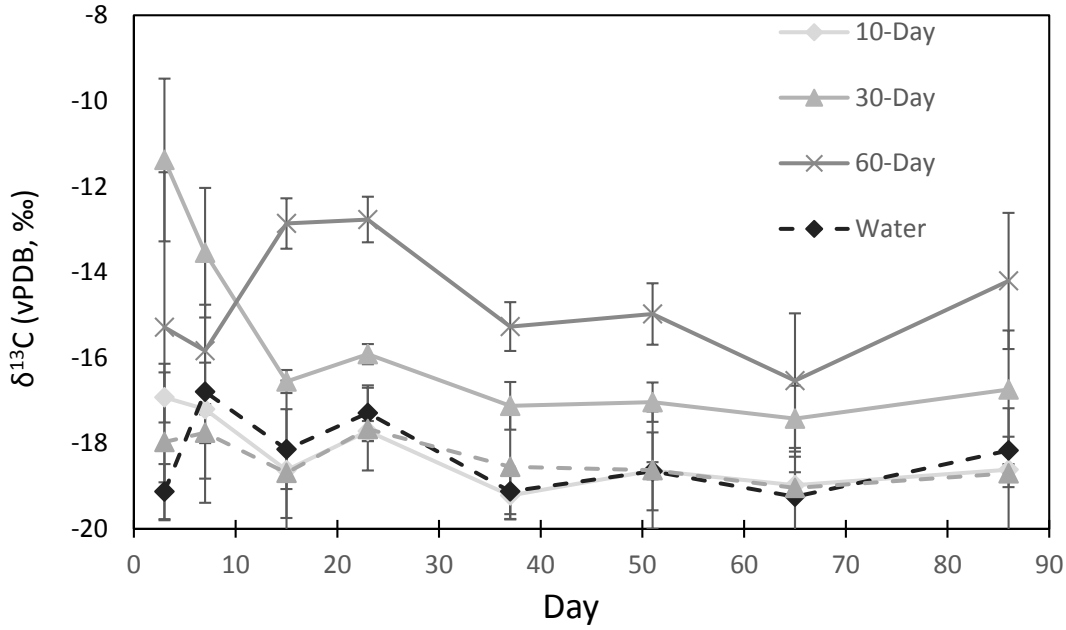

Time (Day)	10 Day	30 Day	60 Day	Water (Control)	Non-irradiated
3	-	-	-	-	-
7	AB	A	AB	AB	B
15	B	B	A	B	B
23	BC	B	A	BC	C
37	B	AB	A	B	B
51	B	AB	A	B	B
65	-	-	-	-	-
86	B	AB	A	B	B

Figure 4.4 Isotope composition of CO_2 respired from soil microcosms (top) and statistical significance (bottom). Treatments without shared letters indicate significant differences between treatments (1-way ANOVA, Tukey's HSD Post-Hoc) ($\alpha = 0.05$) at a given time point. If no letters are present for a time point, no significant differences exist at ($\alpha = 0.05$). Error bars represent standard error.

The largest ^{13}C enrichment in CO_2, +4.5 ‰ compared to the no-C_{60} control, was observed after 23 days of incubation in microcosms containing 60-day irradiated C_{60} (see Figure 4.4). The cumulative ^{13}C mineralized corresponded to a ^{13}C contribution equivalent to approximately 0.125 % of the total mineralized carbon at this time point. Over the course of the entire incubation a total of 15.6 μg of the 60-day irradiated C_{60}, or 0.78% of the original 2 mg of C_{60} added were mineralized. As a result of the high purity of the C_{60} used in this study, enrichment in headspace CO_2 cannot be attributed to mineralization of amorphous impurities in the starting materials. Such impurities account for no more than 5.3 μg of the added C_{60} per microcosm, thus headspace $^{13}CO_2$ must predominately be the result of mineralization of C_{60} photo-products. This finding demonstrates for the first time that prolonged exposure of C_{60} to sunlight can promote further mineralization by soil microorganisms, with a rate of decomposition of 180.9 ng/day for these particular soil microcosms. The photo-products of the solar-spectrum-light-irradiated C_{60} are mineralized much more rapidly than the parent C_{60}. Previous studies have reported no observable mineralization of irradiated C_{60} (Hartmann *et al.* 2011), and minimal mineralization (less than 0.1%) of SWCNT in a liquid culture at a rate less than 0.33 ng/day (Parks *et al.* 2015). Note that neither of these previous studies were conducted with soil, but rather under more ideal growth conditions using liquid media, which likely contributes to the observed differences in mineralization.

The influence of (non-irradiated) C_{60} addition on soil respiration found herein stands in contrast to previous studies (Tong *et al.* 2007; Johansen *et al.* 2008). Tong *et*

al. (2007), using similar C_{60} application rates but in a siltly loam soil with higher carbon-content (4.0 wt % C), reported no signficant differences in soil respiration over the course of a 30-day incubation. Similarly, Johansen *et al.* (2008) reported no effect in soil respiration for a C_{60} treatment applied at a lower rate, 50 mg/kg of soil, in a soil of similar texture and carbon content to our experiment. The differences in findings may be a function of C_{60}/soil C addition rates which varied among the three studies or soil specific microbial community structure and activity. The irradiation of C_{60} acts to oxidize carbon and enriches surface oxygenated groups. The results of our study, demonstrating the enhanced lability of irradiated C_{60}, agrees with previous findings of the lability of oxygenated C_{60}, C_{60} fulerols, by Schreiner et al (2009) who reported that up to 2.86% of ^{13}C-labeled C_{60} fullerol could be mineralized over the course of a 225 day incubation with a white-rot fungus.

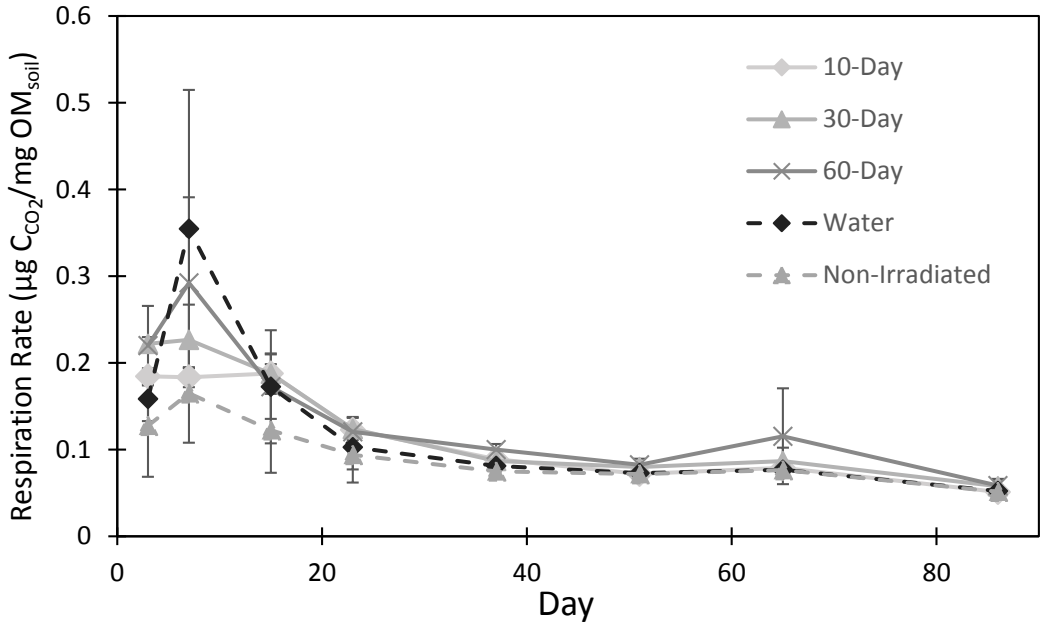

Time (Day)	10 Day	30 Day	60 Day	Water (Control)	Non-irradiated
3	AB	A	AB	AB	B
7	AB	AB	AB	A	B
15	-	-	-	-	-
23	-	-	-	-	-
37	AB	AB	A	AB	B
51	-	-	-	-	-
65	-	-	-	-	-
86	-	-	-	-	-

Figure 4.5 Soil microcosm respiration rate per hour, normalized to soil OM (top) and statistical significance (bottom). Treatments without shared letters indicate significant differences between treatments (1-way ANOVA, Tukey's HSD Post-Hoc) (α = 0.05) at a given time point. If no letters are present for a time point, no significant differences exist at (α = 0.05). Error bars represent standard error.

4.4.3 Oxidative Enzymes

The addition of neither irradiated nor non-irradiated C_{60} had a significant impact on soil laccase activity (Figure 4.6). However, non-irradiated C_{60}, but not the irradiated analog, significantly lowered the activity of peroxidase enzymes (1.59 ± 0.17 µmol product $Hr^{-1}g_{soil}l^{-1}$) in comparison to the no-fullerene control (1.86 ± 0.12 µmol product

$Hr^{-1}g_{soil}l^{-1}$). The lack of an oxidative enzymatic response to in soil containing irradiated C_{60}, even though these treatments exhibited measurable changes in respiration (Figure 4.5) suggests that either extracellular enzymatic oxidation is not the source of the observed CNM mineralization, or that mineralization of irradiated C_{60} occurred without additional enzyme expression as might be expected if the C_{60} were co-metabolized with an additional substrate in soil. However, if co-metabolism were the main degradation mechanism there would likely be strong correlation between mineralization of non-fullerene substrates (and thus respiration rate) and mineralization of $^{13}C_{60}$ (Hamer *et al.* 2004), a relationship that was not noted in this study. Because small clusters of C_{60} have been shown to be taken up into bacterial without a significant loss cell viability (An and Jin 2012) it remains also possible that the fullerene mineralization observed in this study is the result of intercellular enzyme activity as opposed to extracellular enzyme activity, which cannot be investigated using the methods in this study.

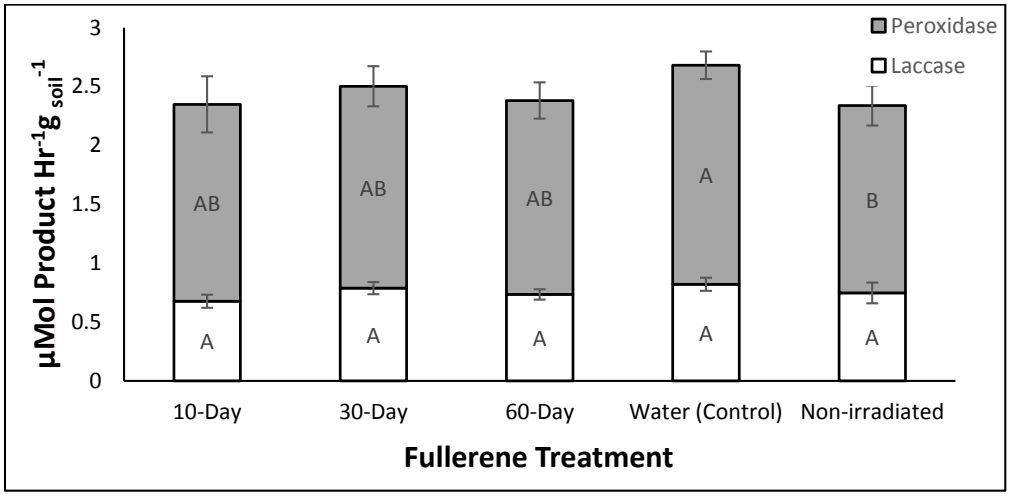

Figure 4.6 Oxidative enzyme activity in soils following incubation. Error bars represent standard deviation. Treatments without shared letters indicate significant differences in enzyme activity (1-way ANOVA, Tukey's HSD Post-Hoc) ($\alpha = 0.05$).

4.4.4 Bacterial Abundance and Community Composition:

Bacterial abundance was determined as the number of copies of the 16S rRNA gene per gram of dry soil by qPCR. Bacterial abundance ranged between $3.8x10^{10}$ copies and $5.8x10^{10}$ copies per gram of soil among the treatments, with no statistical differences observed (Figure 4.7). Microbial community composition by DGGE, however, found significant differences in community composition among the C_{60} treatments. Dice similarities between treatments varied from 70 % to 97 % and formed three clusters: One cluster was formed by microcosms containing C_{60} that been irradiated for 30 and 60 days, which was most similar to a second group comprised of fullerene-free control microcosms and those containing C_{60} that had been irradiated for 10 days. The cluster with the least similarity to other treaments were those containing non-irradiated C_{60} (Figure 4.8).

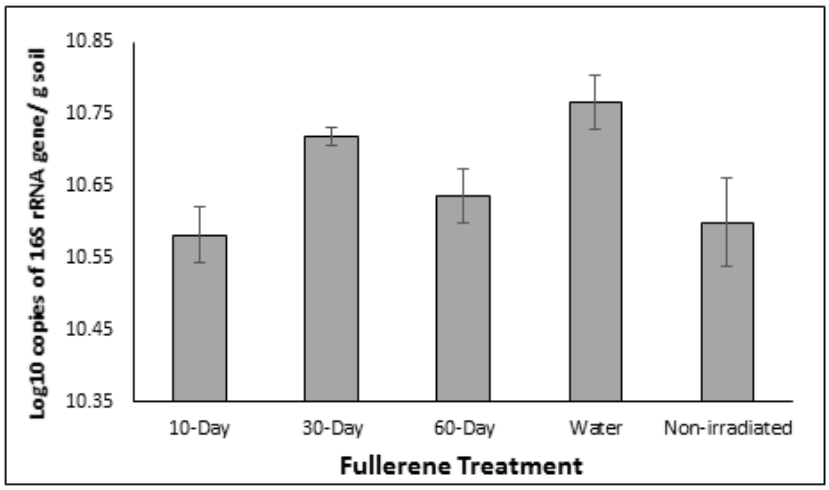

Figure 4.7 Bacterial abundance in microcosm soil following incubation with irradiated C_{60} calculated as the copy number of 16S rRNA gene per gram of dry soil. Each point in the graphic represent the average of nine data points (Triplicate qPCR reactions for each of the microcosm replicates at each time point). Error bars represent standard error. The efficiency of the qPCR was higher than 93 % and with a correlation coefficient > 0.99

Previous studies utilizing DGGE to assess the impact of CNM in a soil with a higher organic and clay content found minimal change in the community structure of this soil with CNM addition. For example, Tong *et al.* reported that C_{60} had little impact on the composition of the microbial community in such a soil (Tong *et al.* 2007) and later reported that, while certain types of SWCNT significantly altered the community composition in a soil with low clay and organic matter content (similar to the current study), these same nanomaterials had little effect when applied to a soil that contained more clay and organic matter (Tong *et al.* 2012).

These studies proposed that soil organic matter and clay are able to mitigate CNM toxicity through strong sorption and aggregation dynamics, however the mechanisms are poorly understood. Interactions with soil dissolved organic matter have been previously studied as important factors in the response of soil to CNM exposure. Espinasse *et al.* (2007) reported that inclusion of tannic acid in aqueous C_{60} suspensions decreased aggregation and enhanced mobility of fullerenes in a porous media (Espinasse *et al.* 2007). Similarly, Chen *et al.* (2007) found that the addition of Suwannee River humic acid to aqueous suspensions of C_{60} dramatically decreased the rate of homoaggregation of C_{60} particles as a result of sorptive interactions that promote colloidal stability (Chen and Elimelech 2007) and can then be expected to limit exposure of soil microorganisms to CNM aggregates (Navarro *et al.* 2008). The prominent clustering of microbial communities in the present study, in a soil lacking significant organic or clay content further reenforces the importance of these properties in controlling microbial interactions with CNMs.

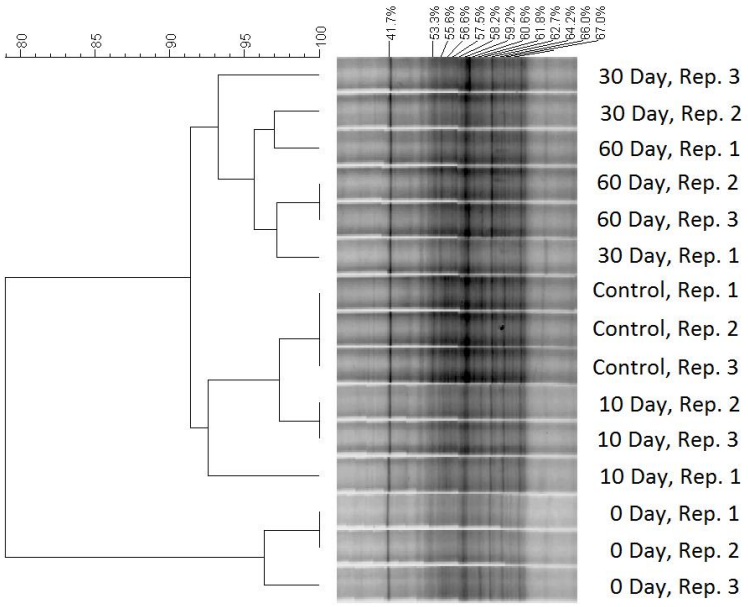

Figure 4.8 Clustering analysis of the bacterial community structure in soil following incubation with irradiated C_{60}. Dendrogram based on Dice similarities and constructed using UPGMA. Each lane corresponds to a single microcosm.

4.5 Conclusions and Implications on the Environmental Fate of CNMs

In this study we investigate the coupled processes of abiotic photochemical transformations C_{60} and subsequent biotic mineralization in soil. We report for the first time the measurable mineralization of irradiated ^{13}C-C_{60} in soil, albeit at very low rates (180.9 ng/day). Given this modest rate of decomposition, it is unlikely that similar photo-chemical transformations in nature, in conjunction with biotic mineralization are sufficient to prevent CNM accumulation in the event of continued environmental release. Even after 60 days of continuous solar wavelength irradiation prior to inclusion in soils only ~0.78 % of added nanocarbon is mineralized after 86 days of incubation.

C_{60} addition altered microbial community composition, with variation depending on irradiation duration, a finding that stands in contrast to previous studies using soils

with a different composition and indicating that edaphic properties may control the microbial impact of CNM exposure. These impacts on microbial community structure indicate that microbial populations in soils with low organic matter and clay content may be vulnerable to fullerene exposure with the potential to affect soil biogeochemical cycles.

We found no evidence of increased oxidative soil enzyme activity with the addition of irradiated C_{60}, even though respirations rates were influenced and C_{60} was mineralized. This has important implications in the study of CNM fate in soils, as a number of studies have investigated the potential of these enzymes to transform and ultimately degrade related CNMs such as MWCNT (Allen *et al.* 2008; Zhao *et al.* 2011) which may not be relevant in systems containing CNMs with less extreme aspect-ratios such as C_{60}.

4.6 Acknowledgements

The authors acknowledge support from the Environmental Protection Agency under EPA STAR award RD-83485801-0 and would like to thank Ms. Lisa Reese and Ms. Laurie Mueller for their assistance in characterizing the C_{60} clusters used in this study.

CHAPTER 5. MICROBIAL MINERALIZATION OF C_{60} FULLEROLS IN TWO AGRICULTURAL SOILS

5.1 Abstract

Despite their status as an emerging pollutant, the environmental fate of functionalized carbon nanomaterials (CNM) such as fullerols is poorly understood, likely as a result of the tendency of researchers to focus on the behavior more condensed, "pristine" nanomaterials in the environment. We present the results of a study investigating the mineralization of ^{13}C-labeled C_{60} fullerols in soils in order to address this knowledge gap and to test the hypothesis posed previously in CHAPTER FOUR that the increased solubility and ease of oxidation that results from the conversion of C_{60} to fullerols would result in greater microbial oxidation and C-uptake. We found that although fullerol addition had little impact on net soil respiration rate or oxidative enzyme activity, the fullerols were rapidly mineralized in soil mesocosms. Soil carbon and clay content had a strong control on the extent of mineralization as determined by ^{13}C-content of the mesocosm head space where a low-carbon soil, Clermont series, exhibited a lower proportional decomposition (~25.9 % of added fullerol C) than the higher C and clay content Drummer series soil, (~59.1 % of added fullerol C mineralized). Analysis of the concentration, composition, and ^{13}C content of soil phospholipid fatty

acids from the fullerol amended soils demonstrated the uptake of fullerol C by the soil microbial community; a result never before demonstrated. Fullerol C uptake varied by microbial guild, with Gram positive bacteria deriving 0.27 % of PLFA carbon from the fullerols and Gram negative bacteria deriving 1.25 % of PLFA from fullerols; this represents approximately 27 % and 125 % of the level of the proportional carbon spike of the fullerol to total soil C. These findings demonstrate for the first time the mineralization of C_{60} fullerol in an environmentally relevant substrate and provide important insights on the microbial populations most active in the CNM degradation and metabolism in agricultural soils.

5.2 Introduction

A number of previous studies on CNM have focused on the importance CNM surface chemistry in controlling the behavior of these materials in the environment, particularly how surface modification may influence their transport, toxicity, and stability (Handy *et al.* 2008; Nowack *et al.* 2012). Surface chemistry is also expected to be a major driver in the degradation of CNM in the environment. For example, mechanistic studies of CNT transformation by oxidative enzymes report increased degradation of surface functionalized nanomaterials in comparison to pristine CNT (Allen *et al.* 2008; Zhao *et al.* 2011) and pure-culture studies report increased enzymatic activity from saprotrophic organisms and bleaching of CNM when surface functionalized (Schreiner *et al.* 2009; Berry *et al.* 2014). Recent works however, have largely focused on the degradation of pristine CNM and report either negligible decay or particle half-lives on the order of 100s of years (Avanasi *et al.* 2014; Flores-Cervantes *et al.* 2014; Parks *et*

al. 2015). The authors of the present study however, have recently found that coupled photo-chemical and biotic degradative processes have the potential to significantly accelerate the degradation of C_{60} fullerenes, likely as a result of photo-chemical disruption of the stable condensed aromatic structure and the inclusion of oxidizable and hydrolysable sp3 and sp2 oxygenated carbon.

We present the results of a novel study investigating the mineralization of ^{13}C-labeled C_{60} fullerols ($^{13}C_{60}(OH)_{19\text{-}27}$) in soils with contrasting edaphic properties. The use of a stable isotope label allowed for the precise determination of degradation rates and microbial uptake of the fullerol C by tracing ^{13}C into respired CO_2 and incorporation into microbial biomass. Fullerols are representative of both manufactured CNM designed for enhanced solubility (e.g. for drug delivery applications) and CNM that have been chemically weathered through processes such as the prolonged exposure to sunlight (Hou and Jafvert 2009; Hou *et al.* 2010; Berry *et al.* 2015). Informed by pure-culture studies demonstrating the significant mineralization of fullerols (Schreiner *et al.* 2009) and enzymatic response of fungi towards functionalized CNM (CHAPTER TWO), we utilized ^{13}C enriched fullerols to investigate the hypothesis that highly functionalized CNM would be rapidly mineralized in soils in comparison to pristine unfunctionalized C_{60}. Denaturing gradient gel electrophoresis and phospholipid fatty acids analysis was used to assess the relative impact of fullerol exposure on the microbial community structure and to ascertain which microbial guilds might drive a soil's response to CNM. We speculate that specific bacterial groups, principally the gram negative bacteria, that have been shown to be facile decomposers of other natural sources of condensed

aromatic carbon like naturally produced pyrogenic organic matter, will be the primary agents for its metabolism over fungi or gram positive bacteria

5.3 Materials and Methods

5.3.1 Fullerols and Soils

The fullerols used in this study were synthesized in partnership with TDA research as in Schreiner *et al.* 2009; briefly, $^{13}C60$ fullerenes (MER Corp., USA) were oxidized in CH_2Cl_2 by 18-crown-6 stabilized KO_2. The precipitant produced in this reaction was collected, washed in CH_2Cl_2, suspended in H_2O and purified by filtration through a 0.45 μM PTFE filter and repeated methanol/water precipitations. Purity of the resulting product was verified by HPLC in which no evidence of amorphous carbon was found (Schreiner *et al.* 2009). The product of the synthesis was stored under argon gas in sealed amber vials until use to prevent degradation.

The fullerols added to the soil microcosms were prepared as an aqueous suspension by dissolving 64.5 mg of $C_{60}(OH)_{19\text{-}27}$ (1.09 atom % ^{13}C) and 15.3 mg of $^{13}C_{60}(OH)_{19\text{-}27}$ (22 atom % ^{13}C, prepared as above, TDA Research, USA) together in 18MΩ/cm ultrapure water to produce a suspension with a concentration of 80 mg/ 20 mL and an isotopic composition of 5 atom % ^{13}C. Two soils were chosen that vary in clay content and organic matter content, factors thought to control CNM interaction and accessibility, Drummer series soil (fine-silty, mixed, superactive, mesic Typic Endoaquoll, 7.8 % organic matter, pH=7) and Clermont series soil (fine-silty, mixed, superactive, mesic Typic Glossaqualf, 2.3 % organic matter, pH=4.8). Each of the two soils has a history of agricultural land use and have been used in a number of previous studies that

investigate the effect of nanomaterials on soil microbiota (Tong *et al.* 2007; Tong *et al.* 2012; Berry *et al.* 2015)). A complete characterization of each soil is available in Table 5.1.

Table 5.1 Physical properties of the soil used in microcosm incubations.

	Clermont Series Soil	**Drummer Series Soil**
Taxonomic Class	Fine-silty, mixed, superactive, mesic Typic Glossaqualf	Fine-silty, mixed, superactive, mesic Typic Endoaquoll
Sand (%)	27	25
Silt (%)	57	49
Clay (%)	16	26
Texture	Silt Loam	Loam
Organic Matter (%)	2.3	7.8
pH	4.8	7.8
MAT* (ºC)	11	11
MAP* (cm)	10.54	9.4
Soil Moisture (%)**	23.72	35.72
*As described in official USDA series description. **Water holding capacity at 1/3 Bar		

5.3.2 Soil Microcosms and Controls

Soil microcosms were constructed as in CHAPTER FOUR, a design modified from Creamer *et al.* (2011). Briefly, microcosms containing 3 grams of air dried soil, sieved to remove large plant fragments and stones (0.5 cm) and 1.5 g of ashed quartz sand (53-250 µm) were mixed and added to 12 mL glass vials with screw-caps fitted with repiercable septa (LabCo, UK). The aqueous fullerol suspension detailed above was added to soils so that fullerol carbon accounted for 1 % of total microcosm organic matter, a fullerol loading of 1.57 mg for Clermont microcosms and 5.33 mg for Drummer

microcosms. Microcosms were then brought to field moisture (water holding capacity at 1/3 bar) sterile ultrapure water. Control soil microcosms receiving only sterile ultrapure water were also constructed.

To help distinguish between abiotic and biotic mineralization of the added fullerols, microbially suppressed soil microcosms were also prepared. These microbially suppressed treatments were prepared by autoclaving microcosms at 121 ºC and 100 kPA for 30 minutes. Autoclaving was repeated 4 times with a 1 day recovery period between sterilization cycles. Fullerol treatments were then added to the autoclaved soil microcosms as above. Five replicates were prepared for each soil/treatment combination. A series of 5 soil-free controls were also prepared to help assess the role of edaphic properties in controlling fullerol oxidation. Each soil-free control contained 4.5 grams of ashed quartz sand and received 1.57 mg of fullerols (equivalent to the loading of the Clermont microcosms).

Following 3 days of pre-incubation each microcosm was gently mixed to improve airflow. Preliminary measurements of CO_2 at this time showed that autoclaved samples had reactivated and so were fumigated with chloroform to further reduce microbial abundance without mineralizing the fullerol in the microcosm. Pre-incubation continued for 4 days for a total pre-incubation period of 7 days. Microcosms were incubated in darkness at 26 ºC for 65 days with caps sealed to prevent moisture loss. When not accumulating headspace for sampling, microcosms were allowed to exchange with air by uncapping under aseptic conditions twice a week. Headspace CO_2 was measured using a Sercon (Crewe, UK) TGA2 trace gas analyzer interfaced to a Sercon

20/20 isotopic ratio mass spectrometer. The ^{13}C isotope composition of headspace is reported in standard delta (δ) notation relative to Vienna Pee Dee Belemnite (vPDB). Two days prior to each headspace sampling, microcosm headspace was flushed (10X headspace volume) with CO_2-free air produced by passing atmospheric air over sodium hydroxide pellets and humidified by bubbling through sterile nanopure water, corresponding to a 48 hour CO_2 accumulation period for each time point. All microcosms, including controls had their headspace analyzed at each timepoint. Microcosm headspace was flushed during trace gas analysis, cumulative carbon respiration was calculated by integrating the measured respiration rates between time points. The relative contribution of soil organic carbon and fullerols was calculated using a simple two-member mixing model. These calculations are detailed in the APPENDIX.

5.3.3 Oxidative Enzyme Assays

Microcosms were disassembled after 65 days of incubation with soil fractions persevered at -80°C for future PLFA and DNA analysis. The activity of phenol oxidase and peroxidase enzymes were assayed colorimetrically using L-3,4-dihydroxyphenylalanine (L-DOPA) as a substrate (Sinsabaugh and Linkins 1988). Soil homogenates were prepared immediately following microcosm disassembly by stirring 750 mg of field moist soil in 50mL of 50 mM sodium acetate buffered to a pH of 5.0 for 30 minutes. Phenol oxidase activity was assayed by combining 750 µL of soil homogenate with 750 µL of an aqueous 20 mM L-DOPA solution directly in the assay cuvettes. Peroxidase assays were prepared by including 10 µL of 3 % hydrogen peroxide

to cuvettes in addition to the soil homogenate and substrate solutions. Preliminary incubations of Clermont and Drummer series soil homogenates found that, due to differences in soil enzyme activity incubation periods of 15 hours and 24 hours provided the most consistent measurements. Cuvettes were incubated in darkness at 26 ºC accordingly before absorbance was measured at 460 nm. Absorbance was corrected against soil homogenate and substrate only blanks.

5.3.4 Soil DNA Extraction, 16S rRNA PCR-DGGE and qPCR

DNA was extracted from ~250 mg of soil using the PowerSoil DNA isolation kit (MOBIO, Carlsbad,CA) as per manufacturer instructions. Agarose gel electrophoresis and spectrometry using a NanoDrop 1000 spectrophotometer (Thermo Scientific, Wilmington, DE) was used to assess DNA quality before fluorometric quantification using the Qubit 2.0 fluorometer and dsDNA BR assay kit (Life Technologies, Grand Island, NY) as per manufacturer instructions.

Amplicons for DGGE analysis were prepared using PerfeCTa qPCR supermix (Quanta Biosciences, MD) and primers 534R and 388F-GC to amplify the V3 region of the 16S rRNA (Muyzer *et al.* 1993). Bacterial abundance was determined by qPCR of the 16S rRNA using the same primers used for PCR-DGGE without the GC clamp. Standard DNA for absolute quantification was constructed using pCR2.1 TOPO TA vector (Life Technologies, Grand Island, NY) containing a full-length copy of the 16S rRNA gene from *Bacillus subtilis*. Primer sequences, reaction composition, and PCR cycle information are as described in CHAPTER 4. Separation of the 16S rRNA gene amplification products was performed by DGGE using a 35 %-70 % denaturing gradient (7 M Urea and 40 %

formamide comprised 100 % denaturant) in 8 % acrylamide gels. Gels were digitalized and analyzed using the GelCompare II software (Applied Maths, Austin, TX). Similarity coefficients were used in clustering analysis with the unweighted pair group method with arithmetic mean (UPGMA) method.

5.3.5 Phospholipid Extraction and Quantification

PLFA were extracted from 3 g subsamples as outlined by Bligh and Dyer (1959) and (White *et al.* 1979) Briefly, lipids were extracted from soils by mixing with chloroform, methanol, and phosphate buffer prepared in a 1:2:08 ratio before being allow to stand 24 hours and centrifuged to separate soil particles from solvent layers. The chloroform layer was then extracted and concentrated by rotary evaporation and blown dry under N_2. Re-suspended total lipid extracts were transferred to silicic acid extraction columns (Creamer *et al.* 2015; Orr *et al.* 2015). Neutral lipid fractions (eluted from columns by chloroform) and glycolipids fractions (eluted by acetone) were discarded prior to elution of PLFA by methanol into clean vials. The eluted PLFA were then split with 90% to be used in compound specific gas chromatography-combustion-isotope ratio mass spectrometry (GC-c-IRMS) and 10 % to be quantified by GC-FID after conversion into fatty acid methyl esters (FAMES) by mild alkaline methanolysis. FAMES were quantified as in Orr *et al.* (2015); briefly, FAMES were separated using a 60 m DB-5 capillary column (0.25 mm ID, 0.25 µm film thickness; J&W Scientific) inside of an Agilent 5975 gas chromatograph/mass spectrometer (Agilent, Santa Clara, USA). FAMES were identified by retention time and fragmentation pattern and quantified by peak area against a standard (Standard #1114, Matreya LLC, Pleasant Gap, PA). PLFA-

FAMEs are referred to using short-hand fatty acid nomenclature following the format "X:YωZ", with X indicates the length of the carbon chain, Y indicates the number of double and Z indicates the position of the double bonds relative to the methyl end of the fatty acid. Double bound geometry is denoted by the suffices *c* and *t* for *cis* and *trans* bonds while the prefixes *i* and *a* indicate *iso*- and *anteiso*- branching of saturated FAMEs. Cyclopropyl groups are denoted with the prefix *cy*-. PLFA-FAMEs were combined into taxonomic guilds as follows; general (14:0, 15:0, 16:0, 17:0, 18:0), gram positive bacteria (i15:0, a15:0, i16:0, i17:0, a17:0), gram negative bacteria (cy17:0, cy19:0), non-specific bacteria (18:1ω9c/t), and fungi (18:2ω6,9c/t,), a classification scheme consistent with a number of previous studies (Frostegard *et al.* 1993; Frostegard *et al.* 2011)

5.3.6 Compound Specific Gas Chromatography-Combustion-Isotope Ratio Mass Spectrometry (GC-C-IRMS) Analysis

Following methanolysis of PLFA as above, ^{13}C content of the resultant FAMES was measured by GC-c-IRMS. FAMES were injected at 280 °C through a cooled injection system (CIS4, Gerstel, Cologne, Germany) into a Hewlett Packard 6890A GC (Agilent, Santa Clara, CA) containing a 60 m RTX-5MX (0.25 mm ID, 0.25 μm film thickness, Restek) column connected to a ceramic microcombustion reactor interfaced to a Sercon 20/22 isotope ratio mass spectrometer (IRMS, Sercon, Crewe, UK). The microcombustion reactor contained wound copper, nickel, and platinum wires as combustion catalysts at a ratio of 2:2:1 and was held at a constant temperature of 1000 ˚C throughout the analysis. Peak separation was achieved using a ramped

temperature program; 50 °C for 5 minutes, 50-120 at 10 °C/minute, 120-250 at 4 °C/minute, 250 °C for 12 minutes. An internal standard of nC15, isotopically verified at a $\delta^{13}C$ value of -30.2 ‰, was added to samples at a concentration of 10.0 ng/µL to correct isotopic values when necessary. Standard calibration curves were also included in each batch of analyses to ensure the consistency of chromatographic and isotopic data. Due to low recovery of PLFA-FAMEs from the Clermont soils, they were not included in CSIA, however a total of 15 FAMEs from the Drummer soils were sufficiently well separated to include (8:0, 10:0, 12:0, i14:0, i15:0, a15:0, i16:0, 16:0, 10Me16, 17:1 ω?, 17:1 ω?(2), 18:0, 18:1ω9c, 18:1 ω?, and cy19; a ? indicates that a FA includes a double bond with a position that could not be determined by GC analysis). Because 18:1ω9c and 18:1 ω? nearly co-eluted, they were integrated and processed together for a combined $\delta^{13}C$ value. A two-member mixing model using PLFA extracted for fullerol-free controls and $^{13}C_{60}(OH)_{19\text{-}27}$ as end-members was used to calculate the relative contribution of fullerol derived carbon to PLFA carbon. The resultant fraction of ^{13}C for a PLFA analyzed by CSIA was then used in conjunction with data on the abundance of the PLFA and knowledge of its molecular formula to determine the total mass of CNM derived carbon in each PLFA which was then normalized to total guild biomass using the assumption that the average bacterial cell has a PLFA content of $1.4X10^{-8}$ nmol (Frostegard and Baath 1996) and contains 30 fg of carbon (Fukuda *et al.* 1998; Loferer-Krossbacher *et al.* 1998). Formulae for the necessary calculations are provided in the APPENDIX.

5.3.7 Statistical Analyses

. Differences in microcosm respiration rates, isotopic composition of CO_2, oxidative enzyme activity, and bacterial abundance were assessed by one-way ANOVA with a Tukey HSD post-hoc test. Statistical analysis was performed with JMP 8 (v8.0.2.0 SAS Institute, Cary, NC, USA) with significance set for $\alpha=0.05$ in all tests. Treatment effects were analyzed separately at each time point (in the respiration experiment) and for each soil type. Principle component analysis using PRIMER 7 (v7.09, PRIMER-E Ltd., Lutton, UK) was used to visual grouping of soil treatments based upon mol% of individual PLFA extracted from microcosms. The similarities of percentages (SIMPER) analysis in PRIMER was used to determine which PLFAs contributed most significantly to the separation of soil treatments. Trace PLFA-FAMES with a relative abundance <1% in all microcosms were excluded from these analyses, leaving a total of 18 PLFA to be included in a characteristic PLFA fingerprint (i14:0, 14:0, i15:0, a15:0, 15:0, 15:1ω?, i16:0, 16:0, 16:1ω9, 17:0, 18:0, 18:1ω9c, 18:1ω9t, 18:1ω?, cy19:0, 20:0, 22:0, 24:0; a ? indicates that a FA includes a double bond with a position that could not be determined by GC analysis).

5.4 Results and Discussion

5.4.1 Fullerols do not significantly impact net respiration

The rate of CO_2 respiration from microcosms demonstrates the distinct nature of the two soils used in the study with regard to relative oxidation of native soil carbon and fullerol amendment (Figure 5.1). Even when normalized to carbon content, the higher SOC containing Drummer series soils respired more rapidly than did the Clermont series

soils. The addition of fullerols to the Drummer soil did not change the rate nor the net amount of CO_2 respired with respect to the water only controls; Drummer microcosms containing fullerol respired 38.9 ± 7.2 mg of CO_2 compared to the 32.1 ± 8.6 mg of CO_2 respired in the water-only controls. The addition in fullerols did however result in one time point, day 30 of the incubation, exhibiting a statistically significant increase above the control (i.e. 2.40 ± 0.12 $\mu g_{CO2}/mg_{soilC}\, d^{-1}$ and 1.87 ± 0.08 $\mu g_{CO2}/mg_{soilC}\, d^{-1}$, respectively). In contrast, the addition of fullerols had no observable impact on the respiration rate of the Clermont series soil at any time point or in the net flux during the total experiment. The increase in respiration rates of the autoclaved and chloroform fumigated microcosms over the course of the incubation indicates that the microbial population in these soils was able to recover, and emphasizes that they should be viewed as microcosms with a suppressed microbial community rather than as purely abiotic controls.

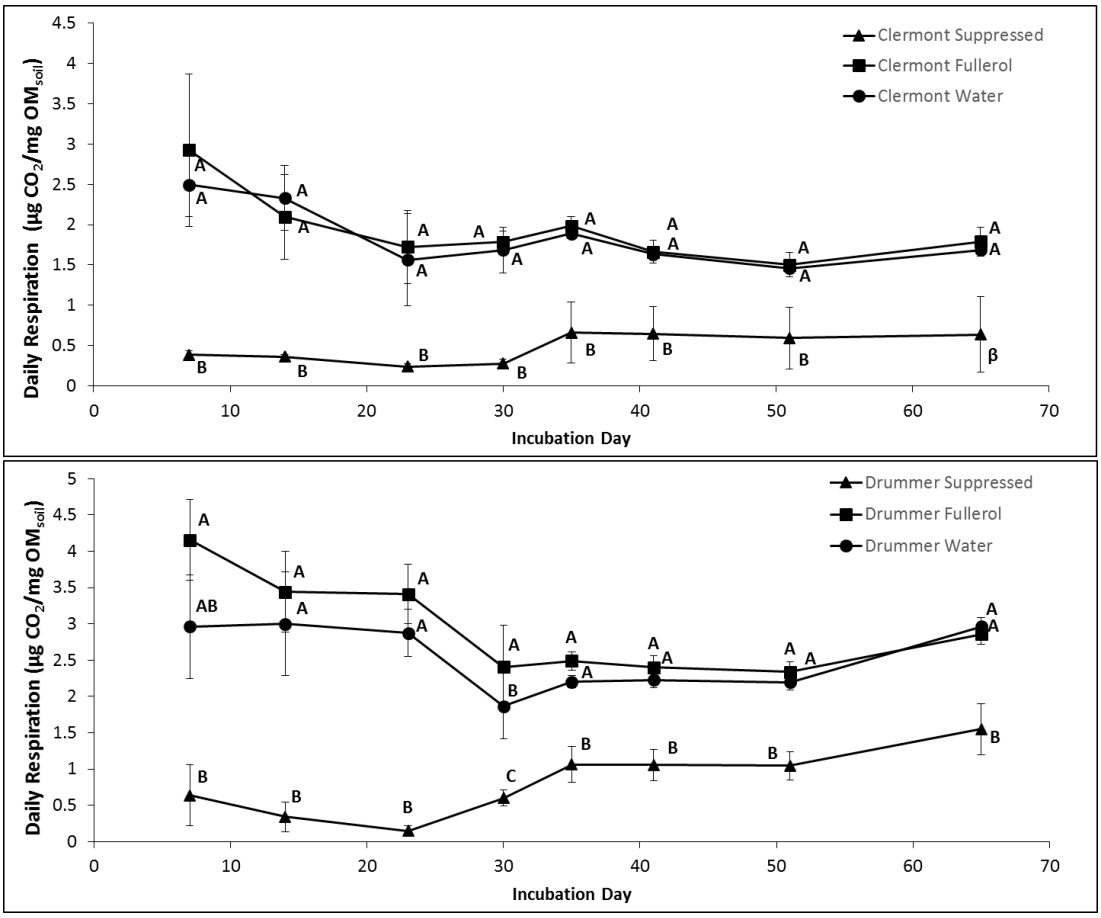

Figure 5.1 Daily respiration of soil microcosms containing Clermont series soil (top) and Drummer series soil (bottom). Treatments without shared letters indicate significant differences between treatments (1-way ANOVA, Tukey's HSD Post-Hoc) ($\alpha = 0.05$) at a given time point. Error bars represent standard error.

Although not statistically significant, the observed increase in soil respiration following addition of fullerols in the Drummer, but not Clermont soil, is noteworthy as it is in contrast to our recent work on the coupled photo-chemical/biotic degradation of C_{60} fullerenes. In that study we found that the addition of pristine fullerenes decreased net respiration in the Clermont series soil (CHAPTER 4), a finding which demonstrates the potential toxicity of these materials to soil microorganisms. No such repression of soil respiration is observed for either soil in the present study, which suggests that

microbial responses to the highly oxygenated fullerols is fundamentally different to the response of pristine fullerenes.

5.4.2 Isotopic composition of headspace and mineralization of ^{13}C-fullerol in controls

In order to assess the contribution of abiotic oxidation of fullerols a series of controls were established including soil-free and microbially suppressed soils. Based upon the amount of carbon evolved from these controls over the course of the 65 day incubation, soil-free controls mineralized 0.06 mg (8.8%) of the added fullerol C. Although care was taken in shielding microcosms from exposure to light, exposure of the controls to light during sampling did occasionally occur. The role of light exposure in mineralizing CNM has been thoroughly researched, and evidence suggests that this mineralization would occur more rapidly with more oxidized CNM (Hou and Jafvert 2009; Su 2013). Fullerols may have been partially mineralized by auto-oxidation; dissolved, condensed aromatic substances such as naturally occurring humic acid have been demonstrated to undergo auto-oxidation (Swift and Posner 1972). The abiotic and dark mineralization of the more condensed C_{60} fullerenes has also been noted, and Su *et al.* reported the transformation of ~10 % of fullerenes after incubation in the dark for 30 days (Su 2013). Unfortunately, the water used to prepare the fullerol suspensions were not purged of dissolved oxygen before incubation and solution oxygen significantly increases the mineralization dissolved organic carbon and fullerenes in both biotic and abiotic studies (Swift and Posner 1972; Bastviken *et al.* 2004; Su 2013). Regardless of the mechanism of mineralization, it is important to note that the soil-free controls mineralized significantly less than microcosms containing living soils.

Headspace of Drummer and Clermont microcosms containing microbially suppressed soils were found to contain ^{13}C-enriched CO_2 from the mineralization of added fullerols. The abundance of ^{13}C-enriched CO_2 produced by microbially suppressed Drummer soil microcosms increased over time reaching a maximum value of 22.5 ± 6.2 ‰ at day 65 which may be a result of the progressive recovery of the soil microbial community over time (Figure 5.2). This recovery is also evident in the increased respiration rate of these microcosms over time (Figure 5.1). The $\delta^{13}C$ values of the microbially suppressed Clermont soils were statistically indistinguishable from the healthy soils that contained fullerols. However, over the first 23 days the suppressed microcosms exhibited lower (though not significantly at $\alpha = 0.05$) ^{13}C-enrichment than the healthy treatments. As with the suppressed Drummer microcosms, Clermont headspace CO_2 became progressively more ^{13}C enriched over the course of the incubation, particularly following day 23. Soil respiration also increased over this time period suggesting that the microbial community may have recovered enough to significantly mineralize fullerols by this time. Despite the observable difference in headspace ^{13}C enrichment between healthy and suppressed Clermont microcosms, ANOVA was unable to determine that these differences were statistically significant. We attribute this to the significant variability in headspace ^{13}C between replicates of the suppressed Clermont soils. Respiration occurred so slowly in these soils that occasionally the quantity of CO_2 accumulated fell below the calibration range of the instrument, resulting in decreased analytical precision with very small sample volumes. This effect can be seen in the size of the error bars corresponding to the suppressed

Clermont microcosms in Figure 5.2, particularly early in the incubation when respiration rates were lowest.

The $\delta^{13}C$ values of the CO_2 respired by the water-only controls in the Drummer (between -18.4 ± 1.2 ‰ and -20.3 ± 0.3 ‰) and Clermont microcosms (between -16.4 ± 0.79 ‰ and -20.7 ± 0.12 ‰, see figure 5.2) are expected values for the two soils given their bulk carbon isotopic composition of -18.7 ‰ and -20.8 ‰ respectively (Table 5.1). Although the relationship between the isotopic composition of soils and the CO_2 respired from SOC varies with time, these values tend range within -2 and +3 ‰ of the mean soil values using similar microcosm designs (Creamer *et al.* 2011).

5.4.3 Differentiation of ^{13}C-fullerol and native soil carbon respiration

The inclusion of ^{13}C-enriched fullerols resulted in a significant enrichment of ^{13}C in headspace CO_2, indicating that the fullerols were readily mineralized in the soils (Figure 5.2). Microcosms containing Drummer soil respired CO_2 with an isotopic composition of 157.9 ± 20.1 ‰ when first sampled at day 7 of the incubation. The headspace in these microcosms became progressively less ^{13}C enriched as the incubation progressed, at an average rate of 2.8 ‰ per day for the first 30 days. Between days 30 and 65 headspace CO_2 remained relatively consistent between 84.6 ± 8.3 ‰ and 93.9 ± 5.4 ‰. Headspace in Clermont microcosms was less enriched at the first time point (43.0 ± 7.9 ‰) than were Drummer microcosms. However, Clermont microcosm headspace became more enriched in ^{13}C over the course of the incubation, reaching a maximum isotopic composition of 103.0 ± 7.1 ‰ on day 51.

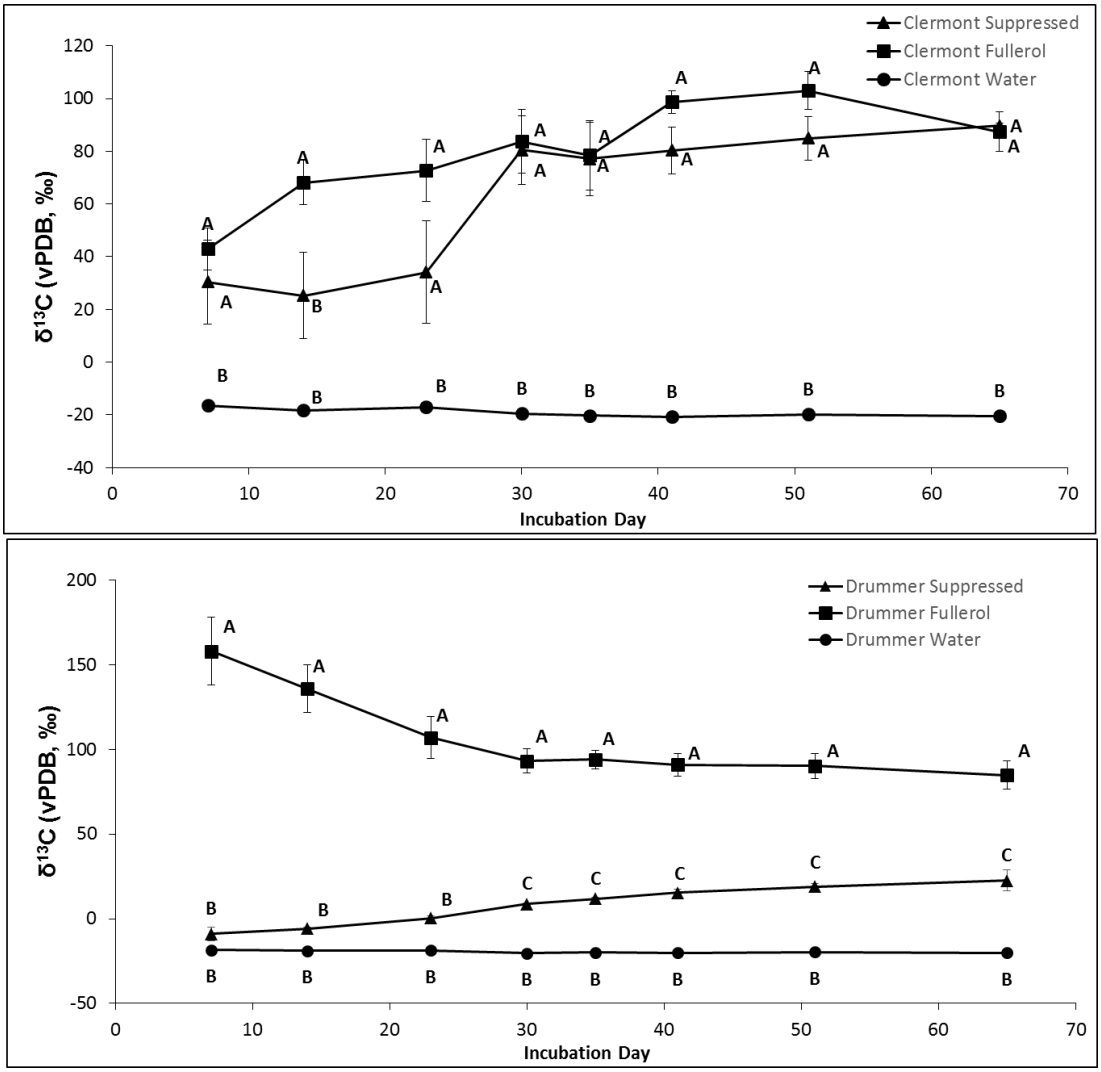

Figure 5.2 Isotopic composition of headspace CO_2 respired from soil microcosms containing Clermont series soil (top) and Drummer series soil (bottom). Treatments without shared letters indicate significant differences between treatments (1-way ANOVA, Tukey's HSD Post-Hoc) ($\alpha = 0.05$) at a given time point. Error bars represent standard error.

Based upon isotopic composition of respired CO_2 the mass of fullerol C mineralized could be calculated (see APPENDIX). Over the course of the 65 day incubation, significant quantities of fullerol were mineralized; live Drummer microcosms mineralized an average of 1.38 ± 0.32 mg of C_{60} fullerol C, equivalent to 59.1 % of the

added fullerol. The microbially suppressed Drummer microcosms mineralized on average 0.09 ± 0.06 mg of fullerol C, corresponding to degradation of 4.07 % of added fullerol C. Living and suppressed Clermont microcosms mineralized 0.18 ± 0.05 mg (25.9%) and 0.05 ± 0.02 mg (6.7%) of added fullerol C, respectively.

The lower rate of fullerol mineralization in the Clermont series soil as a result of fullerol addition is also interesting in that soils with comparatively lower clay content have been shown to be relatively more sensitive to the degradation of highly condensed contaminants (e.g. polyaromatic hydrocarbons (PAHs) and CNM) than are higher clay soils, likely as a result of the considerably affinity of some clay minerals for binding these contaminants (Muller *et al.* 2007). For example, Carmichael *et al*. found silt and clay content was inversely related to PAH degradation in a range of soils and was in fact a larger driver of PAH transformation than either microbial community or PAH structure (Carmichael and Pfaender 1997). If soil clay content did sorb fullerols, soils with low clay content (e.g. Clermont) might be expected to mineralize them rapidly than a more clay rich soil (e.g. Drummer). The impact of clay sorption of condensed compounds may be offset in this study by a number of other differences between the Drummer and Clermont soils. The Drummer series soil has a higher abundance of bacteria (Figure 5.4) and organic matter (Table 5.1). Natural organic matter has been observed to stabilize CNM in suspension (Chen and Elimelech 2007; Hyung *et al.* 2007) decreasing aggregation and increasing transport throughout the soil (Espinasse *et al.* 2007; Chae *et al.* 2015). Thus the relatively high organic matter content of the Drummer soil might

facilitate transport of the fullerols throughout the soils, increasing their exposure to and degradation by resident soil microorganisms.

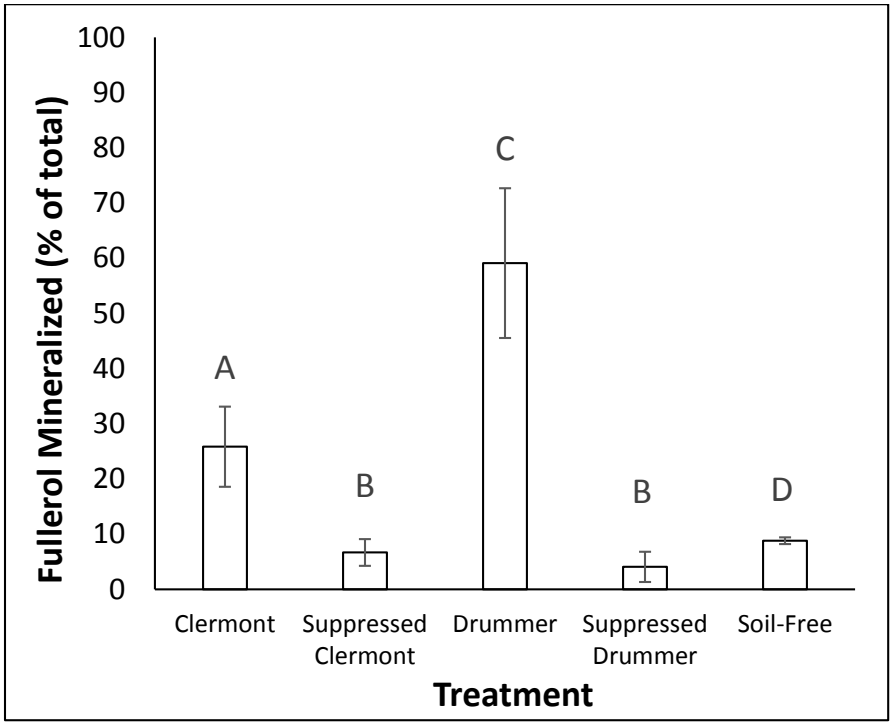

Figure 5.3 Percentage of total fullerols mineralized to CO_2 in each microcosm. Treatments without shared letters indicate significant differences between treatments ($\alpha = 0.05$). Error bars represent standard error.

The decay rates observed for fullerols in this study are substantially higher than those reported for pristine or low functionality CNM such as C_{60} fullerenes or CNT. Hartmann *et al.* (2011) found no measurable mineralization of fullerenes following prolonged exposure to indirect lighting, while a recent study by Parks *et al.* (2015) found a SWCNT degradation rate of <0.33 ng/day in liquid cultures, a rate corresponding to the degradation of less than 21.5 ng of SWCNT over a 65 day incubation In a companion study to this fullerol degradation work (CHAPTER FOUR) we investigated the degradation rate of a photo-chemically oxidized C_{60} added to the same Clermont series

soil and found that the irradiated C_{60} fullerenes degraded at an average rate of 180.9 ng/day; more than a 10 fold slower rate compared to the fullerol degradation rate (2.7 µg/day) reported herein. This distinction underscores the multiple effects of increased surface functionalization found in fullerols, as we should expect highly solubility and greater ease of bond cleavage with lower aromaticity and increased hydroxyl content of the synthetic fullerol. The only other study to date investigating the biotic degradation of fullerols, Schreiner *et al.,* reported the mineralization of 1 mg of fullerols over a 16 week period, giving an average mineralization rate of 8.9 µg/day. However, the CNM loading in that study was significantly higher than in the present study (35 mg vs. 5.3 mg for Drummer microcosms). As a result the mineralization presented in Schreiner *et al.* corresponds to the mineralization of only 2.86 % of fullerol mineralized over a 16 week incubation which is significantly less than the observed mineralization of 59.1% over 4 weeks by the Drummer series soil in the present study. This discrepancy is not surprising however, as single-culture studies investigating contaminant degradation typically report much lower rates of mineralization than do studies involving complex microbial consortia (e.g. those found in soils), as few microorganisms possess the necessary suite of degradative enzymes to fully convert a xenobiotic molecule to CO_2 themselves (De Schrijver and De Mot 1999; Haritash and Kaushik 2009). In fact, Schreiner *et al.,* found that one the major transformations of the fullerols in single-culture system studied was the fungal bleaching of fullerols without complete oxidation or metabolic update. Similarly, Boonchan *et al.* reports that significant degradation of high molecular-weight PAH occurs only in fungal-bacterial cocultures, and does not

occur when in axenic cultures. The rapid mineralization of CNM reported in this study thus underscores the importance of both CNM surface chemistry and incubation substrate when considering the environmental fate of a nanomaterial.

5.4.4 Fullerol degradation is laccase and peroxidase independent

Oxidative enzyme activity was measured by incubation of soil homogenates with L-DOPA and spectroscopic quantitation of the reaction product, dopachrome, at 460nm. The inclusion of C_{60} fullerols to soil microcosms did not significantly impact the activity of oxidative enzymes in the phenol oxidase and peroxidase enzyme family, regardless of soil type. Phenol oxidase activity in Clermont microcosms containing fullerol was found to be 0.488 ± 0.05 and 0.546 ± 0.08 µmol dopachrome $Hr^{-1}g_{soi}l^{-1}$ in microcosms containing only water. Peroxidase activity was found to be 2.34 ± 0.17 and 2.36±0.16 µmol dopachrome $Hr^{-1}g_{soi}l^{-1}$ in fullerol and water only Clermont microcosms respectively. Drummer microcosms containing fullerols had an average phenol oxidase activity of 0.584 ± 0.10 and a peroxidase activity of 1.32 ± 0.20, while corresponding water only microcosms had respective activities of 0.530 ± 0.11 and 1.33 ± 0.20 µmol dopachrome $Hr^{-1}g_{soi}l^{-1.}$ The inability of C_{60} fullerol to alter activity of these enzymes is noteworthy as a previous study using similar methods reported that pristine C_{60} fullerenes decreased the apparent activity of peroxidase enzymes by 14.5% (Berry *et al.* 2015) while pure culture studies utilizing carbon nanotubes report increased activity of these enzymes when the nanotubes are functionalized with oxygen containing groups (Allen *et al.* 2008; Zhao *et al.* 2011; Berry *et al.* 2014). Schreiner *et al.* (2009) observed bleaching of fullerols in growth media when incubated with the wood decay fungi

Trametes versicolor and Phlebia tremellosa, fungi known to produce an array of powerful oxidative enzymes (Schreiner *et al.* 2009) and suggested an extracellular degradation pathway involving both hydrolytic and oxidative enzymes. In this study we report significant degradation of C_{60} fullerols in the apparent absence of increased oxidative enzyme activity, which suggests that either intracellular oxidative or non-oxidative extracellular are the primary drivers of CNM degradation certain soils. In light of this potentially conflicting data on the role of oxidative enzymes in CNM degradation it is important to acknowledge that findings from such cell-free and pure culture studies are not always directly transferable to more complex systems such as soils where many additional variables such as sorption of clay and mineral surfaces can control apparent enzyme activity (Sinsabaugh *et al.* 2009; Sinsabaugh 2010).

5.4.5 Bacterial Abundance and Microbial Community Structure

Bacterial abundance, defined herein as the number of copies of the 16S rRNA gene per gram of dry soil as determined by qPCR was significantly altered with the addition of fullerols in both soils. Clermont microcosms containing fullerol had an average bacterial abundance of 3.83×10^7 copies per gram soil compared to 2.58×10^7 copies per gram in microcosms that did not contain fullerols. Bacterial abundance in Drummer soil microcosms similarly increased from 2.49×10^8 to 3.57×10^8 copies per gram soil when fullerol was included. As intended, soils of both types that had been autoclaved and fumigated had significantly fewer copies of the 16S rRNA gene with suppressed Drummer soils containing 1.34×10^7 copies per gram soil. Despite the decrease in abundance achieved by the sterilization protocols used, bacteria are still

quite abundant by the end of the incubation period. Insufficient DNA was extracted from suppressed Clermont microcosms for successful qPCR analysis

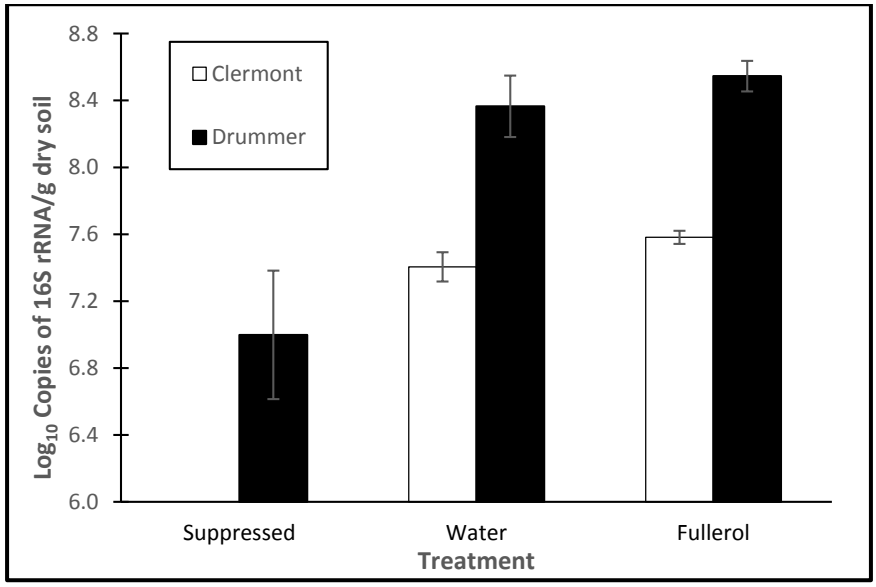

Figure 5.4 Bacterial abundance in Clermont and Drummer soils for different treatments, calculated as the copy number of 16S rRNA gene per gram of dry soil. Each point in the graphic represent the average of fifteen data points (Triplicate qPCR reactions for each of the replicates from each treatment), and error bars represent standard error. The efficiency of the qPCR was higher than 97% (slopes ~-3.3) and the correlation coefficient higher than 0.99. DNA concentration of microbially suppressed Clermont soils was below threshold for successful qPCR and is omitted.

Although both soils had an increase in bacterial abundance when incubated with fullerols, only the Drummer series soil had significant differences in microbial community structure as determined by DGGE fingerprinting. Cluster analysis indicates that differences in community structure are small, with the cluster predominantly populated with water only microcosms having a Dice similarity of ~90 % to the cluster comprised entirely of fullerol containing microcosms. Although relatively small, the difference in microbial community in the clay and organic rich Drummer soil but not the

Clermont soil with less organic content is noteworthy because previous studies on the impact of CNM on microbial community structure that used Drummer series soils consistently report no difference following addition of C_{60} fullerenes (Tong *et al.* 2007) or CNTs (Tong *et al.* 2012). The inability of CNM additions to induce changes in microbial community in this soil (while readily causing changes in other soils) is often attributed to the high organic matter content which is thought to be able to stabilize CNM suspensions through sorption effects, as discussed above (Tong *et al.* 2012). While stabilization of CNM by organic matter may help to increase dispersal throughout a soil by preventing aggregate formation (Chen and Elimelech 2007; Espinasse *et al.* 2007; Chen and Elimelech 2008), this same process may act to decrease CNM toxicity (Li *et al.* 2008). Although the fullerols in this study have a high surface oxygen content and are readily soluble in water, properties of the soil solution are still expected to be a major driver in CNM suspension stability (Yang *et al.* 2013). The simultaneous increase in bacterial abundance and facile mineralization of added fullerols suggests that changes in microbial community structure under these conditions may be the result of CNM being used as a carbon source rather than a toxin, a role that is facilitated by increased stabilization and transport of C_{60} fullerol in the microcosm soil.

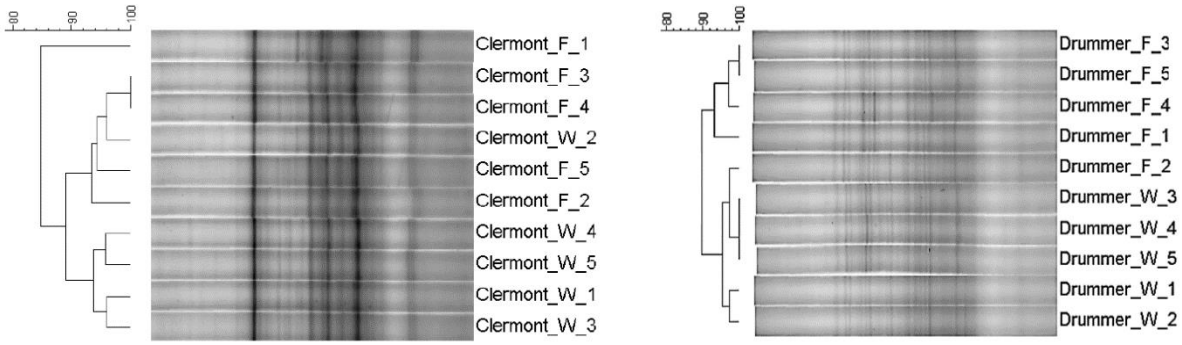

Figure 5.5 Clustering analysis of the bacterial community structure in Clermont (left) and Drummer (right) soils after different treatments. Dendrogram based on Dice similarities and constructed using UPGMA. Each lane corresponds to a soil sample, each treatment has 5 replicates. First number after the name of the soil corresponds to the treatment (F = fullerol, W = water), and the following number represents the technical replica.

5.4.6 Microbial uptake of fullerol C

. No significant differences in the PLFA abundance of individual guilds was noted (figure 5.6). In general the PLFA profile of both Clermont and Drummer soils was dominated by Gram positive bacteria. For the Clermont soil, 34.22 ± 0.94 and 34.11 ± 1.20 % of the PLFA were Gram positive in the water-only and fullerol treatments, respectively. Drummer soils have similar Gram positive abundance at 32.80 ± 0.78 and 31.02 ± 1.22 for water and fullerol treatments, respectively. Drummer soils had significantly more PLFA from Gram negative sources than the Clermont series (Drummer Water = 11.21 ± 1.69, Drummer Fullerol = 12.27 ± 1.27, Clermont Water = 2.08 ± 0.24, Clermont Fullerol = 2.24 ± 0.31). Notably absent from the PLFA of either soil used in this study are the commonly used fungal biomarkers 18:2ω6,9c and 18:2ω6,9t. As a result, there are no PLFA that can be clearly attributed to fungi in the two soils used herein. This finding is contrasted by a recent PLFA analysis of a Drummer series soil that

reported at a fungal contribution of at least 17% (Orr *et al.* 2015). However, it that study 18:1ω9c/t were considered fungal biomarkers. Although 18:1ω9c/t are occasionally used as a fungal biomarkers (Bird *et al.* 2011; Creamer *et al.* 2015) we have not included them in this grouping in our analyses, as previous studies have found that 18:1ω9c/t is poorly correlated with fungal biomass in the absence of 18:2ω6,9c/t, especially in agricultural soils like those used in this study (Frostegard *et al.* 2011). Instead we opted to classify 18:1ω9c/t as a non-specific bacterial biomarker as it is frequently cited as being a significant component of bacterial phospholipids (Zelles 1999; Schoug *et al.* 2008). Although fungi are often significantly less plentiful in agricultural soils, likely as a result of increased sensitivity to tillage practices (Guggenberger *et al.* 1999; Six *et al.* 2004; Six *et al.* 2006) it is unlikely that fungi are completely absent from the soil. Instead, the other less specific biomarkers likely include fungal biomass.

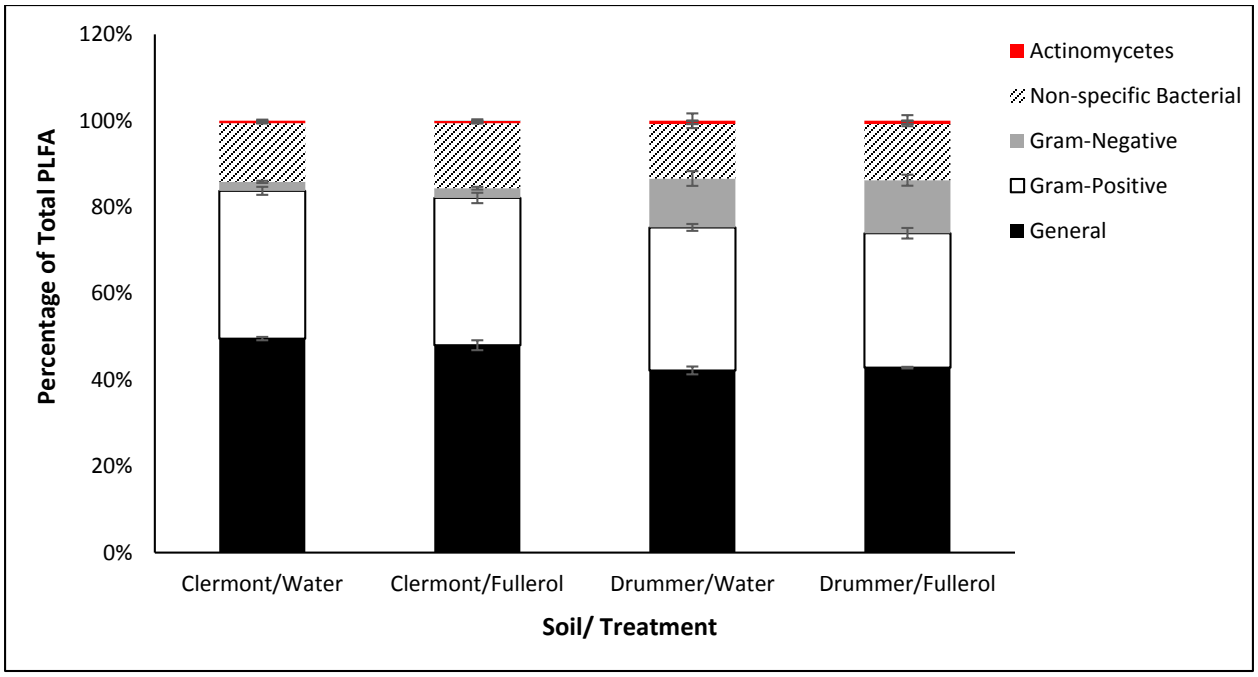

Figure 5.6 Percent contributions of microbial guilds to total PLFA extracted. Error bars indicate standard error.

Principle component analysis of PLFA extracted from microcosms highlights differences in microbial community structure between microcosms of in the contrasting soils and receiving different treatments (Figure 5.6). PLFA from the different soils separate along PC1, which accounts for 51.1 % of the total observed variance. Treatment type is partially separated along PC2 (accounting for 26.7% of variance) with autoclaved Drummer microcosms very clearly segregating along this axis while separation among Clermont soil microcosms is less complete. While soil type clearly has a significant impact on the PLFA composition of the microbial community ($p = 0.001$ with PERMANOVA), the impact of fullerol exposure on the PLFA composition of the community is not significant ($p = 0.516$ for all soils). This finding is broadly consistent with our previous characterization of soil microbial communities by DGGE, which found

only small shifts in community structure following fullerol addition. However, while DGGE found a significant difference in clustering between treatments, we do not observe the same significant shift in PLFA composition. These results are consistent with shifts in the microbial community structure of the soil, but within the microbial guild as assessed by PLFA analysis (e.g. the substitution of one gram bacteria for another with a similar PLFA profile).

While fullerol treatment did not have a significant impact on the overall PLFA fingerprint, individual PLFA were found to significantly contribute to separation between treatments using the SIMPER analysis in PRIMER. The monounsaturated PLFA 16:1ω9c is a major driver of separation between both soils and treatment groups, contributing 44.6% to the separation between Clermont and Drummer soils when all treatments are considered. Separation between treatments in the Drummer series soil was also dominated by this PLFA (accounting for 41.8% of the observed separation). Discounting the autoclaved treatment, the largest drivers of separation between water and fullerol treatments when considering both soils are the mono-unsaturated PLFAs 16:1ω9c and 18:1ω9c (56.2 and 13.81 % separation respectively) and the branched-chain PLFA i15:0 (9.6 % of separation).

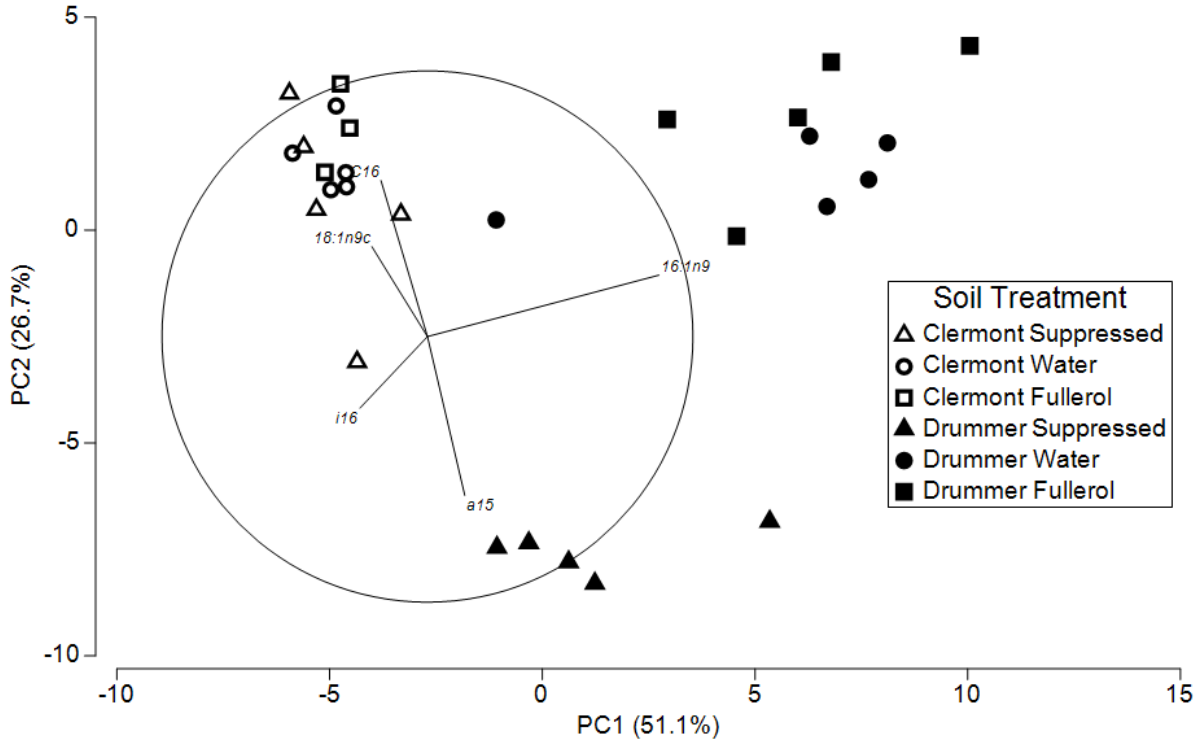

Figure 5.7 Principal component analysis of the proportional mol% of PLFA extracted from soil microcosms following incubation. Percentage of variance explained by a PC is given on the respective axis, the two PC plotted explain a total of 77.8% of the total variance. The overlaid vector map displays PLFA with Pearson correlations >0.30 along the PCs, with line length indicating size of loading along the axes. Due to formatting constraints imposed by the software, the PLFA previously described as 16:0 is labelled as C16 in the above figure.

The use of ^{13}C enriched fullerol in this study allows, for the first time, the quantification of microbial uptake of fullerol derived carbon in a soil. Table 5.2 lists the difference between the isotopic composition of PLFA extracted from fullerol treated Drummer microcosms and those extracted from fullerol-free controls. These values were used to calculate fractional contribution of fullerol C to microbial lipids and biomass C (as described in materials and methods and the APPENDIX). Of the 15 PLFA

Analyzed by CSIA, 12 were found to be significantly enriched in ^{13}C with respect to SOC and the corresponding PLFA grown in controls containing only water.

Table 5.2 Difference in ^{13}C content between PLFA extracted from fullerol and water only microcosms and the corresponding contribution of fullerol derived carbon to the total carbon content of the PLFA. Asterisks indicate a significant difference in isotopic composition between a PLFA extracted from fullerol containing soil and the corresponding PLFA from the water only controls ($\alpha = 0.05$).

PLFA	$\delta C_{Fullerol\ Lipid} - \delta C_{Control\ Lipid}$	Percent C from Fullerol
8:0	3.58 ± 1.81	0.10
10:0	0.55 ± 3.15	<0.05
12:0	2.40 ± 3.47	0.06
i14:0	4.96 ± 1.75*	0.13
i15:0	12.05 ± 2.09*	0.33
a15:0	7.82 ± 1.83*	0.21
i16:0	9.29 ± 1.15*	0.25
16:0	20.93 ± 4.72*	0.57
10Me16	42.81 ± 4.25*	1.16
17:1n?	9.57 ± 1.39*	0.26
17:1n?(2)	9.56 ± 2.01*	0.26
18:0	45.46 ± 3.11*	1.23
18:1ω9c/ 18:1n?	61.74 ± 2.55*	1.67
cy19	46.26 ± 3.31*	1.25

Using the mass and $\delta^{13}C$ of each PLFA, the fractional contribution of the fullerol sourced ^{13}C can be used to estimate the total mass of fullerol C incorporated into PLFA and biomass for both gram positive and gram negative microbial guilds (Table 5.3). This calculation is useful for distinguishing microorganisms actively engaged in uptake of

CNM carbon from those may be abundant but are less involved in assimilation of mineralized CNM. The Gram positive bacteria, accounting for 31.02 % of all extracted PLFA in the fullerol treated Drummer soil, derived just 0.27 % of PLFA carbon from fullerols while the Gram negative bacteria, with only 12.27 % of the total PLFA ascribed to their guild, derived 1.25 % of their PLFA carbon from the fullerols.

The affinity of Gram negative bacteria for labile fractions of condensed soil amendments has been previously noted in CSIA studies involving the degradation of pyrogenic organic matter (PYOM) (Steinbeiss *et al.* 2009; Bird *et al.* 2011). Conversely, Gram positive bacteria are frequently associated with more slowly degraded pools of soil carbon (Kramer and Gleixner 2008; Bird *et al.* 2011). These observations may help explain the difference in microbial uptake of CMN carbon by these groups in the present study; the highly soluble $^{13}C_{60}(OH)_{19\text{-}27}$ are degraded more readily by Gram negative bacteria as they are better suited to quickly utilize dissolved carbon sources rather than expend energy on extracelluar enzymes to break down complex organic matter, indeed previous studies have observed the uptake of C_{60} into Gram negative bacteria with minimal losses to viability (An and Jin 2012). If this generalization does indeed hold for CNM, one might expect Gram positive bacterial to preferentially incorporate carbon from less-functionalized (or pristine) CNM into their biomass.

Table 5.3 Contribution of Fullerol C to PLFA and Total Microbial Biomass.

	Characteristic PLFA	Total PLFA C (ng/microcosm)	Fullerol PLFA C (ng/microcosm)	Fullerol C Uptake (%)	Fullerol C in total Biomass (µg)
Gram Positive Bacteria	i14:0, i15:0, a15:0, i16:0	1646.1	4.4	0.27	0.25 ± 0.019
Gram Negative Bacteria	cy19	84.9	1.1	1.25	0.05 ± 0.007
Actinomycetes	10Me16	45.6	0.5	1.16	0.03 ± 0.002
Non-specific Bacteria	Unknown monounsaturated, 18:1ω9c	1059.8	16.4	1.56	0.71 ± 0.112
General	8:0, 10:0, 12:0, 16:0	1742.2	12.2	0.70	0.64 ± 0.044
Whole Soil	All of Above	4578.6	34.6	0.76	1.78 ± 0.163

The only previous study to assess the uptake of fullerol derived carbon into microbial biomass reported a CNM contribution to PLFA C of < 0.14 % by the cultured white-rot fungi *Phlebia tremellosa* (Schreiner *et al.* 2009). As discussed above in the context of CNM mineralization to CO_2, it is not surprising that a complex mixture of microorganisms was able to better incorporate nanocarbon, as numerous complimentary degradative systems are able to behave synergistically (Bouchez *et al.* 1999; Boonchan *et al.* 2000; Peng *et al.* 2008). This finding is reinforced by the observation that a diverse group of microorganisms can be seen to incorporate nanocarbon into their biomass in the present study, indicating that multiple microbial guilds are utilizing the CNM as a carbon source.

In total, the PLFA of soil microbial community accounts for the uptake of 34.6 ng of the fullerol C added to the Drummer microcosms while total biomass (calculated as described in the materials and methods) is estimated to contain 1.78 µg fullerol carbon. Since CNM were added to these microcosms at loading of 2.34 mg fullerol C, estimated

total biomass uptake accounts for ~0.08% of fullerol C. As the Drummer soil community oxidized 1.31 mg of added fullerols (live Drummer soil minus suppressed controls) the uptake of only 1.78 µg indicates a strong preference for microbial oxidation of fullerols over uptake (uptake : mineralization = 0.0014 : 1). Although microbial biomass was observed to contain significantly more fullerol derived carbon in this study than in *Schreiner* et al., it is important to note that the rate of incorporation reported herein is small in comparison to more conventional microbial substrates (e.g. Wood or plant litter). For example *Santos* et al. reported that soil PLFA were found to incorporate 16.2 % of carbon from the degradation of pine wood over only 42 days (Santos *et al.* 2012). However, studies focusing on the degradation of more condensed natural substrates (e.g. PyOM) report mineralization rates and microbial uptake similar to those found in the current study (Kuzyakov *et al.* 2009). It is important to note that only a small component of total microbial biomass is being assessed in this study.

5.5 Conclusions

As a follow-up to the work presented in CHAPTER FOUR, this study examines CNM degradation and microbial substrate utilization by utilizing ^{13}C-enriched C_{60} fullerols as a sensitive tracer of the environmental fate of highly functionalized CNM. Using these CNM, we report for the first time the rates of microbially driven mineralization of C_{60} fullerols in soils and the subsequent incorporation of CNM derived carbon into microbial biomass. As hypothesized, the fullerols in this study were rapidly mineralized following addition to both soils. The mineralization observed in this study stands in stark contrast to the negligible mineralization reported in previous studies of

more condensed CNM such as CNT (Parks *et al.* 2015) and C_{60} fullerenes (Hartmann *et al.* 2011) and indicates the crucial roles of surface chemistry when assessing the environmental fate of similar materials. The use of two agricultural soils with contrasting properties also allow us to gauge importance of soil properties on facilitating the mineralization of CNM. While we found that the more clay and organic rich Drummer series soil was able more readily mineralize fullerol than a sandier, less organic soil (59.1 versus 25.9 % CNM mineralization) it was not possible to determine whether this was the result of edaphic properties of the unique microbial communities of the two soils. Finally, by using CSIA to trace ^{13}C into microbial PLFA, we were able to determine for the first time which microbial populations might be best suited for the degradation of CNM. The findings of this study should prove useful in informing future works on the degradation of CNM in soils by identifying important processes and microbial communities that can expected to control the environmental fate of CNM.

5.6 Acknowledgements

The authors acknowledge support from the Environmental Protection Agency under award RD-83485801-0

CHAPTER 6. CONCLUSIONS AND FUTURE DIRECTIONS

6.1 Summary

As the synthesis of CNM continues to grow with lowering production costs and increasing applications, so too does their potential to accumulate in the environment (De Volder *et al.* 2013, Zhang *et al.* 2013). In order to understand the environmental risks imposed by CNM, it is important to study more than their potential toxicity; we must also understand the processes and properties that contribute to their transformation and decay. Without this knowledge it is impossible to assess the potential threats of CNM accumulation in the environment.

Each study in this dissertation helps to further the current understanding on the properties that control CNM degradation by microorganisms. In CHAPTER TWO we demonstrated the crucial role of surface functionalization in the enzymatic response of the saprotrophic fungi *T. versicolor* and *P. tremellosa* towards CNT. With a powerful arsenal of degradative enzymes these organisms have the potential to be major degraders of CNM in certain environments (Schreiner *et al.* 2009, Berry *et al.* 2014). These model fungi did not respond enzymatically to the presence of purified and unfunctionalized CNT, they did however exhibit increased enzyme activity when grown with impure or surface functionalized tubes. Surface functionalized CNT contained

within polymer composites had little impact on enzyme activity, further emphasizing the importantance of CNM surface/microbial interaction in stimulating enzyme production (CHAPTER THREE).

While previous studies on the mineralization of the CNM reported negligible or very slow decomposition of CNM (Hartmann *et al.* 2011, Avanasi *et al. 2014,* Parks *et al.* 2015) we found that when coupled with abiotic processes such as photo-degradation, ~0.78 of C_{60} fullerenes added to soil were mineralized over the course of a two month incubation (CHAPTER FOUR). Mineralization of fullerenes in this study was related to photo-irradiation duration, providing a strong link between light induced surface oxygenation of CNM and subsequent degradation in soil (Hou *et al.* 2009, 2010). These results were the first to link abiotic surface changes to measurable decay in an environmental substrate. A follow-up study using highly functionalized ^{13}C-enriched fullerols further demonstrated the relationship between surface functionalization and mineralization in soils (CHAPTER FIVE). The amount of fullerols mineralized over the 65 day incubation varied between soils, with the more clay and organic matter rich Drummer series soil mineralizing ~59.1% of added fullerols and the lower-carbon Clermont series soil degrading ~25.9% of the added fullerols. This difference indicates that edaphic properties may serve as significant controls on the biotic mineralization of CNM, especially when highly functionalized. The use of a stable isotope label also allowed for the tracing of fullerol carbon into microbial PLFA and the determination of the microbial communities most activity in the uptake of mineralized fullerols. We found that Gram negative bacteria were able to incorporate significantly more fullerol

carbon into their biomass than Gram positive bacteria (including Actinomycetes) were. This is the first ever study to report the incorporation of CNM derived carbon into microbial biomass extracted from an environmental substrate.

Together, these studies reveal that, as hypothesized, surface chemistry is a major control on the microbial degradation of CNM by influencing the production of extracellular oxidative enzymes (CHAPTER TWO) and facilitating degradation in soils (CHAPTERS FOUR and FIVE). We also demonstrated the importance of considering abiotic transformative processes when investigating biotic mineralization of CNM, as these processes are coupled. The importance of the environmental processes and CNM properties studied herein in controlling the microbial degradation of CNM will be a useful in informing future studies investigating the environmental fate of CNM.

6.2 Future Directions

Although this dissertation contributes important insights on environmental degradation of CNM, there are still plenty of unanswered questions surrounding the environmental fate of these materials. One important question left unanswered is the role of extracellular enzymes in degrading CNM. The results of enzyme assays conducted in CHAPTER TWO and CHAPTERS FOUR and FIVE reveal a potential disconnect between degradation studies conducted on different CNM and in different substrates. While the white-rot fungi in CHAPTER TWO exhibited increased enzymatic activity in the presence of surface functionalized CNT, exploring the mechanism behind this response was beyond the scope of the study. Furthermore, despite obvious mineralization of both C_{60} fullerenes and fullerols in soil, no elevation in either laccase

or peroxidase enzymes was observed despite the presence of surface functionalized CNM. There are a number of potential explanations for this observation; agricultural soils, especially those that have undergone tillage in the past are frequently depleted in fungi (Guggenberger *et al.* 1999, Six *et al.* 2006) the organisms most frequently associated with the production of the enzymes (Leonowicz *et al.* 1999, Thurston 1994). However, the possibility remains extracellular enzyme production is only promoted when the organism encounters a CNM that it cannot possibly degrade intracellularly. A CNT might have an aspect ratio of 1:1,000,000 making cellular uptake impossible while C_{60} is significantly smaller; Gram negative bacteria have been observed taking up fullerene particles with little loss in viability. One potential study that would help clarify the relationship between soil, CNM, and enzymatic response would involve conducting incubations of both purified, unfunctionalized SWCNT and functionalized SWCNT in a forest soil with a large population of fungi.

The precise role of soil properties on controlling the microbial response to CNM is also poorly understood. Although clay minerals have been observed adsorbing and protecting PAH from degradation (Carmichael and Pfaender 1997), the same process has not be observed to occur with CNM. The role of dissolved organic matter on CNM solutions is better understood, as numerous studies have reported that DOM is able to stabilize CNM, preventing aggregation and promoting transport (Chen and Elimelech 2009; Espinasse *et al.* 2007). However, only a single study has attempted to investigate the impacts of clay and organic matter content in soils with CNM degradation, and that study was conducted using CNM in which mineralization is poorly observed, even under

the most favorable circumstances (Avanasi *et al.* 2014). Future microcosm incubation studies examining the mineralization of CNM should include enough different soils to generate a factorial experimental design that includes varying levels of clay and organic matter. Mineralization studies could then be conducted with CNM of different functionalities to help elucidate the interactions between CNM surface chemistry, edaphic properties, and mineralization in an environmentally relevant study.

These suggested experiments address only a few of the many unknown factors that control the environmental fate of CNM. As this dissertation demonstrates the role of surface functionalization in promoting CNM degradation, future studies should take care to address the potential interactions between CNM surface chemistry and environmental substrates when studying microbial degradation of CNM.

REFERENCES

REFERENCES

Adekunle, A. E., Wang F., Hu J. H., Ma A. Z., Guo C., Zhuang G. Q. and Liu C. Z. (2015). "Chitosan multiple addition enhances laccase production from trametes versicolor." Bioprocess and Biosystems Engineering **38**(10): 1973-1981.

Allan, C. R. and Hadwiger L. A. (1979). "Fungicidal effect of chitosan on fungi of varying cell-wall composition." Experimental Mycology **3**(3): 285-287.

Allen, B. L., Kichambare P. D., Gou P., Vlasova, II, Kapralov A. A., Konduru N., Kagan V. E. and Star A. (2008). "Biodegradation of single-walled carbon nanotubes through enzymatic catalysis." Nano Letters **8**(11): 3899-3903.

An, H. J. and Jin B. (2012). "Impact of fullerene particle interaction on biochemical activities in fermenting zymomonas mobilis." Environmental Toxicology and Chemistry **31**(4): 712-716.

Antolini, E. (2009). "Carbon supports for low-temperature fuel cell catalysts." Applied Catalysis B-Environmental **88**(1-2): 1-24.

Arias, L. R. and Yang L. J. (2009). "Inactivation of bacterial pathogens by carbon nanotubes in suspensions." Langmuir **25**(5): 3003-3012.

Auffan, M., Bottero J. Y., Chaneac C. and Rose J. (2010). "Inorganic manufactured nanoparticles: How their physicochemical properties influence their biological effects in aqueous environments." Nanomedicine **5**(6): 999-1007.

Ausman, K. D., Piner R., Lourie O., Ruoff R. S. and Korobov M. (2000). "Organic solvent dispersions of single-walled carbon nanotubes: Toward solutions of pristine nanotubes." Journal of Physical Chemistry B **104**(38): 8911-8915.

Avanasi, R., Jackson W. A., Sherwin B., Mudge J. F. and Anderson T. A. (2014). "C-60 fullerene soil sorption, biodegradation, and plant uptake." Environmental Science & Technology **48**(5): 2792-2797.

Avouris, P. (2002). "Molecular electronics with carbon nanotubes." Accounts of Chemical Research **35**(12): 1026-1034.

Bachilo, S. M., Benedetto A. F. and Weisman R. B. (2001). "Triplet state dissociation of c-120, the dimer of c-60." Journal of Physical Chemistry A **105**(43): 9845-9850.

Bakry, R., Vallant R. M., Najam-Ul-Haq M., Rainer M., Szabo Z., Huck C. W. and Bonn G. K. (2007). "Medicinal applications of fullerenes." International Journal of Nanomedicine **2**(4): 639-649.

Baldrian, P. (2003). "Interactions of heavy metals with white-rot fungi." Enzyme and Microbial Technology **32**(1): 78-91.

Baldrian, P. and Gabriel J. (1997). "Effect of heavy metals on the growth of selected wood-rotting basidiomycetes." Folia Microbiologica **42**(5): 521-523.

Bastviken, D., Persson L., Odham G. and Tranvik L. (2004). "Degradation of dissolved organic matter in oxic and anoxic lake water." Limnology and Oceanography **49**(1): 109-116.

Batley, G. E., Kirby J. K. and McLaughlin M. J. (2013). "Fate and risks of nanomaterials in aquatic and terrestrial environments." Accounts of Chemical Research **46**(3): 854-862.

Bell, A. A. and Wheeler M. H. (1986). "Biosynthesis and functions of fungal melanins." Annual Review of Phytopathology **24**: 411-451.

Bell, P. F., Chaney R. L. and Angle J. S. (1991). "Free metal activity and total metal concentrations as indexes of micronutrient availability to barley hordeum-vulgare (l) klages." Plant and Soil **130**(1-2): 51-62.

Berry, T. D., Clavijo A., Turco R. F. and Filley T. R. (2015). "Soil microbial response to photo-degraded c60 fullerenes." Environmental Pollution.

Berry, T. D., Filley T. R. and Blanchette R. A. (2014). "Oxidative enzymatic response of white-rot fungi to single-walled carbon nanotubes." Environmental Pollution **193**: 197-204.

Bianco, A., Kostarelos K. and Prato M. (2005). "Applications of carbon nanotubes in drug delivery." Current Opinion in Chemical Biology **9**(6): 674-679.

Bird, J. A., Herman D. J. and Firestone M. K. (2011). "Rhizosphere priming of soil organic matter by bacterial groups in a grassland soil." Soil Biology & Biochemistry **43**(4): 718-725.

Blanchette, R. A. (1991). "Delignification by wood-decay fungi." Annual Review of Phytopathology **29**: 381-403.

Boonchan, S., Britz M. L. and Stanley G. A. (2000). "Degradation and mineralization of high-molecular-weight polycyclic aromatic hydrocarbons by defined fungal-bacterial cocultures." Applied and Environmental Microbiology **66**(3): 1007-1019.

Bottini, M., Bruckner S., Nika K., Bottini N., Bellucci S., Magrini A., Bergamaschi A. and Mustelin T. (2006). "Multi-walled carbon nanotubes induce t lymphocyte apoptosis." Toxicology Letters **160**(2): 121-126.

Bouchez, M., Blanchet D., Bardin V., Haeseler F. and Vandecasteele J. P. (1999). "Efficiency of defined strains and of soil consortia in the biodegradation of polycyclic aromatic hydrocarbon (pah) mixtures." Biodegradation **10**(6): 429-435.

Camarero, S., Sarkar S., Ruiz-Duenas F. J., Martinez M. J. and Martinez A. T. (1999). "Description of a versatile peroxidase involved in the natural degradation of lignin that has both manganese peroxidase and lignin peroxidase substrate interaction sites." Journal of Biological Chemistry **274**(15): 10324-10330.

Capek, I. (2009). "Dispersions, novel nanomaterial sensors and nanoconjugates based on carbon nanotubes." Advances in Colloid and Interface Science **150**(2): 63-89.

Carmichael, L. M. and Pfaender F. K. (1997). "Polynuclear aromatic hydrocarbon metabolism in soils: Relationship to soil characteristics and preexposure." Environmental Toxicology and Chemistry **16**(4): 666-675.

Chae, S. R., Noeiaghaei T., Jang H. C., Sahebi S., Jassby D., Shon H. K., Park P. K., Kim J. O. and Park J. S. (2015). "Effects of natural organic matter on separation of the hydroxylated fullerene nanoparticles by cross-flow ultrafiltration membranes from water." Separation and Purification Technology **140**: 61-68.

Chae, S. R., Watanabe Y. and Wiesner M. R. (2011). "Comparative photochemical reactivity of spherical and tubular fullerene nanoparticles in water under ultraviolet (uv) irradiation." Water Research **45**(1): 308-314.

Chen, C. Y. and Jafvert C. T. (2011). "The role of surface functionalization in the solar light-induced production of reactive oxygen species by single-walled carbon nanotubes in water." Carbon **49**(15): 5099-5106.

Chen, K. L. and Elimelech M. (2007). "Influence of humic acid on the aggregation kinetics of fullerene (c60) nanoparticles in monovalent and divalent electrolyte solutions." Journal of Colloid and Interface Science **309**(1): 126-134.

Chen, K. L. and Elimelech M. (2008). "Interaction of fullerene (c-60) nanoparticles with humic acid and alginate coated silica surfaces: Measurements, mechanisms, and environmental implications." Environmental Science & Technology **42**(20): 7607-7614.

Coleman, J. N., Khan U., Blau W. J. and Gun'ko Y. K. (2006). "Small but strong: A review of the mechanical properties of carbon nanotube-polymer composites." Carbon **44**(9): 1624-1652.

Collins, P. G., Zettl A., Bando H., Thess A. and Smalley R. E. (1997). "Nanotube nanodevice." Science **278**(5335): 100-103.

Collins, P. J., Kotterman M. J. J., Field J. A. and Dobson A. D. W. (1996). "Oxidation of anthracene and benzo a pyrene by laccases from trametes versicolor." Applied and Environmental Microbiology **62**(12): 4563-4567.

Creamer, C. A., de Menezes A. B., Krull E. S., Sanderman J., Newton-Walters R. and Farrell M. (2015). "Microbial community structure mediates response of soil c decomposition to litter addition and warming." Soil Biology & Biochemistry **80**: 175-188.

Creamer, C. A., Filley T. R., Boutton T. W., Oleynik S. and Kantola I. B. (2011). "Controls on soil carbon accumulation during woody plant encroachment: Evidence from physical fractionation, soil respiration, and delta c-13 of respired co2." Soil Biology & Biochemistry **43**(8): 1678-1687.

D'Annibale, A., Ricci M., Leonardi V., Quaratino D., Mincione E. and Petruccioli M. (2005). "Degradation of aromatic hydrocarbons by white-rot fungi in a historically contaminated soil." Biotechnology and Bioengineering **90**(6): 723-731.

Darlington, A. B. and Rauser W. E. (1988). "Cadmium alters the growth of the ectomycorrhizal fungus paxillus-involutus - a new growth-model accounts for changes in branching." Canadian Journal of Botany-Revue Canadienne De Botanique **66**(2): 225-229.

De Schrijver, A. and De Mot R. (1999). "Degradation of pesticides by actinomycetes." Critical Reviews in Microbiology **25**(2): 85-119.

De Volder, M. F. L., Tawfick S. H., Baughman R. H. and Hart A. J. (2013). "Carbon nanotubes: Present and future commercial applications." Science **339**(6119): 535-539.

Degryse, F., Smolders E. and Parker D. R. (2009). "Partitioning of metals (cd, co, cu, ni, pb, zn) in soils: Concepts, methodologies, prediction and applications - a review." European Journal of Soil Science **60**(4): 590-612.

Dice, L. R. (1945). "Measures of the amount of ecologic association between species." Ecology **26**(3): 297-302.

Dilek, F. B., Erbay A. and Yetis U. (2002). "Ni(ii) biosorption by polyporous versicolor." Process Biochemistry **37**(7): 723-726.

Dunford, H. B. and Stillman J. S. (1976). "Function and mechanism of action of peroxidases." Coordination Chemistry Reviews **19**(3): 187-251.

Espinasse, B., Hotze E. M. and Wiesner M. R. (2007). "Transport and retention of colloidal aggregates of c-60 in porous media: Effects of organic macromolecules, ionic composition, and preparation method." Environmental Science & Technology **41**(21): 7396-7402.

Fenoglio, I., Greco G., Tornatis M., Muller J., Rayrnundo-Pinero E., Beguin F., Fonseca A., Nagy J. B., Lison D. and Fubini B. (2008). "Structural defects play a major role in the acute lung toxicity of multiwall carbon nanotubes: Physicochemical aspects." Chemical Research in Toxicology **21**(9): 1690-1697.

Flores-Cervantes, D. X., Maes H. M., Schaffer A., Hollender J. and Kohler H. P. E. (2014). "Slow biotransformation of carbon nanotubes by horseradish peroxidase." Environmental Science & Technology **48**(9): 4826-4834.

Fogarty, R. V. and Tobin J. M. (1996). "Fungal melanins and their interactions with metals." Enzyme and Microbial Technology **19**(4): 311-317.

Forrester, I. T., Grabski A. C., Burgess R. R. and Leatham G. F. (1988). "Manganese, mn-dependent peroxidases, and the biodegradation of lignin." Biochemical and Biophysical Research Communications **157**(3): 992-999.

Fortner, J. D., Lyon D. Y., Sayes C. M., Boyd A. M., Falkner J. C., Hotze E. M., Alemany L. B., Tao Y. J., Guo W., Ausman K. D., Colvin V. L. and Hughes J. B. (2005). "C-60 in water: Nanocrystal formation and microbial response." Environmental Science & Technology **39**(11): 4307-4316.

Franklin, A. D., Luisier M., Han S. J., Tulevski G., Breslin C. M., Gignac L., Lundstrom M. S. and Haensch W. (2012). "Sub-10 nm carbon nanotube transistor." Nano Letters **12**(2): 758-762.

Frostegard, A. and Baath E. (1996). "The use of phospholipid fatty acid analysis to estimate bacterial and fungal biomass in soil." Biology and Fertility of Soils **22**(1-2): 59-65.

Frostegard, A., Tunlid A. and Baath E. (1993). "Phospholipid fatty-acid composition, biomass, and activity of microbial communities from 2 soil types experimentally exposed to different heavy-metals." Applied and Environmental Microbiology **59**(11): 3605-3617.

Frostegard, A., Tunlid A. and Baath E. (2011). "Use and misuse of plfa measurements in soils." Soil Biology & Biochemistry **43**(8): 1621-1625.

Fukuda, R., Ogawa H., Nagata T. and Koike I. (1998). "Direct determination of carbon and nitrogen contents of natural bacterial assemblages in marine environments." Applied and Environmental Microbiology **64**(9): 3352-3358.

Gabriel, J., Baldrian P., Hladikova K. and Hakova M. (2001). "Copper sorption by native and modified pellets of wood-rotting basidiomycetes." Letters in Applied Microbiology **32**(3): 194-198.

Gadd, G. M. (1993). "Interactions of fungi with toxic metals." New Phytologist **124**(1): 25-60.

Galhaup, C. and Haltrich D. (2001). "Enhanced formation of laccase activity by the white-rot fungus trametes pubescens in the presence of copper." Applied Microbiology and Biotechnology **56**(1-2): 225-232.

Garbeva, P., van Veen J. A. and van Elsas J. D. (2004). "Microbial diversity in soil: Selection of microbial populations by plant and soil type and implications for disease suppressiveness." Annual Review of Phytopathology **42**: 243-270.

Gast, C. H., Jansen E., Bierling J. and Haanstra L. (1988). "Heavy-metals in mushrooms and their relationship with soil characteristics." Chemosphere **17**(4): 789-799.

Ge, C. C., Li W., Li Y. F., Li B., Du J. F., Qiu Y., Liu Y., Gao Y. X., Chai Z. F. and Chen C. Y. (2011). "Significance and systematic analysis of metallic impurities of carbon nanotubes produced by different manufacturers." Journal of Nanoscience and Nanotechnology **11**(3): 2389-2397.

Georgakilas, V., Tagmatarchis N., Pantarotto D., Bianco A., Briand J. P. and Prato M. (2002). "Amino acid functionalisation of water soluble carbon nanotubes." Chemical Communications(24): 3050-3051.

Gorczyca, A., Kasprowicz M. J. and Lemek T. (2009). "Physiological effect of multi-walled carbon nanotubes (mwcnts) on conidia of the entomopathogenic fungus, paecilomyces fumosoroseus (deuteromycotina: Hyphomycetes)." Journal of Environmental Science and Health Part a-Toxic/Hazardous Substances & Environmental Engineering **44**(14): 1592-1597.

Gottschalk, F. and Nowack B. (2011). "The release of engineered nanomaterials to the environment." Journal of Environmental Monitoring **13**(5): 1145-1155.

Gramss, G., Kirsche B., Voigt K. D., Gunther T. and Fritsche W. (1999). "Conversion rates of five polycyclic aromatic hydrocarbons in liquid cultures of fifty-eight fungi and the concomitant production of oxidative enzymes." Mycological Research **103**: 1009-1018.

Guggenberger, G., Frey S. D., Six J., Paustian K. and Elliott E. T. (1999). "Bacterial and fungal cell-wall residues in conventional and no-tillage agroecosystems." Soil Science Society of America Journal **63**(5): 1188-1198.

Guldi, D. M. and Asmus K. D. (1997). "Photophysical properties of mono- and multiply-functionalized fullerene derivatives." Journal of Physical Chemistry A **101**(8): 1472-1481.

Hamer, U., Marschner B., Brodowski S. and Amelung W. (2004). "Interactive priming of black carbon and glucose mineralisation." Organic Geochemistry **35**(7): 823-830.

Handy, R. D., von der Kammer F., Lead J. R., Hassellov M., Owen R. and Crane M. (2008). "The ecotoxicology and chemistry of manufactured nanoparticles." Ecotoxicology **17**(4): 287-314.

Haritash, A. K. and Kaushik C. P. (2009). "Biodegradation aspects of polycyclic aromatic hydrocarbons (pahs): A review." Journal of Hazardous Materials **169**(1-3): 1-15.

Hartmann, N. B., Buendia I. M., Bak J. and Baun A. (2011). "Degradability of aged aquatic suspensions of c-60 nanoparticles." Environmental Pollution **159**(10): 3134-3137.

Hatakka, A. (1994). "Lignin-modifying enzymes from selected white-rot fungi: Production and role from in lignin degradation." FEMS Microbiology Reviews **13**(2-3): 125-135.

Hatakka, A. I., Niemenmaa O. V., Lankinen V. P. and Lundell T. K. (1992). Production and characterization of lignin peroxidases and laccase from the white-rot fungi phlebia-radiata and phlebia-(merulius)-tremellosa. Chichester, Ellis Horwood Ltd.

Heinonsalo, J., Kabiersch G., Niemi R. M., Simpanen S., Ilvesniemi H., Hofrichter M., Hatakka A. and Steffen K. T. (2012). "Filter centrifugation as a sampling method for miniaturization of extracellular fungal enzyme activity measurements in solid media." Fungal Ecology **5**(2): 261-269.

Hernandez-Soriano, M. C. and Jimenez-Lopez J. C. (2012). "Effects of soil water content and organic matter addition on the speciation and bioavailability of heavy metals." Science of the Total Environment **423**: 55-61.

Hierold, C., Jungen A., Stampfer C. and Helbling T. (2007). "Nano electromechanical sensors based on carbon nanotubes." Sensors and Actuators a-Physical **136**(1): 51-61.

Hirsch, A. (2002). "Functionalization of single-walled carbon nanotubes." Angewandte Chemie-International Edition **41**(11): 1853-1859.

Hofrichter, M., Ziegenhagen D., Sorge S., Ullrich R., Bublitz F. and Fritsche W. (1999). "Degradation of lignite (low-rank coal) by ligninolytic basidiomycetes and their manganese peroxidase system." Applied Microbiology and Biotechnology **52**(1): 78-84.

Holden, P. A., Nisbet R. M., Lenihan H. S., Miller R. J., Cherr G. N., Schimel J. P., Gardea-Torresdey J. L. and Univ C. (2013). "Ecological nanotoxicology: Integrating nanomaterial hazard considerations across the subcellular, population, community, and ecosystems levels." Accounts of Chemical Research **46**(3): 813-822.

Hou, W. C. and Jafvert C. T. (2009). "Photochemical transformation of aqueous c-60 clusters in sunlight." Environmental Science & Technology **43**(2): 362-367.

Hou, W. C. and Jafvert C. T. (2009). "Photochemistry of aqueous c-60 clusters: Evidence of o-1(2) formation and its role in mediating c-60 phototransformation." Environmental Science & Technology **43**(14): 5257-5262.

Hou, W. C., Kong L. J., Wepasnick K. A., Zepp R. G., Fairbrother D. H. and Jafvert C. T. (2010). "Photochemistry of aqueous c-60 clusters: Wavelength dependency and product characterization." Environmental Science & Technology **44**(21): 8121-8127.

Hu, C. W., Zhang L. J., Wang W. L., Cui Y. B. and Li M. (2014). "Evaluation of the combined toxicity of multi-walled carbon nanotubes and sodium pentachlorophenate on the earthworm eisenia fetida using avoidance bioassay and comet assay." Soil Biology & Biochemistry **70**: 123-130.

Hu, H., Zhao B., Itkis M. E. and Haddon R. C. (2003). "Nitric acid purification of single-walled carbon nanotubes." Journal of Physical Chemistry B **107**(50): 13838-13842.

Hwang, Y. S. and Li Q. L. (2010). "Characterizing photochemical transformation of aqueous nc(60) under environmentally relevant conditions." Environmental Science & Technology **44**(8): 3008-3013.

Hyung, H., Fortner J. D., Hughes J. B. and Kim J. H. (2007). "Natural organic matter stabilizes carbon nanotubes in the aqueous phase." Environmental Science & Technology **41**(1): 179-184.

Iijima, S. (1991). "Helical microtubules of graphitic carbon." Nature **354**(6348): 56-58.

Itkis, M. E., Perea D. E., Niyogi S., Rickard S. M., Hamon M. A., Zhao B. and Haddon R. C. (2003). "Purity evaluation of as-prepared single-walled carbon nanotube soot by use of solution-phase near-ir spectroscopy." Nano Letters **3**(3): 309-314.

Jaisi, D. P. and Elimelech M. (2009). "Single-walled carbon nanotubes exhibit limited transport in soil columns." Environmental Science & Technology **43**(24): 9161-9166.

Jia, G., Wang H. F., Yan L., Wang X., Pei R. J., Yan T., Zhao Y. L. and Guo X. B. (2005). "Cytotoxicity of carbon nanomaterials: Single-wall nanotube, multi-wall nanotube, and fullerene." Environmental Science & Technology **39**(5): 1378-1383.

Johansen, A., Pedersen A. L., Jensen K. A., Karlson U., Hansen B. M., Scott-Fordsmand J. J. and Winding A. (2008). "Effects of c(60) fullerene nanoparticles on soil bacteria and protozoans." Environmental Toxicology and Chemistry **27**(9): 1895-1903.

Journet, C., Maser W. K., Bernier P., Loiseau A., delaChapelle M. L., Lefrant S., Deniard P., Lee R. and Fischer J. E. (1997). "Large-scale production of single-walled carbon nanotubes by the electric-arc technique." Nature **388**(6644): 756-758.

Kang, S., Mauter M. S. and Elimelech M. (2009). "Microbial cytotoxicity of carbon-based nanomaterials: Implications for river water and wastewater effluent." Environmental Science & Technology **43**(7): 2648-2653.

Kang, S., Pinault M., Pfefferle L. D. and Elimelech M. (2007). "Single-walled carbon nanotubes exhibit strong antimicrobial activity." Langmuir **23**(17): 8670-8673.

Karakoti, A. S., Hench L. L. and Seal S. (2006). "The potential toxicity of nanomaterials - the role of surfaces." Jom **58**(7): 77-82.

Kasel, D., Bradford S. A., Simunek J., Putz T., Vereecken H. and Klumpp E. (2013). "Limited transport of functionalized multi-walled carbon nanotubes in two natural soils." Environmental Pollution **180**: 152-158.

Khodakovskaya, M. V., de Silva K., Nedosekin D. A., Dervishi E., Biris A. S., Shashkov E. V., Galanzha E. I. and Zharov V. P. (2011). "Complex genetic, photothermal, and photoacoustic analysis of nanoparticle-plant interactions." Proceedings of the National Academy of Sciences of the United States of America **108**(3): 1028-1033.

Kim, D. Y. and Rhee Y. H. (2003). "Biodegradation of microbial and synthetic polyesters by fungi." Applied Microbiology and Biotechnology **61**(4): 300-308.

Klaine, S. J., Alvarez P. J. J., Batley G. E., Fernandes T. F., Handy R. D., Lyon D. Y., Mahendra S., McLaughlin M. J. and Lead J. R. (2008). "Nanomaterials in the environment: Behavior, fate, bioavailability, and effects." Environmental Toxicology and Chemistry **27**(9): 1825-1851.

Kong, M., Chen X. G., Xing K. and Park H. J. (2010). "Antimicrobial properties of chitosan and mode of action: A state of the art review." International Journal of Food Microbiology **144**(1): 51-63.

Kramer, C. and Gleixner G. (2008). "Soil organic matter in soil depth profiles: Distinct carbon preferences of microbial groups during carbon transformation." Soil Biology & Biochemistry **40**(2): 425-433.

Kroto, H. W., Heath J. R., Obrien S. C., Curl R. F. and Smalley R. E. (1985). "C-60 - buckminsterfullerene." Nature **318**(6042): 162-163.

Kuzyakov, Y., Subbotina I., Chen H. Q., Bogomolova I. and Xu X. L. (2009). "Black carbon decomposition and incorporation into soil microbial biomass estimated by c-14 labeling." Soil Biology & Biochemistry **41**(2): 210-219.

Leonowicz, A., Cho N. S., Luterek J., Wilkolazka A., Wojtas-Wasilewska M., Matuszewska A., Hofrichter M., Wesenberg D. and Rogalski J. (2001). "Fungal laccase: Properties and activity on lignin." Journal of Basic Microbiology **41**(3-4): 185-227.

Leonowicz, A., Matuszewska A., Luterek J., Ziegenhagen D., Wojtas-Wasilewska M., Cho N. S., Hofrichter M. and Rogalski J. (1999). "Biodegradation of lignin by white rot fungi." Fungal Genetics and Biology **27**(2-3): 175-185.

Li, D., Lyon D. Y., Li Q. and Alvarez P. J. J. (2008). "Effect of soil sorption and aquatic natural organic matter on the antibacterial activity of a fullerene water suspension." Environmental Toxicology and Chemistry **27**(9): 1888-1894.

Lilly, W. W., Wallweber G. J. and Lukefahr T. A. (1992). "Cadmium absorption and its effects on growth and mycelial morphology of the basidiomycete fungus, schizophyllum-commune." Microbios **72**(292-93): 227-237.

Lin, S. J., Reppert J., Hu Q., Hudson J. S., Reid M. L., Ratnikova T. A., Rao A. M., Luo H. and Ke P. C. (2009). "Uptake, translocation, and transmission of carbon nanomaterials in rice plants." Small **5**(10): 1128-1132.

Liu, J., Rinzler A. G., Dai H. J., Hafner J. H., Bradley R. K., Boul P. J., Lu A., Iverson T., Shelimov K., Huffman C. B., Rodriguez-Macias F., Shon Y. S., Lee T. R., Colbert D. T. and Smalley R. E. (1998). "Fullerene pipes." Science **280**(5367): 1253-1256.

Liu, X. Y., Gurel V., Morris D., Murray D. W., Zhitkovich A., Kane A. B. and Hurt R. H. (2007). "Bioavailability of nickel in single-wall carbon nanotubes." Advanced Materials **19**(19): 2790-+.

Loferer-Krossbacher, M., Klima J. and Psenner R. (1998). "Determination of bacterial cell dry mass by transmission electron microscopy and densitometric image analysis." Applied and Environmental Microbiology **64**(2): 688-694.

Lopacka, J. (2013). "Nanoparticles used to improve physical properties of polymer composites for food packaging materials." Polimery **58**(11-12): 864-868.

Lyon, D. Y., Adams L. K., Falkner J. C. and Alvarez P. J. J. (2006). "Antibacterial activity of fullerene water suspensions: Effects of preparation method and particle size." Environmental Science & Technology **40**(14): 4360-4366.

Lyon, D. Y., Fortner J. D., Sayes C. M., Colvin V. L. and Hughes J. B. (2005). "Bacterial cell association and antimicrobial activity of a c-60 water suspension." Environmental Toxicology and Chemistry **24**(11): 2757-2762.

Melechko, A. V., Merkulov V. I., McKnight T. E., Guillorn M. A., Klein K. L., Lowndes D. H. and Simpson M. L. (2005). "Vertically aligned carbon nanofibers and related structures: Controlled synthesis and directed assembly." Journal of Applied Physics **97**(4).

Muller, S., Totsche K. U. and Kogel-Knabner I. (2007). "Sorption of polycyclic aromatic hydrocarbons to mineral surfaces." European Journal of Soil Science **58**(4): 918-931.

Muyzer, G., Dewaal E. C. and Uitterlinden A. G. (1993). "Profiling of complex microbial-populations by denaturing gradient gel-electrophoresis analysis of polymerase chain reaction-amplified genes-coding for 16s ribosomal-rna." Applied and Environmental Microbiology **59**(3): 695-700.

Mwaura, J. K., Pinto M. R., Witker D., Ananthakrishnan N., Schanze K. S. and Reynolds, Jr. (2005). "Photovoltaic cells based on sequentially adsorbed multilayers of conjugated poly(p-phenylene ethynylene)s and a water-soluble fullerene derivative." Langmuir **21**(22): 10119-10126.

Nakamura, E. and Isobe H. (2003). "Functionalized fullerenes in water. The first 10 years of their chemistry, biology, and nanoscience." Accounts of Chemical Research **36**(11): 807-815.

Nasibulin, A. G., Anisimov A. S., Pikhitsa P. V., Jiang H., Brown D. P., Choi M. and Kauppinen E. I. (2007). "Investigations of nanobud formation." Chemical Physics Letters **446**(1-3): 109-114.

Navarro, E., Baun A., Behra R., Hartmann N. B., Filser J., Miao A. J., Quigg A., Santschi P. H. and Sigg L. (2008). "Environmental behavior and ecotoxicity of engineered nanoparticles to algae, plants, and fungi." Ecotoxicology **17**(5): 372-386.

Niyogi, S., Hamon M. A., Hu H., Zhao B., Bhowmik P., Sen R., Itkis M. E. and Haddon R. C. (2002). "Chemistry of single-walled carbon nanotubes." Accounts of Chemical Research **35**(12): 1105-1113.

Novotny, C., Erbanova P., Sasek V., Kubatova A., Cajthaml T., Lang E., Krahl J. and Zadrazil F. (1999). "Extracellular oxidative enzyme production and pah removal in soil by exploratory mycelium of white rot fungi." Biodegradation **10**(3): 159-168.

Nowack, B., Ranville J. F., Diamond S., Gallego-Urrea J. A., Metcalfe C., Rose J., Horne N., Koelmans A. A. and Klaine S. J. (2012). "Potential scenarios for nanomaterial release and subsequent alteration in the environment." Environmental Toxicology and Chemistry **31**(1): 50-59.

Nyberg, L., Turco R. F. and Nies L. (2008). "Assessing the impact of nanomaterials on anaerobic microbial communities." Environmental Science & Technology **42**(6): 1938-1943.

Ollikka, P., Alhonmaki K., Leppanen V.-M., Glumoff T., Raijola T. and Suominen I. (1993). "Decolorization of azo, triphenyl methane, heterocyclic, and polymeric dyes by lignin peroxidase isoenzymes from phanerochaete chrysosporium." Applied and Environmental Microbiology **59**(12): 4010-4016.

Orr, M. J., Gray M. B., Applegate B., Volenec J. J., Brouder S. M. and Turco R. F. (2015). "Transition to second generation cellulosic biofuel production systems reveals limited negative impacts on the soil microbial community structure." Applied Soil Ecology **95**: 62-72.

Parks, A. N., Chandler G. T., Ho K. T., Burgess R. M. and Ferguson P. L. (2015). "Environmental biodegradability of c-14 single-walled carbon nanotubes by trametes versicolor and natural microbial cultures found in new bedford harbor sediment and aerated wastewater treatment plant sludge." Environmental Toxicology and Chemistry **34**(2): 247-251.

Pasquini, L. M., Hashmi S. M., Sommer T. J., Elimelech M. and Zimmerman J. B. (2012). "Impact of surface functionalization on bacterial cytotoxicity of single-walled carbon nanotubes." Environmental Science & Technology **46**(11): 6297-6305.

Peng, R. H., Xiong A. S., Xue Y., Fu X. Y., Gao F., Zhao W., Tian Y. S. and Yao Q. H. (2008). "Microbial biodegradation of polyaromatic hydrocarbons." Fems Microbiology Reviews **32**(6): 927-955.

Rabea, E. I., Badawy M. E. T., Stevens C. V., Smagghe G. and Steurbaut W. (2003). "Chitosan as antimicrobial agent: Applications and mode of action." Biomacromolecules **4**(6): 1457-1465.

Rabinovich, M. L., Bolobova A. V. and Vasil'chenko L. G. (2004). "Fungal decomposition of natural aromatic structures and xenobiotics: A review." Applied Biochemistry and Microbiology **40**(1): 1-17.

Rinzler, A. G., Liu J., Dai H., Nikolaev P., Huffman C. B., Rodriguez-Macias F. J., Boul P. J., Lu A. H., Heymann D., Colbert D. T., Lee R. S., Fischer J. E., Rao A. M., Eklund P. C. and Smalley R. E. (1998). "Large-scale purification of single-wall carbon nanotubes: Process, product, and characterization." Applied Physics a-Materials Science & Processing **67**(1): 29-37.

Riva, S. (2006). "Laccases: Blue enzymes for green chemistry." Trends in Biotechnology **24**(5): 219-226.

Rodrigues, D. F., Jaisi D. P. and Elimelech M. (2013). "Toxicity of functionalized single-walled carbon nanotubes on soil microbial communities: Implications for nutrient cycling in soil." Environmental Science & Technology **47**(1): 625-633.

Rodriguez-Yanez, Y., Munoz B. and Albores A. (2013). "Mechanisms of toxicity by carbon nanotubes." Toxicology Mechanisms and Methods **23**(3): 178-195.

Rogalski, J., Lundell T., Leonowicz A. and Hatakka A. (1991). "Production of laccase, lignin peroxidase and manganese-dependent peroxidase by various strains of trametes-versicolor depending on culture conditions." Acta Microbiologica Polonica **40**(3-4): 221-234.

Ruoff, R. S. and Lorents D. C. (1995). "Mechanical and thermal-properties of carbon nanotubes." Carbon **33**(7): 925-930.

Santos, F., Torn M. S. and Bird J. A. (2012). "Biological degradation of pyrogenic organic matter in temperate forest soils." Soil Biology & Biochemistry **51**: 115-124.

Sayes, C. M., Liang F., Hudson J. L., Mendez J., Guo W. H., Beach J. M., Moore V. C., Doyle C. D., West J. L., Billups W. E., Ausman K. D. and Colvin V. L. (2006). "Functionalization density dependence of single-walled carbon nanotubes cytotoxicity in vitro." Toxicology Letters **161**(2): 135-142.

Schoug, A., Fischer J., Heipieper H. J., Schnuerer J. and Hakansson S. (2008). "Impact of fermentation ph and temperature on freeze-drying survival and membrane lipid composition of lactobacillus coryniformis si3." Journal of Industrial Microbiology & Biotechnology **35**(3): 175-181.

Schreiner, K. M., Filley T. R., Blanchette R. A., Bowen B. B., Bolskar R. D., Hockaday W. C., Masiello C. A. and Raebiger J. W. (2009). "White-rot basidiomycete-mediated decomposition of c-60 fullerol." Environmental Science & Technology **43**(9): 3162-3168.

Scott-Fordsmand, J. J., Krogh P. H., Schaefer M. and Johansen A. (2008). "The toxicity testing of double-walled nanotubes-contaminated food to eisenia veneta earthworms." Ecotoxicology and Environmental Safety **71**(3): 616-619.

Shimao, M. (2001). "Biodegradation of plastics." Current Opinion in Biotechnology **12**(3): 242-247.

Sinsabaugh, R. L. (2010). "Phenol oxidase, peroxidase and organic matter dynamics of soil." Soil Biology and Biochemistry **42**(3): 391-404.

Sinsabaugh, R. L., Hill B. H. and Shah J. J. F. (2009). "Ecoenzymatic stoichiometry of microbial organic nutrient acquisition in soil and sediment." Nature **462**(7274): 795-798.

Sinsabaugh, R. L. and Linkins A. E. (1988). "Exoenzyme activity associated with lotic epilithon." Freshwater Biology **20**(2): 249-261.

Six, J., Bossuyt H., Degryze S. and Denef K. (2004). "A history of research on the link between (micro)aggregates, soil biota, and soil organic matter dynamics." Soil and Tillage Research **79**(1): 7-31.

Six, J., Frey S. D., Thiet R. K. and Batten K. M. (2006). "Bacterial and fungal contributions to carbon sequestration in agroecosystems." Soil Science Society of America Journal **70**(2): 555-555.

Smith, B., Wepasnick K., Schrote K. E., Cho H. H., Ball W. P. and Fairbrother D. H. (2009). "Influence of surface oxides on the colloidal stability of multi-walled carbon nanotubes: A structure-property relationship." Langmuir **25**(17): 9767-9776.

Star, A. and Stoddart J. F. (2002). "Dispersion and solubilization of single-walled carbon nanotubes with a hyperbranched polymer." Macromolecules **35**(19): 7516-7520.

Steinbeiss, S., Gleixner G. and Antonietti M. (2009). "Effect of biochar amendment on soil carbon balance and soil microbial activity." Soil Biology & Biochemistry **41**(6): 1301-1310.

Su, D. (2013). Photo mineralization of aqueous fullerene clusters: Headspace analysis and product characterization. Civil Engineering, Purdue University. **Master of Science**.

Svoboda, L., Havlickova B. and Kalac P. (2006). "Contents of cadmium, mercury and lead in edible mushrooms growing in a historical silver-mining area." Food Chemistry **96**(4): 580-585.

Swift, R. S. and Posner A. M. (1972). "Autoxidation of humic acid under alkaline conditions." Journal of Soil Science **23**(4): 381-393.

Taylor, R. and Walton D. R. M. (1993). "The chemistry of fullerenes." Nature **363**(6431): 685-693.

Thess, A., Lee R., Nikolaev P., Dai H. J., Petit P., Robert J., Xu C. H., Lee Y. H., Kim S. G., Rinzler A. G., Colbert D. T., Scuseria G. E., Tomanek D., Fischer J. E. and Smalley R. E. (1996). "Crystalline ropes of metallic carbon nanotubes." Science **273**(5274): 483-487.

Thompson, B. C. and Frechet J. M. J. (2008). "Organic photovoltaics - polymer-fullerene composite solar cells." Angewandte Chemie-International Edition **47**(1): 58-77.

Thurston, C. F. (1994). "The structure and function of fungal laccases." Microbiology **140**: 19-26.

Tong, Z. H., Bischoff M., Nies L., Applegate B. and Turco R. F. (2007). "Impact of fullerene (c-60) on a soil microbial community." Environmental Science & Technology **41**(8): 2985-2991.

Tong, Z. H., Bischoff M., Nies L. F., Myer P., Applegate B. and Turco R. F. (2012). "Response of soil microorganisms to as-produced and functionalized single-wall carbon nanotubes (swnts)." Environmental Science & Technology **46**(24): 13471-13479.

Trojanowicz, M. (2006). "Analytical applications of carbon nanotubes: A review." Trac-Trends in Analytical Chemistry **25**(5): 480-489.

Turco, R. F., Bischoff M., Tong Z. H. and Nies L. (2011). "Environmental implications of nanomaterials: Are we studying the right thing?" Current Opinion in Biotechnology **22**(4): 527-532.

Vance, E. D., Brookes P. C. and Jenkinson D. S. (1987). "An extraction method for measuring soil microbial biomass c." Soil Biology and Biochemistry **19**(6): 703-707.

Wang, T. and Keddie J. L. (2009). "Design and fabrication of colloidal polymer nanocomposites." Advances in Colloid and Interface Science **147-48**: 319-332.

Wariishi, H., Akileswaran L. and Gold M. H. (1988). "Manganese peroxidase from the basidiomycete phanerochaete chrysosporium: Spectral characterization of the oxidized states and the catalytic cycle." Biochemistry **27**(14): 5365-5370.

Wariishi, H., Valli K. and Gold M. H. (1992). "Manganese(ii) oxidation by manganese peroxidase from the basidiomycete phanerochaete chrysosporium. Kinetic mechanism and role of chelators." Journal of Biological Chemistry **267**(33): 23688-23695.

Westerhoff, P. K., Kiser A. and Hristovski K. (2013). "Nanomaterial removal and transformation during biological wastewater treatment." Environmental Engineering Science **30**(3): 109-117.

White, D. C., Davis W. M., Nickels J. S., King J. D. and Bobbie R. J. (1979). "Determination of the sedimentary microbial biomass by extractible lipid phosphate." Oecologia **40**: 51-62.

Wiesner, M. R., Lowry G. V., Jones K. L., Hochella M. F., Di Giulio R. T., Casman E. and Bernhardt E. S. (2009). "Decreasing uncertainties in assessing environmental exposure, risk, and ecological implications of nanomaterials." Environmental Science & Technology **43**(17): 6458-6462.

Yang, J., Bitter J. L., Smith B. A., Fairbrother D. H. and Ball W. P. (2013). "Transport of oxidized multi-walled carbon nanotubes through silica based porous media: Influences of aquatic chemistry, surface chemistry, and natural organic matter." Environmental Science & Technology **47**(24): 14034-14043.

Yang, Y., Yu Z. C., Nosaka T., Doudrick K., Hristovski K., Herckes P. and Westerhoff P. (2015). "Interaction of carbonaceous nanomaterials with wastewater biomass." Frontiers of Environmental Science & Engineering **9**(5): 823-831.

Yetis, U., Ozcengiz G., Dilek F. B., Ergen N. and Dolek A. (1998). "Heavy metal biosorption by white-rot fungi." Water Science and Technology **38**(4-5): 323-330.

Yu, M. F., Lourie O., Dyer M. J., Moloni K., Kelly T. F. and Ruoff R. S. (2000). "Strength and breaking mechanism of multiwalled carbon nanotubes under tensile load." Science **287**(5453): 637-640.

Zelles, L. (1999). "Fatty acid patterns of phospholipids and lipopolysaccharides in the characterisation of microbial communities in soil: A review." Biology and Fertility of Soils **29**(2): 111-129.

Zeng, H. L., Gao C. and Yan D. Y. (2006). "Poly(epsilon-caprolactone)-functionalized carbon nanotubes and their biodegradation properties." Advanced Functional Materials **16**(6): 812-818.

Zhang, Q., Huang J. Q., Qian W. Z., Zhang Y. Y. and Wei F. (2013). "The road for nanomaterials industry: A review of carbon nanotube production, post-treatment, and bulk applications for composites and energy storage." Small **9**(8): 1237-1265.

Zhang, X., Li C. R., Wang W. C., Xue J., Huang Y. L., Yang X. X., Tan B., Zhou X. P., Shao C., Ding S. J. and Qiu J. F. (2016). "A novel electrochemical immunosensor for highly sensitive detection of aflatoxin b-1 in corn using single-walled carbon nanotubes/chitosan." Food Chemistry **192**: 197-202.

Zhao, B., Hu H., Yu A. P., Perea D. and Haddon R. C. (2005). "Synthesis and characterization of water soluble single-walled carbon nanotube graft copolymers." Journal of the American Chemical Society **127**(22): 8197-8203.

Zhao, H. F., Fan W., Dong J. J., Lu J., Chen J., Shan L. J., Lin Y. and Kong W. B. (2008). "Evaluation of antioxidant activities and total phenolic contents of typical malting barley varieties." Food Chemistry **107**(1): 296-304.

Zhao, Y., Allen B. L. and Star A. (2011). "Enzymatic degradation of multiwalled carbon nanotubes." Journal of Physical Chemistry A **115**(34): 9536-9544.

Zhao, Y. and Jafvert C. T. (2015). "Environmental photochemistry of single layered graphene oxide in water." Environmental Science Nano.

Zhao, Y. C. and Jafvert C. T. (2015). "Environmental photochemistry of single layered graphene oxide in water." Environmental Science-Nano **2**(2): 136-142.

APPENDIX

APPENDIX

A.1. C_{60} mineralization calculations

Head-space analysis using the Sercon TGA2 trace gas analyzer requires evacuation of the microcosm headspace and quantifies total headspace CO_2. The respiration rate of a microcosm can then be calculated by the quantity of CO_2 by the time the microcosm was allowed to accumulate before sampling.

$$Respiration\ Rate\ = \frac{Headspace\ CO_2}{Accumlation\ Time} \qquad \text{Equation 1}$$

As headspace was flushed during each sampling, the quantity of carbon respired between samplings was calculated by integrating the measured respiration rates between time points using the trapezoidal approximation. Cumulative CO_2 is the summation of these trapezoidal approximations and was calculated using the equation below.

$$Total\ CO_2\ Respired = \sum\left(\frac{RR_{T_n}+RR_{T_{n+1}}}{2} \times (T_n\ - T_{n+1})\right) \qquad \text{Equation 2}$$

Where T_N is the time of sampling in the incubation and T_{N+1} is the time of the subsequent sampling. RR_{TN} and RR_{TN+1} correspond to the respiration rates at sampling time points T_n and T_{n+1} respectively (as calculated in Equation 1. Care must be taken to insure that units used to define T_n are consistent with the units used in the calculation of RR_{Tn} (i.e. if RR_{Tn} is measured in mg C/hour, T_n must represent the time in hours during which the headspace CO_2 was sampled)

The fractional contribution of mineralized C_{60} fullerene (in CHAPTER FOUR) and C_{60} fullerol (CHAPTER FIVE) to the total CO_2 efflux from soil microcosms at a given time point is calculated using a simple two member mixing model (Equation 3).

$$FC_{60} = \frac{(\delta^{13}C_{C60\ Headspace} - \delta^{13}C_{Control\ Headspace})}{(\delta^{13}C_{C60} - \delta^{13}C_{Control\ Headspace})} \quad \text{Equation 3}$$

In which $\delta^{13}C_{C60\ Headspace}$ and $\delta^{13}C_{Control\ Headspace}$ are the isotopic compositions of the headspace CO_2 from microcosms containing C_{60} and C_{60}-free controls respectively and $\delta^{13}C_{60}$ is the isotopic composition of the added C_{60} (3683.73 ‰).

Finally, the quantity of C_{60} mineralized into CO2 over the course of the incubation is computed as the summation of fractional contribution of C60 to headspace CO_2 multiplied by the CO_2 respired (Equation 4).

$$Total\ C_{60}\ Mineralized = \sum(FC_{60_T} \times CO_{2_T}) \quad \text{Equation 4}$$

A2. PLFA-FAME Calculations

PLFA extracted from microcosm soils were converted by mild alkaline methanolysis into the corresponding FAMEs to enable analysis by GC. The measured isotopic composition of the FAMES analyzed by CSIA were corrected to remove the contribution of the carbon atom added during methanolysis with Equation 5.

$$\delta^{13}C_{Lipid} = \frac{(\delta^{13}C_{FAME} \times N) - \delta^{13}C_{MeOH}}{(N-1)} \quad \text{Equation 5}$$

Where $\delta^{13}C_{FAME}$ is the isotopic composition of the FAME, $\delta^{13}C_{MeOH}$ is the isotopic composition the methyl group added by methanolysis, and N is the number of carbon atoms in the FAME. A mixing model equation similar to Equation 3 was then used to compute the fractional contribution of carbon from C_{60} fullerols to the microbial PLFA.

$$F_{C60} = \frac{(\delta^{13}C_{C60\ Lipid} - \delta^{13}C_{Control\ Lipid})}{(\delta^{13}C_{C60} - \delta^{13}C_{Control\ Lipid})}$$ Equation 6

Where $\delta^{13}C_{C60\ Lipid}$ and $\delta^{13}C_{Control\ Lipid}$ are the isotopic compositions a PLFA extracted from the fullerol containing and fullerol-free microcosms, respectively. The quantity of fullerol taken up into PLFA of a microbial guild is calculated by multiplying the fractional contribution of fullerol (calculated with Equation 6) to biomass by the actual quantity of PLFA carbon for each characteristic PLFA and summing the results as in Equation 7.

$$C60\ Uptake_{Guild\ PLFA} = \sum(F_{C60} \times PLFA_C)$$ Equation 7

Where $PLFA_c$ is total carbon in an individual PLFA. The ratio of this value to the total guild PLFA carbon pool gives the ratio of C_{60} carbon to other carbon in all of the guild's PLFA.

$$Biomass\ Uptake\ Ratio = \frac{C60\ Uptake_{Guild\ PLFA}}{Total\ Guild\ PLFA_C}$$ Equation 8

Finally, this is used to estimate total fullerol uptake into total microbial guild biomass by multiplying guild PLFA abundance (normalized to soil SOM) by the average quantity of PLFA in a bacterial cell (1.4E-8 nmol/Cell, Frostegard *et al.* 1996) and the total carbon content of a bacterial cell (3E-11mg/Cell, Fukada *et al.* 1998 and Loferer-Krossbacher *et al.* 1998) .

$$C60\ uptake_{Guild\ Total} = Biomass\ Uptake\ Ratio \times \frac{\frac{nmol_{Guild\ PLFA}}{g\ SOM}}{1.4\times10^{-8} nmol\ PLFA/Cell} \times (3 \times 10^{-11} mg_C/cell)$$

VITA

VITA

Timothy Berry

Education

Ph.D. in Earth, Atmospheric, and Planetary Science/Interdisciplinary Life Science — 2015
Dissertation: *Microbial Controls on the Environmental Fate of Carbon Nanomaterials*
Purdue University, West Lafayette, IN

B.S. in Microbiology — 2010
Michigan State University, East Lansing, MI

Research Experience

Research Assistant — 2011- present
Purdue Stable Isotope/ Soil Geochemistry Lab
Purdue University, West Lafayette, IN

Rotating Research Assistant — 2010-2011
Purdue Stable Isotope/ Soil Geochemistry Lab
Purdue University, West Lafayette, IN

Undergraduate Research Assistant — 2009-2010
Microbial Ecology Lab
Michigan State University, East Lansing, MI

Volunteer Research Assistant — 2008-2009
Genomics, Evolution, and Development Lab
Michigan State University, East Lansing, MI

Teaching Experience

EAPS 312: Capstone: Environmental Science for Elementary Educators (Laboratory Instructor) — 2014, 2015

Fellowships, Grants, and Awards

Outstanding Graduate Instructor, Purdue Teaching Academy	2015
Travel Grant, Purdue University Life Sciences (PULSe)	2015
Outstanding Graduate Student Poster, Earth, Atmospheric, and Planetary Sciences	2014
Lynn Graduate Fellowship	2010

Service and Outreach

Science in Schools Program, Lafayette Public Schools 2010-2014
Developed and conducted simple, hands on science experiments with 3rd, 4th, and 5th graders in public schools to foster K-12 scientific engagement

PULSe Peer Mentor 2011-2013
Mentored first-year graduate students in the PULSe program. Included recruitment and speaking responsibilities

Activities Coordinator, **PULSe Graduate Student Organization** 2011-2012
Planned and organized community outreach and social events in addition to seminars for graduate students

Publications

Berry, T.D.; Filley, T.R.; Blanchette, R.A.; Oxidative enzymatic response of white-rot fungi to single-walled carbon nanotubes. *Environmental Pollution (2014), pp. 197-204*

Berry, T.D.; Clavijo A.; Zhao, Y.; Jafvert, C.T.; Turco, R.F.; Filley, T.R.; Soil microbial response to photo-degraded C60 Fullerenes. (*In Press), Environmental Pollution*

Gibson, C.D.; **Berry, T.D.;** Wang, R.; Johnston, C.T.; Jiang, Y.; Bird, J.A.; Blanchette, R.A.; Filley, T.R.; Weathering of pyrogenic organic matter induces fungal oxidative enzyme response in single culture inoculation experiments. (*In Press), Organic Geochem.*

Berry, T.D.; Clavijo A.; Bischoff Gray, M.; Turco, R.F.; Filley, T.R.; Microbial Mineralization of $^{13}C_{60}$ Fullerols in Two Agricultural Soils. (*In prep*.) Target Journal: Environmental Science and Pollution

BeigzadehMilani, S.; **Berry, T.D.**; Filley, T.R.; Goodwin, D.J.; Fairbrother, D.H.; Jafvert, C.T; Aqueous Photochemistry of Carboxylated Single-Walled Carbon Nanotubes: CO2

Formation and Wavelength Dependency. (*In prep.)* Target Journal: Environmental Science: Nano

Presentations

Berry, T.D.; Filley, T.R.; Measuring nanocarbon fluxes by tracing stable isotope labelled nanomaterials. Oral presentation, 2015, *249th National Meeting of the American Chemical Society*

Berry, T. D.; Gibson, C. D.; Filley, T. R.; Jafvert, C. T., Response of cultured saprotrophic fungi to single-walled carbon nanotube exposure. Poster, 2014*, Purdue Earth, Atmospheric, and Planetary Sciences Research Expo*

Berry, T. D.; Gibson, C. D.; Filley, T. R.; Jafvert, C. T., Response of cultured saprotrophic fungi to single-walled carbon nanotube exposure. Poster, 2013*, 246th National Meeting of the American Chemical Society*

Filley, T.R.; **Berry, T. D.**; Gibson, C. D; Wang, R.Z., Sequential photochemical-biochemical decay pathways for condensed aromatic carbon in the terrestrial environment. Poster, 2013*, 246th National Meeting of the American Chemical Society*

Gibson, C. D.; **Berry, T. D**.; Wang, R. Z.; Filley, T. R.; Bird, J., Priming effects of black carbon additions on carbon mineralization in malt extract media by the white-rot fungus, *Trametes versicolor*. Poster, 2013*, 246th National Meeting of the American Chemical Society*

Organizational Affiliations

American Chemical Society – Geochemistry and Environmental Chemistry Divisions 2011-2015